
NUCLEAR ENERGY RESEARCH INITIATIVE

7. Fundamental Nuclear Science

This element includes 25 NERI projects to date of which 13 were awarded in FY 1999, 1 in FY 2000, 5 in FY 2001, and 6 in FY 2002. It addresses the long-term R&D goal of developing new technologies for nuclear energy applications, of educating young scientists and engineers and training a technical workforce, and of contributing to the broader scientific and technological enterprise.

Today's U.S. reactors, which are based largely on technology from the 1970s, operate under close supervision in a conservative regulatory environment. Although the knowledge base is adequate for these purposes, improvements in the Nation's knowledge base and reduction of the inherent uncertainties concerning nuclear reactors could bring costs savings to current reactor operations and reduce the costs of future reactors. They could also enable innovative designs that reduce the need for excessively conservative and costly safety and reliability factors, and significantly extend safe operating lifetimes. Future reactor technologies are likely to involve higher operating temperatures, advanced fuels, higher fuel burn-up, longer plant lifetimes, better materials for cladding and containment vessels, and alternative coolants. To implement such features, substantial research must be carried out in fundamental science and engineering to supplement applied research on individual promising design concepts. Such fundamental research need not and should not be directed to any specific design. Although motivated in part by the need for new nuclear reactor system designs, the research would also have a far-reaching impact elsewhere in engineering and technology.

The five broad topics identified in the Long-Term R&D Plan related to fundamental nuclear sciences include the following:

- Environmental effects on materials, in particular the effects of the radiation, chemical, and thermal environments, and aging
- Thermal fluids, including multiphase fluid dynamics and fluid structure interactions
- The mechanical behavior of materials, including fracture mechanics, creep, and fatigue
- Advanced material processes and diagnostics
- Reactor physics

Projects currently selected under this element include R&D in fundamental science in the fields of material science, chemical science, computational science, nuclear physics, or other applicable basic research fields. Selected research subjects include irradiation, chemistry, and corrosion effects on nuclear plant materials; advanced new materials research; innovative computational models; and, the investigation of nuclear isomers that could prove beneficial in civilian applications.

NUCLEAR ENERGY RESEARCH INITIATIVE

Directory of Fundamental Nuclear Sciences Project Summaries and Abstracts

99-010 Effects of Water Radiolysis in Water Cooled Nuclear Reactors.225
99-039 Measurements of the Physics Characteristics of Lead-Cooled Fast Reactors and Accelerator Driven Systems229
99-072 Mapping Flow Localization Processes in Deformation of Irradiated Reactor Structural Alloys233
99-101 A Novel Approach to Materials Development for Advanced Reactor Systems237
99-134 Complete Numerical Simulation of Subcooled Flow Boiling in the Presence of Thermal and Chemical Interactions239
99-155 Developing Improved Reactor Structural Materials Using Proton Irradiation as a Rapid Analysis Tool241
99-202 An Investigation of the Mechanism of IGA/SCC of Alloy 600 in Corrosion Accelerating Heated Crevice Environments243
99-233 Interfacial Transport Phenomena and Stability in Molten Metal-Water Systems247
99-254 Fundamental Thermal Fluid Physics of High Temperature Flows in Advanced Reactor Systems249
99-269 An Innovative Reactor Analysis Methodology Based on a Quasidiffusion Nodal Core Model251
99-276 Radiation-Induced Chemistry in High Temperature and Pressure Water and Its Role in Corrosion253
99-280 Novel Concepts for Damage-Resistant Alloy in Next Generation Nuclear Power Systems257
99-281 Advanced Ceramic Composites for High-Temperature Fission Reactors259
00-123 Isomer Research: Energy Release Validation, Production and Applications263
01-084 Random Grain Boundary Network Connectivity as a Predictive Tool for Intergranular Stress-Corrosion Cracking267
01-124 Reactor Physics and Criticality Benchmark Evaluations for Advanced Nuclear Fuel.273
01-130 Fundamental Understanding of Crack Growth in Structural Components of Generation-IV Supercritical Light Water Reactors277
01-137 New Design Equations for Swelling and Irradiation Creep in Generation IV Reactors281
01-140 Development and Validation of Temperature Dependent Thermal Neutron Scattering Laws for Applications and Safety Implications in Generation IV Nuclear Reactor Designs285
02-042 Oxidation of Zircaloy Fuel Cladding in Water-Cooled Nuclear Reactors289
02-044 Incorporation of Integral Fuel Burnable Absorbers Boron and Gadolinium into Zirconium-Alloy Fuel Clad Material293
02-060 Neutron and Beta/Gamma Radiolysis of Supercritical Water295
02-075 Innovative Approach to Establish Root Causes for Cracking in Aggressive Reactor Environments297
02-110 Design of Radiation-Tolerant Structural Alloys for Generation IV Nuclear Energy Systems299
02-146 Enhanced Control of PWR Primary Coolant Water Chemistry Using Selective Separation Systems for Recovery and Recycle of Enriched Boric Acid301

NUCLEAR ENERGY RESEARCH INITIATIVE

NUCLEAR ENERGY RESEARCH INITIATIVE

Effects of Water Radiolysis in Water Cooled Nuclear Reactors

Primary Investigator: Simon M. Pimblott, University of Notre Dame Radiation Laboratory (NDRL)

Project Number: 99-010

Collaborators: Georgia Institute of Technology (GIT)

Project Start Date: August 1999

Project End Date: May 2003

Research Objectives

The aim of this project is to develop an experiment- and theory-based model for the radiolysis of non-standard aqueous systems like those that will be encountered in the Advanced Light Water Reactor (ALWR). Three aspects of the radiation chemistry of aqueous systems at elevated temperatures are considered in the project. They are the radiation-induced reaction within the primary track and with additives, the homogeneous production of H_2O_2 at high radiation doses, and the heterogeneous reaction of the radiation-induced species escaping the track.

The goals for the latter stages of the program are as follows:

- Development of an algorithm and the testing of code to simulate high-Linear Energy Transform (LET) heavy-ion track structure in water
- Simulation of H_2 saturated solutions at ambient temperature
- Development of an experimental protocol for H_2O_2 measurement from gamma irradiation
- Measurements of the effect of H_2 on H_2O_2 yields in gamma irradiated solutions at high doses
- Design of a cell for pulse radiolysis at elevated temperatures
- Irradiation of heavy loaded suspensions of metal oxides in water at ambient temperature
- Determination of the effect of surface potential on escape depth from narrow band-gap oxide materials
- Testing of Electron Parametric Resonance (EPR) and conductivity techniques to measure the charge escape of electrons and holes from these oxides

- Determination of electronic band structures of doped zirconia
- Controlled irradiation of iron oxide covered with water
- Integrity measurements on the zirconia and iron-oxide/water over-layers

Research Progress

The principal focus of this program is to construct an experiment and theory-based model for the radiolysis of non-standard aqueous systems found in nuclear power plants. The research project has two complementary aspects, one simulation-based and one experimental. A methodology was developed for evaluating the energy loss properties of non-relativistic light and heavy ions in condensed media, and calculations were performed for a variety of radiation types in gaseous and in liquid water. The agreement between calculated stopping powers and ranges and available experimental data is excellent over the range of specific energies (E/amu) of radiation chemical interest, 0.1-100 MeV/amu. The NDRL suite of computer codes, TRACKSIM and TRACKKIN, for the simulation of low-linear energy transfer (LET) track structure and chemistry in condensed media was extended to include radiation particles with moderately high LET in liquid water. These codes address two aspects of the radiolysis: the structure of the radiation track (TRACKSIM) and the chemistry of the resulting spatially non-homogeneous distribution of radiation induced reactants (TRACKKIN). The track structure is simulated using a collision-to-collision methodology, employing the newly developed cross-sections for liquid water mentioned above. The Independent Reaction Times methodology, employed for modeling the radiation chemical kinetics, relies upon the generation of random reaction times from initial coordinate positions from reaction time distribution functions.

To incorporate a significant section of heavy ion track structure, extensive modifications of the simulation methodology were made. Calculations were performed to investigate the radiation chemistry induced by ^1H , ^4He , ^7Li , and ^{12}C ions and in aqueous solutions over the temperature range 0°C to 300°C . The results obtained for these well-characterized solutions reproduced yields obtained experimentally (see Figure 1), implying that the technique may be reliably used to model radiation chemical effects in less well-defined, but more relevant systems.

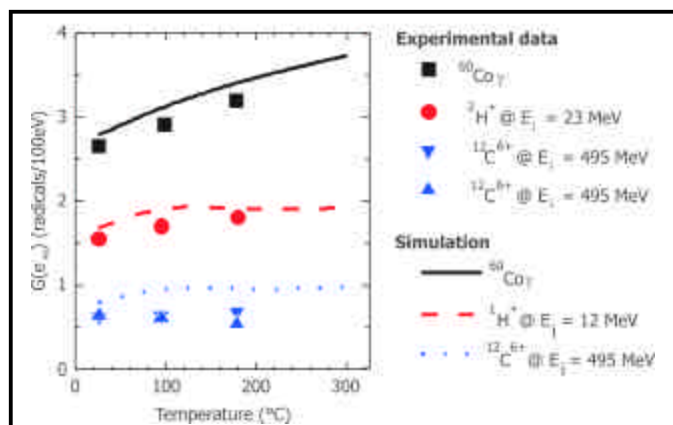


Figure 1. The graph illustrates the effect of temperature on the yield of the hydrated electron produced in the gamma, ^1H and ^{12}C ion radiolysis of water. The points refer to the experimental data of Elliot (1994) while the lines are the predictions of stochastic simulation.

The bulk, homogeneous radiation chemistry of aqueous solutions of hydrated electron and hydroxyl radical scavengers was modeled using yields derived from non-homogeneous stochastic simulations. In some cases, the predictions of these calculations differ from similar more conventional calculations using radical escape yields. These differences are due to intra-track and scavenger chemistry modifying the yields.

One component of the experimental research effort at NDRL has focused on several of the factors that affect the production of hydrogen peroxide in the radiolysis of aqueous solutions. Hydrogen peroxide is the major stable oxidizing product produced in the radiolysis of water and is of considerable interest for the initiation or propagation of corrosion processes. Molecular hydrogen is commonly added to coolant water to lower the steady-state level of hydrogen peroxide. The mechanism for this process was examined with both γ -rays and heavy ions to predict the effects due to the mixed fields associated with reactors. Nuclear reactors typically operate at elevated temperatures

so the radiolytic production and decay of hydrogen peroxide was examined up to a temperature of 150°C . Since the radiolytic production of hydrogen peroxide is so important in reactor water chemistry, its mechanism of formation was thoroughly probed using scavengers for both oxidizing and reducing precursors.

The addition of molecular hydrogen was found to significantly lower the steady-state concentration of hydrogen peroxide in the γ -radiolysis of water. This process is due to the initiation of a chain process by the H atoms and OH radicals produced during water radiolysis. Increasing the concentration of hydrogen to its saturation level lowers the hydrogen peroxide concentration to below detectable levels. The results with high LET particles are considerably different. Above about 20 eV/nm the amount of radicals escaping the radiation track is too low to initiate the chain reaction and the steady-state concentration of hydrogen peroxide increases continuously with dose. Simple deterministic models were found to predict the results with γ -rays, but not with heavy ions.

The non-homogeneous nature of energy deposition by ionizing radiation results in high local concentrations of reactive species. An increase in temperature affects both the recombination rates of the reactive species and the diffusive relaxation of the non-homogeneous distribution. In the case of hydrogen peroxide, an increase in temperature decreases its yield due to the lower probability of OH radical combination reactions. The hydrogen peroxide yield at 150°C is only 60 percent of that at 25°C . It was also noticed that hydrogen peroxide is extremely thermal sensitive and readily decays at high temperatures.

In addition to the studies on hydrogen peroxide, pulse radiolysis experiments were conducted on ZrO_2 suspensions at high particle concentrations in order to examine the escape of electrons and holes into the aqueous interface. The yield of reducing and oxidizing species was measured in the presence of electron and hole acceptors. At heavy loading of ZrO_2 , a significant fraction of the energy is absorbed by the solid particles, but the amount of reducing and oxidizing equivalents measured in the aqueous phase and at the interface increases (significantly). This result suggests that energy that was initially deposited in the particles appears in the liquid phase. Furthermore, the increase in the concentration of aqueous reduction and oxidation products is higher than the increase in the energy absorbed by the samples (i.e., higher than the increase in sample density), implying that early-time recombination and trapping

processes in ZrO_2 particles are less efficient than early recombination in water. Effects of the charge of the scavengers and their interaction with the surface potential were also studied. The yield of electrons escaping the solid is higher than the yield of holes. As a result, charge accumulates in the solid. Contrary to the yield of aqueous redox-radical products, the yield of molecular hydrogen strongly decreases upon increasing ZrO_2 concentration. A back-reaction between hydrogen atoms at the interface and the excess holes trapped in the particles is invoked to rationalize this sharp decrease.

The GIT group has completed a series of experiments on proton and molecular desorption from water-covered ZrO_2 . The results in the high coverage limit are consistent with previously measured yields from amorphous ice. However, the yields in the low coverage limit are very small, indicating that the probability of producing a two-hole state is very low on the ZrO_2 surface. This implies that the neutral yields may increase due to single-hole recombination events at the surface, which may resemble an exciton transfer but is actually mediated by a charged carrier. The molecular hydrogen yields were measured as a function of coverage and incident electron/photon energy to examine the importance of exciton, hole, or electron transfer. The proton yields rise monotonically with coverage whereas the HD and D_2 yields increase in the manner expected for a two-body or two-step process. In addition, resonance-enhanced multiphoton ionization (REMPI) spectroscopy has been used to measure the yields of the atomic and molecular hydrogen desorbed.

All of the topics mentioned in the program objectives for Phase 2 above have been addressed, although only significant accomplishments have been discussed here. The knowledge obtained is providing a sound basis for Phase 3 of the program.

Planned Activities

In developing the experiment and theory-based model, two different aspects of the radiation chemistry of water in the nuclear power plant environment will be considered: the initial non-homogeneous reaction of the primary radiation-induced radicals and ions within the radiation track and their reaction with various additives, and the bulk, homogeneous and heterogeneous reaction of the oxidizing and reducing radicals and the molecular products escaping from the track. Thus far, modeling studies have focused on the non-homogeneous and bulk, homogeneous aspects of the radiation chemistry. Final stages of the project will focus on the effects of oxide surfaces and will involve the incorporation into the chemistry model of information about heterogeneous systems that was supplied by the experimental tasks.

Two experimental objectives remain under investigation at NDRL. A remaining goal of the program is the design of a high-temperature radiolysis cell for future studies using high LET radiation. This design is nontrivial due to the thin windows required for heavy ion radiolysis experiments. Experiments will probably be limited to conditions of about $100^\circ C$, because of the relatively low ion energies obtained using the local accelerator. In addition, radiation experiments will be performed with surface-modified and core-shell particles, to study specifically the effects of over-layers of silica on hematite and zirconia on the escape of carriers from the particle to the electrolyte, and to determine the effects of these combinations on dissolution rates and on radical rates.

Currently, the GTI group is measuring the yields of the atomic and molecular hydrogen produced during 100 eV electron-beam bombardment on water-covered ZrO_2 , using REMPI spectroscopy.

Although this research program is scheduled to end in April 2003, numerous avenues for future advances have been opened by the studies performed.

NUCLEAR ENERGY RESEARCH INITIATIVE

Measurements of the Physics Characteristics of Lead Cooled Fast Reactors and Accelerator Driven Systems

Primary Investigator: Phillip J. Finck, Argonne National Laboratory (ANL)

Project Number: 99-039

Collaborators: French Atomic Energy Commission, Commissariat à l'Energie Atomique (CEA)

Project Start Date: August 1999

Project End Date: September 2002

Research Objectives

Several recent studies in the United States and in other countries have indicated a strong interest in the potential development of lead-cooled critical and sub-critical systems. In order to permit the eventual industrial deployment of these systems, several key technical areas need to be carefully investigated, and solutions for potential technical problems need to be found and implemented.

The neutronic behavior of a lead-cooled fast spectrum system is believed to be relatively poorly known; difficulties arise both from nuclear data uncertainties and from methods-related deficiencies. The French Atomic Energy Commission (CEA) has recognized this situation and has launched an ambitious experimental program aimed at measuring the physics characteristics of lead-cooled critical and sub-critical systems in an experimental facility located at the Cadarache Research Center. A complete analytical program is associated with the experimental program and aims at understanding and resolving potential discrepancies between calculated and measured values. The final objective of the two programs is to reduce the uncertainties in predictive capabilities to a level acceptable for industrial applications.

ANL teams are now participating in the experimental design, measurements, and analytical tasks associated with this effort. In exchange for ANL's participation, all experimental data will be made available to ANL staff.

This program will have three critical outcomes: (1) High-quality experimental data representative of the physics of lead-cooled cores will be available to the U.S. programs, (2) U.S. neutronics codes will be validated for calculating lead-cooled systems, and (3) potential deficiencies in U.S. nuclear data and codes will be identified.

Research Progress

Efforts this past year were concentrated in two areas: analysis of the MUSE 4 experiment through its associated benchmark configuration, and development of experimental techniques for the measurement of time-dependent data.

Highlights of the progress made follow:

- The first reference configuration of the MUSE 4 experimental program went critical on January 9, 2001. A preliminary analysis of this configuration was performed, followed by the analysis of the international benchmark exercise that was launched in relation with the experimental program (Figure 1 illustrates the configuration used for the study). Deterministic and Monte Carlo methods have been used with JEF2.2, ENDF/B-V and ENDF/B-VI data files. Results obtained by using the cell code ECCO in conjunction with JEF2.2 data are extremely good. Discrepancies have been observed between the VIM Monte Carlo calculations using the ENDF/B-VI data and the corresponding MC²-2 calculations, as well as between the ECCO and MC²-2 calculations with JEF2.2 data. Perturbation calculations have been carried out in order to better understand these discrepancies. They have been attributed to differences in the evaluated data for Fe⁵⁶, Cr⁵², and Pu²³⁹.

Following these findings, an attempt was made at first to correct the long-standing deficiency in MC²-2 ultra-fine-group (ufg) scattering cross sections for Fe, Ni, Cr, Mn, and Pb due to their resonance-like structures above the resolved resonance cutoff energies. The correction was necessary to account for the self-shielding effect. Corrections were negligible (less than 100 p.c.m.) for JEF2.2 and ENDF/B-VI data and

approximately 200 p.c.m. for ENDF/B-V. Finally the discrepancy was resolved by using the total cross section weighted by the current. This effect is very important for structural material in a reflector medium. When this correction was made, results of MC²-2 agreed with those of ECCO and Monte Carlo codes.

- A major breakthrough was obtained on reaction rate distributions close to the core/reflector boundaries. Up to now, relatively large discrepancies were obtained in the analysis of these quantities. In the course of these studies investigators have shown that using a large number of energy groups (~1,000) significantly improves the agreement between experimental and computational results. The impact of the large number of groups on the eigenvalue calculation is also not negligible for these kinds of configurations where the reflector is in direct contact with the core region and there is no blanket region in the middle. Subsequently, a new computational collapsing procedure has been implemented in order to reproduce the same type of results obtained with a very large number of groups (~1,000), but this time, using a broad-group energy structure (33 groups). The method is iterative and based on the conservation of reaction rates.

Finally, kinetic calculations were performed in order to allow, test, and validate the analysis of the time-dependent experimental results. ²³⁵U fission rate for several detectors as a function of the time for the deuteron-tritium source pulse in have been calculated. The deuteron beam is assumed to have a time structure of 1 second pulses repeated at 1 kHz. The time step and range were of

1 second and 500 second respectively. Calculations were performed for pulse #1 and for pulse after equilibrium ($n \rightarrow \alpha$). Figure 2 shows time dependent rates using the direct method for the solution of the kinetic neutronic equations. No significant differences were observed when the quasi-static method was used.

Significant spatial effects were observed. The greater the distance of the detectors from the external source (from detectors A, B, C and D in the

reflector to the detectors H,J,K and G in the shielding), the more the solution is extended in time. The maximum value is also reached at a different time.

- In the experimental field, the effort has focused on dynamic experimental methods based on the reactor kinetics and neutron noise theory, using time series data. A specific acquisition system has been developed in order to achieve this objective. The time-series-based techniques that have been used are the inverse kinetics method, the pulsed neutron source (PNS) method, the Rossi- α method, and the Feynman- α method. In these dynamic techniques, one makes use of the fact that kinetic behavior in a reactor is related to the reactivity. However, each method is a little different in terms of sensitivity to

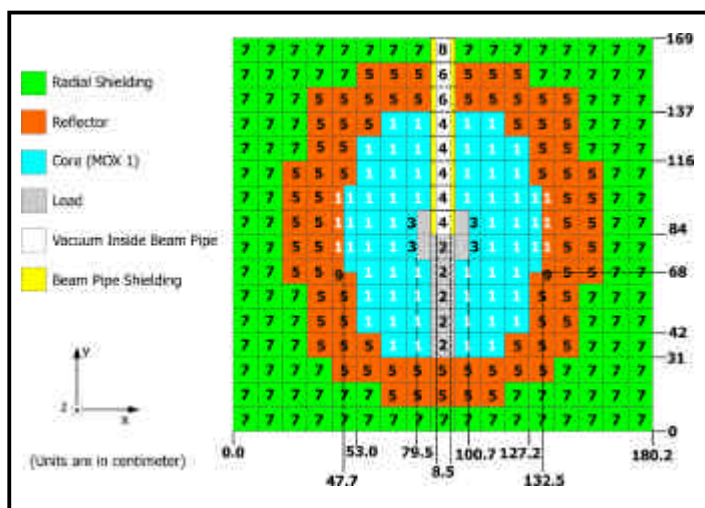


Figure 1: The graphic illustrates the MUSE4 critical (1,112 cells) configuration (top view at half-height)

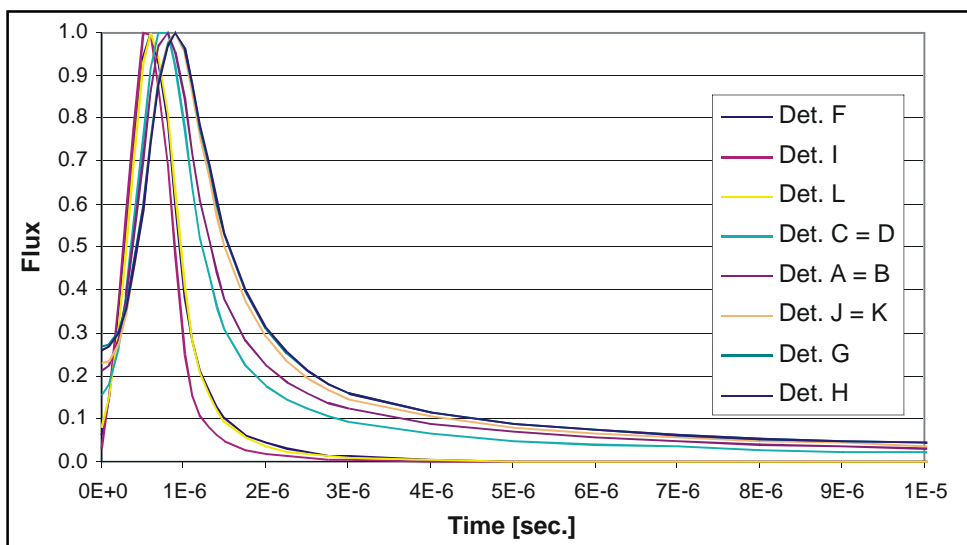


Figure 2. The figure shows time-dependent rates when the direct method is used to solve the kinetic neutronic equations.

other parameters such as background fission rate, detector efficiencies, or kinetic parameters such as the delayed neutron constants.

The PNS, Rossi- α , and Feynman- α techniques have been used to infer the ratio β/Λ , a parameter that determines the time scale of kinetic behavior of a reactor system. A fairly large spread (up to 20 percent) has been observed in the determination of this parameter as the system is perturbed by the insertion of a control rod. Two trends were seen in the α -values (prompt neutron decay constant). As the reactivity of the system is lowered, lower α -values than one would expect are obtained. Additionally, as investigators move from detectors in the core, to detectors in the reactor, and finally to detectors in the shield, a decrease in the α -values is also seen. At the present time, the assumption is that this phenomenon is due to the slowing-down of neutrons in the reactor and shield regions, which increases the detector efficiency. This has the effect of increasing the effective generation time in these outer regions.

- The time-dependent measurements have just begun in the MASURCA¹ facility, and the preliminary results are encouraging. However, many more such measurements are needed before investigators can infer the sub-critical reactivity with an uncertainty on the order of 5 percent or less.

Planned Activities

Although the NERI project has been completed, the ANL activities related to the MUSE experimental program will continue and will be funded under the AFCI program. Both the analysis and experimental tasks will focus on the subsequent subcritical configurations of the program where the GENEPI² accelerator will be used in order to insure the sustainability of the system.

¹ A fast neutron reactor

² A small fast neutron reactor coupled to a deuteron accelerator

NUCLEAR ENERGY RESEARCH INITIATIVE

Mapping Flow Localization Processes in Deformation of Irradiated Reactor Structural Alloys

Primary Investigator: Kenneth Farrell, Oak Ridge National Laboratory (ORNL)

Project Number: 99-072

Collaborators: University of Tennessee

Project Start Date: August 1999

Project End Date: September 2002

Research Objectives

Ferritic steels, austenitic stainless steels, and zirconium alloys are materials used in the construction of nuclear power reactors and are normally quite ductile and workable. After exposure to neutron irradiation they lose much of their ductility and may even become brittle. This degradation of mechanical properties is governed by the way the metals respond to plastic deformation. In the unirradiated condition they undergo plastic flow homogeneously, and the deformation microstructure consists of uniformly distributed tangled dislocations. After irradiation, the deformation mode is markedly changed to highly localized strain in narrow bands or channels, and sometimes in twin bands. This intensification of strain and stress by dislocation channel deformation (DCD) reduces the work-hardening ability of the metal and causes loss of ductility. The degree of degradation is related to the nature and the details of the dominant deformation mode, which are functions of the radiation exposure and of the mechanical test conditions.

Radiation damage raises the tensile yield strength and ultimate tensile strength (UTS), induces yield point drops in materials that do not normally show sharp yield points, reduces the work-hardening rate and the elongation, and causes premature plastic instability and failure. All of these changes are now known or suspected to involve DCD but only a few quantitative correlations have been made.

Such correlations involve measuring the mechanical properties of the metals as functions of neutron fluence and degree of plastic strain, then performing transmission electron microscopy (TEM) examinations of the strained materials to determine their deformation modes. Maps can then be constructed in which the regions and boundaries of the deformation modes are plotted in terms of plastic strain and neutron fluence. Mechanical properties

representing the different deformation modes can be overlaid on the maps, and the maps become pictorial repositories of knowledge relevant to the irradiation behavior of the materials.

The goal of this project is to determine deformation mode maps for A533B ferritic steel, 316 stainless steel, and Zircaloy-4.

Research Progress

Tensile specimens of the three alloys were irradiated in the hydraulic tube facility of the High Flux Isotope Reactor at Oak Ridge National Laboratory to fast neutron fluences of 6×10^{20} , 6×10^{21} , 6×10^{22} , 6×10^{23} , and 5.3×10^{24} n.m⁻², $E > 1\text{MeV}$, corresponding to nominal doses of 0.0001, 0.001, 0.01, 0.1, and 0.9 displacements per atom (dpa). The irradiation temperature was 65 to 100°C. Post-irradiation tensile properties were measured at room temperature at a strain rate of 10^{-3} s⁻¹. All three materials underwent progressive irradiation hardening and loss of ductility with increasing dose. Flow stresses were increased, yield point drops were developed, work-hardening rates were reduced, elongations were severely reduced, and early onset of failure occurred by plastic instability. Four modes of deformation identified were three-dimensional dislocation cell formation, planar dislocation activity, DCD (in which radiation damage structure has been swept away), and fine-scale twinning. These modes varied with material, dose, and strain level.

In the body-centered cubic A533B steel, deformation in the unirradiated specimens was homogeneous and occurred by interaction and tangling of dislocations to form dislocation cells (Figure 1). In those specimens of A533B steel irradiated to the two lowest doses, no radiation damage structure (RDS) was detected and there was only minor radiation hardening; the deformation behavior was similar to the unirradiated material. At the

middle dose of 0.01 dpa, no RDS was seen but there was considerable radiation strengthening and the work hardening rate was reduced almost to zero. For this dose, the arrangement of strain dislocations was more linear, consistent with the decreased work hardening rate, but there was still some dislocation cell structure. At the highest dose, black spot radiation damage with a mean defect size of 1.3 nm and concentration of about $6.5 \times 10^{22} \text{ m}^{-3}$ was evident. In the two highest dose specimens prompt plastic instability failures occurred at the yield stress. Some DCD was observed but the strain in the tensile specimens was too highly localized to allow retrieval of truly representative TEM specimens from the deformed regions. The channels were about 40 nm wide.

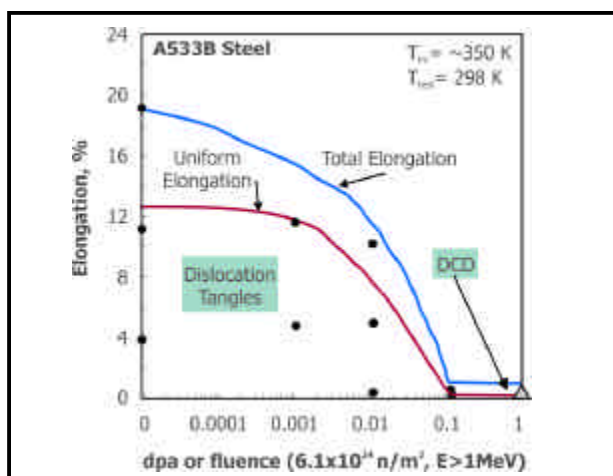


Figure 1. The graph is a deformation mode map for A533B steel neutron-irradiated at 65°C to 100°C and tested at room temperature.

The fluence dependence of the tensile properties of the hexagonal close-packed Zircaloy-4 alloy was found to be of similar form as for the A533B steel, with the exception that the degree of radiation-hardening was higher at the lower doses and lower at the higher doses. No RDS was visible at the lowest dose of 0.0001 dpa. At 0.001, 0.01, 0.1, and 0.8 dpa there was fine black spot damage, reaching a size of 1.4 nm and a concentration of $6.1 \times 10^{22} \text{ m}^{-3}$ at 0.8 dpa. For a dose of 0.001 dpa, and in the unirradiated Zircaloy, plastic deformation during tension testing occurred primarily by coarsely dispersed planar slip in dislocation bands on a single slip system, $\{1000\} \langle 1120 \rangle$ (Figure 2). At 0.01 dpa, the deformation mode was still primarily planar slip, but now occurred on intersecting slip systems, $\{1000\} \langle 1120 \rangle$ and $\{0111\} \langle 1120 \rangle$. At the two highest doses, where plastic instability failure was entered at the yield stress, the deformation mode was dislocation channeling on the same slip systems. Channel widths were on the order of 50 nm.

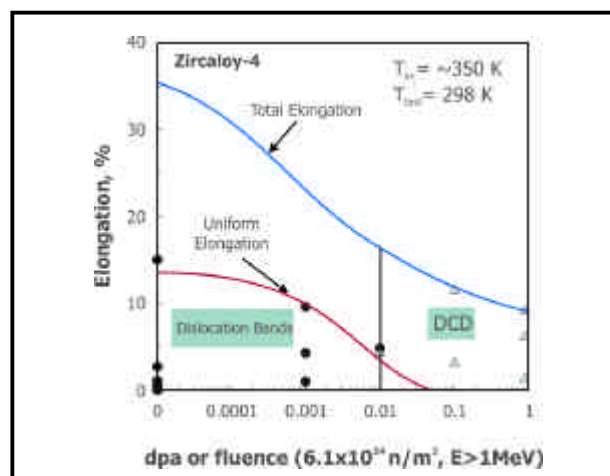


Figure 2. The graph is a deformation mode map for Zircaloy-4 neutron-irradiated at 65°C-100°C and tested at room temperature.

The austenitic 316 stainless steel, which has a face-centered cubic lattice and low stacking fault energy, behaved quite differently from the other two alloys. It displayed a similar degree of radiation hardening as the A533B steel, yet it retained substantial work-hardening and uniform elongation at all doses. In its unirradiated condition, and at the two lowest fluences, where no RDS was visible, it deformed by planar slip on its $\{111\} \langle 110 \rangle$ slip systems (Figure 3). As the level of strain was increased, the slip bands became more pronounced and tangled dislocations appeared in the matrix between the bands. Streaks from fine twins appeared in electron diffraction patterns. Dark field microscopy revealed that the twins were located within the deformation bands. At an irradiation dose of 0.01 dpa, some black spot RDS was found, but the deformation mode was not altered. For the two highest doses, where black spot-type RDS was strong, dislocation channels were cleared through the RDS

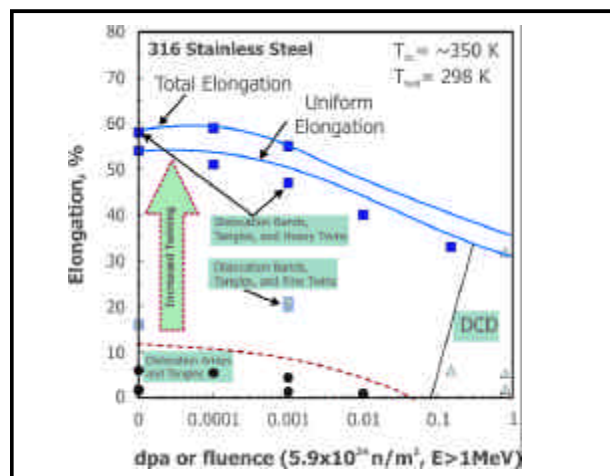


Figure 3. The graph is a deformation mode map for 316 austenitic stainless steel neutron-irradiated at 65°C-100°C and tested at room temperature.

primarily on the easy slip systems. In specimens irradiated to 0.1 dpa, most of the channels were superimposed on the dislocation bands; there were also some very narrow channels containing neither dislocations nor twins. At the highest dose, where the black spot concentration was $4 \times 10^{23} \text{ m}^{-3}$ with a mean size of 1.8 nm, the dislocation bands and microtwins and channels were superimposed in the deformation bands and were very pronounced. Channel widths were about 20 nm. With increasing strain, the blocks of material between the heavy channel bands became subdivided into smaller blocks by development of new channel bands.

The deformation behavior of austenitic stainless steel is different from the other two alloys. Even in its unirradiated condition it deforms in a planar manner. After irradiation, when channels form they are not devoid of dislocations as in the other two alloys. They contain extended dislocations with stacking fault ribbons that are overlapped to form microtwins. Of the three alloys investigated here, the stainless steel has the narrowest channels at a given dose and it is the most resistant to necking. It is suggested that the presence of stacking faults and microtwins in the channels moderates the behavior of glide dislocations in the channels and helps retain some work hardening in the channels, thereby reducing the concentrations of stress and strain in the channels and delaying necking.

Analyses of the fluence (ϕt) dependencies of the increases in tensile yield strengths (ΔYS) for all three alloys were made in terms of the relationship $\Delta YS \propto (\phi t)^n$. Values of the radiation hardening exponent, n , were in the range 0.36-0.38 for fluences up to $6 \times 10^{23} \text{ nm}^{-2}$ (0.1 dpa). Saturation in hardening was noted at higher fluences and was concurrent with acceleration of gross strain localization.

The final phase of the project (Year 3) switched the deformation mapping emphasis to an elevated temperature and higher strain rate. In Years 1 and 2, the irradiations were made at 65°C-100°C and the tensile tests were conducted at a strain rate of 10^{-3} s^{-1} at room temperature. For Year 3, the research focused on an irradiation and test temperature of approximately 300°C, and a strain rate of 10^{-1} to 1.0 per second. Therefore, new irradiations were made in the HFIR hydraulic tube irradiation facility. A new tensile irradiation capsule was designed to accommodate 14 miniature tensile specimens of each of the three alloys, with a specimen irradiation design temperature of 300°C. The specimens were irradiated to doses of 0.01, 0.1, and 0.8 dpa in March

2002. When the specimens were tensile tested the amount of radiation hardening was considerably less than expected. For the goal irradiation and test temperature of 300°C, published data indicate that a dose of 0.01 dpa should raise the tensile yield strength of annealed stainless steel by about 170 MPa. In the present tests no increase in yield strength was found for the stainless steel and the A533B steel, and only a small increase was discerned in Zircaloy-4. Tests conducted at high strain rates of 100 s^{-1} at 288°C, and further tests made at room temperature, showed no significant effects of irradiation on the tensile properties. No radiation damage microstructure and no dislocation channeling were found in TEM of the tested specimens.

Radioactivity readings on the specimens were consistent with their goal neutron exposures. The conclusion is that the temperatures of the specimen in these uninstrumented capsules during irradiation exceeded the goal level and were too high for significant radiation hardening to occur for the investigated damage levels. Postirradiation measurements on passive SiC temperature monitors included in the irradiation capsules indicate that the specimen temperatures were probably in the range 350°C-400°C. This is consistent with sparse literature results showing that the temperatures at which self-annealing of radiation damage will occur during irradiation are 350°C-400°C for the three alloys. Investigation of the cause of overheating during irradiation has focused on two potential culprits: an error in the thermal/hydraulics calculations used to design the internal configuration of the capsule, and unusually low readings of coolant water flow noted in the hydraulic tube system since the reactor cycle in which the capsules were irradiated. Reanalysis of the capsule thermal/hydraulics calculations indicates that the original design had sufficient leeway to allow the specimen irradiation temperature to reach 20°C-30°C higher than desired. Thermal/hydraulics calculations for the low flow condition indicate that the specimen temperature could have increased by approximately 60°C compared to the standard flow condition. The question of reduced coolant flow rate will not be resolved until January 2003 when new flow gauges will be installed in the hydraulic tube irradiation facility. Although these Year 3 results are disappointing for the program goals, they do provide valuable information for irradiation temperature and dose regimes where very little data currently exist; they demonstrate that the upper temperature limit of radiation damage and radiation hardening in these materials at modest neutron doses is only about 350°C.

Planned Activities

The NERI Project has been completed.

NUCLEAR ENERGY RESEARCH INITIATIVE

A Novel Approach to Materials Development for Advanced Reactor Systems

Primary Investigator: Gary S. Was, University of Michigan

Project Number: 99-101

Collaborators: Pacific Northwest National Laboratory, Oak Ridge National Laboratory

Project Start Date: September 1999

Project End Date: August 2002

Research Objectives

Component degradation by irradiation is a primary concern in current reactor systems as well as in future reactors with advanced designs and concepts where the demand for higher efficiency and performance will be considerably greater. In advanced reactor systems, core components will be expected to operate under increasingly hostile conditions (temperature, pressure, radiation flux, dose, and other parameters). The current strategy for assessing radiation effects in order to develop new reactor materials is impractical because the costs and time required to conduct reactor irradiations are becoming increasingly prohibitive, and the facilities for conducting these irradiations are becoming increasingly scarce. Although the next-generation reactors will be designed for more extreme conditions, the capability for assessing materials is significantly weaker than it was 20 years ago. Short of building new test reactors, advanced tools and capabilities are needed now for studying radiation damage in materials that can keep pace with design development requirements.

The most successful of these irradiation tools has been high-energy (several MeV) proton irradiation. Proton irradiation to several tens of displacements per atom (dpa) can be conducted in a short amount of time (weeks), with relatively inexpensive accelerators, and result in negligible residual radioactivity. Together, these factors provide a radiation damage assessment tool that reduces the time and cost to develop and gauge reactor materials by factors of 10 to 100. What remains to be accomplished is the application of this tool to specific materials problems and the extension of the technique to a wider range of problems in preparation for developing and assessing advanced reactor materials.

The objective of this project is to identify the material changes following irradiation that contribute to stress

corrosion cracking (SCC) of stainless steels, embrittlement of pressure vessel steels, and physical and mechanical property changes of Zircaloy fuel cladding. Until such changes are identified, no further progress can be made on developing mitigation strategies for existing core components and radiation-resistant alloys or microstructures that are essential for the success of advanced reactor designs.

Research Progress

Progress is reported separately for the three materials under study.

Stainless Steels: A set of five hardened conditions of commercial 304SS was studied in which the level of hardening remained fixed while the contributions from irradiation and cold work varied. As illustrated in Figure 1, combinations of cold work and proton irradiation were used to achieve a fixed hardness increase of about 180 kg/mm² for a total hardness of 380 kg/mm². Proton irradiation was conducted with 3.2 MeV protons at 360°C at a rate of 7×10^{-6} dpa/s on samples that were previously cold-worked. Magnetic susceptibility tests verified the absence of martensite following cold work. The specimens were then subjected to stress corrosion cracking (SCC) tests in 288°C water, typical of normal water chemistry (NWC) in boiling water reactor (BWR) service conditions. Only the 0 percent cold work + 1.67 dpa and 10 percent cold work + 0.55 dpa samples exhibited irradiation assisted stress corrosion cracking (IASCC), despite the fact that all samples were at a near constant hardness of 380 kg/mm² (± 5 percent). All other samples failed without any evidence of intergranular (IG) cracking. This result suggests that radiation hardening, in contrast to cold working, is most important in the IASCC process.



NUCLEAR ENERGY RESEARCH INITIATIVE

Complete Numerical Simulation of Subcooled Flow Boiling in the Presence of Thermal and Chemical Interactions

Primary Investigator: Vijay K. Dhir, University of California, Los Angeles

Project Number: 99-134

Project Start Date: August 1999

Project End Date: April 2003

Research Objective

The key objective of the proposed research is to develop a mechanistic basis for the thermal and chemical interactions that occur during subcooled boiling in the reactor core. The axial offset anomalies (AOA) are influenced by local heat flux for subcooled nucleate boiling, the nucleation site density on the fuel cladding, and the concentration of boron and lithium in the primary coolant. The approach proposed in this work is very different from that employed in the past, in that complete numerical simulations of the boiling process are to be carried out along with thermal, hydraulic, and concentration fields in the vicinity of the cladding surface. This approach is considered to be the only viable one that can provide, simultaneously, a mechanistic basis for the portioning of the wall heat flux among vapor and liquid and the concentration of boron and lithium, at, and adjacent to, the heated surface. The model is to be validated with data from detailed experiments.

A building block type of approach will be used. By starting with a bubble at a single nucleation site, the complexity of the numerical model and experiments will be increased to include merger of bubbles at the wall as well as interaction of the detached bubbles with the bubbles present on the heated surface. The concentration of boron and system pressure will be important variables of the problem.

Research Progress

Since the start of the project, both the numerical and experimental effort has been expanded to develop a mechanistic basis for thermal and chemical interactions that occur during subcooled boiling in the core of a nuclear reactor. The numerical effort has so far been focused on a single vapor bubble in either pool or flow boiling. In carrying out the numerical simulations, the conservation equations of mass, momentum, and energy

for the two phases along with the conservation of species equation for chemicals present in water have been solved simultaneously. The level set method is used in the numerical simulation. The results of numerical simulation using orthoboric acid as the chemical species present in water reveal that during growth and departure phases of a bubble, the concentration of orthoboric acid varies both spatially and temporally. The highest concentration occurs adjacent to the vapor liquid interface. In regions very close to the wall, this concentration can exceed the solubility limit. In flow boiling, the bubbles are found to slide along the surface before lift-off. The bubble growth continues from departure of the bubble from the cavity to lift-off.

An experimental apparatus for the flow boiling studies has been developed and experiments using silicon strips made from a polished silicon wafer with a microfabricated cavity have been performed. The strips are heated with strain gage heaters that are bonded on the back side. To measure the transient concentration of boron during the bubble evolution, a special probe was developed. Figure 1 shows the measured concentration as a function of distance from the interface when the liquid pool had a boron concentration of 3,000 ppm. Consistent with numerical predictions, the highest concentration occurs near the vapor-liquid interface and decreases with increased distance from the interface. However, the highest concentration observed experimentally near the interface is smaller than that predicted from numerical simulation. One reason for the difference is that the probe yields a concentration that is averaged over a larger volume than calculated through the computations. Plate-out of boron on the silicon surface in the vicinity of a single nucleation site after three hours of subcooled boiling is shown in Figure 2. The plate-out is off-center of the cavity because of the asymmetric growth of the bubble under flow boiling conditions. Most of the plate-out

occurs because of evaporation in the microlayer underneath the bubble.

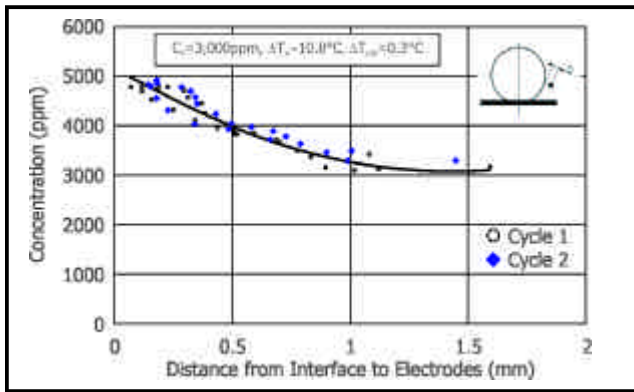


Figure 1. The graph illustrates the measured concentration vs. distance from interface to electrodes.

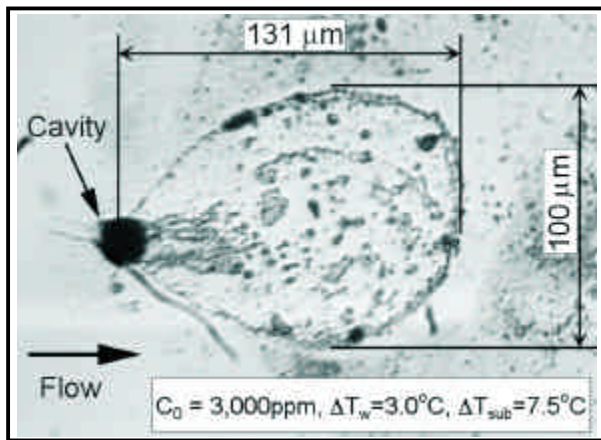


Figure 2. The photo shows boron deposition in subcooled boiling.

Experiments with boron in water were also carried out on a 9 rod bundle. It was found that with 7,000 ppm of boron in the solution, boron crud on the zircalloy cladding was found to reach a thickness of about 30 μm , after 12 hours of boiling on the surface. Because of increased nucleation site density with boron deposits on the cladding, nucleate boiling heat transfer was higher than that on a clean surface. The single phase heat coefficient, however, was lower because of additional thermal resistance of the crud.

A paper based on numerical work was presented at the 2001 IMECE conference; another paper documenting experimental work will be presented at the 2002 IMECE.

Planned Activities

During the remaining period of the project life, effort will be expanded to carry out numerical simulations of flow boiling with boron. The numerical simulations will be carried out for a range of subcoolings in which bubbles either remain attached to the surface or slide and lift off from the surface. For both cases, the possible plate-out of boron on the solid surface will be quantified. The experimental effort will be expanded to determine the thickness of the boron crust on the test surface and a comparison will be made of the predictions from numerical simulations with the data.

NUCLEAR ENERGY RESEARCH INITIATIVE

Developing Improved Reactor Structural Materials Using Proton Irradiation as a Rapid Analysis Tool

Primary Investigator: Todd R. Allen, Argonne National Laboratory-West

Project Number: 99-155

Collaborators: University of Michigan

Project Start Date: August 1999

Project End Date: March 2003

Research Objective

The overall goal of the project is to develop austenitic stainless steel structural materials with enhanced radiation resistance. For this project, the term "radiation resistance" is being used to describe resistance to dimensional changes caused by void swelling and resistance to material failures caused by irradiation-assisted stress corrosion cracking (IASCC). IASCC has been linked to both hardening and changes in grain boundary composition during irradiation. To achieve such enhanced radiation resistance, three experimental paths have been chosen: bulk composition engineering, grain boundary composition engineering, and grain boundary structural engineering. The program involves the use of high-energy proton irradiation as a rapid screening tool to systematically test combinations of alloy composition and thermomechanical treatment conditions to isolate the controlling mechanisms and develop an understanding of how these factors can be engineered to improve material properties.

The alloys chosen for the study have been modeled after commercially available grades of stainless steel commonly used in reactor applications. The model alloys include the following nominal compositions: Fe-18Cr-8Ni-1.75Mn (base 304), Fe-18Cr-40Ni-1.25Mn (Base 330), Fe-18Cr-9.5Ni-1.25Mn + Zr additions (Base 304 + Zr), Fe-16Cr-13Ni-1.25Mn (Base 316), Fe-16Cr-13Ni-1.25Mn + Mo (Base 316 + Mo), Fe-16Cr-13Ni-1.25Mn + Mo + P (Base 316 + Mo + P). Each of the alloying additions was chosen for a specific purpose. Fe-18Cr-40Ni-1.25Mn was chosen because higher bulk nickel concentration is known to reduce swelling, but its effect on IASCC is unknown. Fe-18Cr-8Ni-1.25Mn+Zr alloys were chosen because Zr is an oversized element that might trap point defects and prevent swelling, grain boundary segregation, and other radiation damage. Fe-16Cr-13Ni-1.25Mn, Fe-16Cr-13Ni-1.25Mn+Mo, and Fe-16Cr-13Ni-1.25Mn+Mo+P were chosen to determine why 316 stainless steel is more

resistant to swelling and IASCC than 304 stainless steel. The alloys are naturally classified in three groups: the "316 series" (Fe-16Cr-13Ni-1.25Mn, Fe-16Cr-13Ni-1.25Mn+Mo, and Fe-16Cr-13Ni-1.25Mn+Mo+P), the "Zr series" (Fe-18Cr-8Ni-1.75Mn and Fe-18Cr-8Ni-1.75Mn+Zr), and the "Ni-series" (Fe-18Cr-8Ni-1.75Mn, Fe-16Cr-13Ni-1.25Mn, and Fe-18Cr-40Ni-1.25Mn).

Research Progress

In the first year of the project, the bulk composition engineering path was emphasized. Fe-18Cr-8Ni-1.25Mn, Fe-18Cr-40Ni-1.25Mn, Fe-18Cr-8Ni-1.25Mn+Zr, and Fe-16Cr-13Ni-1.25Mn were studied to determine the effect of bulk composition on swelling and radiation-induced segregation (RIS) at grain boundaries. Samples were irradiated using 3.2 MeV protons at 400°C to 1 displacement per atom (dpa). Swelling was characterized by measuring the void size distribution using a transmission electron microscope (TEM). Radiation-induced grain boundary segregation was measured using a field emission gun scanning transmission electron microscope (FEG-STEM). Microhardness measurements were performed on irradiated and non-irradiated alloys to estimate the effect of irradiation on strength.

Results revealed that alloys with greater bulk nickel concentration have greater RIS. They also have increased hardening and Cr depletion, theoretically making the alloy more susceptible to IASCC. Molybdenum additions did not have a significant impact on the swelling and RIS behavior of the 316 series model alloys, but the addition of phosphorus led to a substantial refinement of the dislocation microstructure, suppression of void formation, and a reduction in the extent of Cr depletion at grain boundaries.

During the second year of the project, the effect of pre-irradiation heat treatments on thermal non-equilibrium

grain boundary segregation and subsequent radiation-induced grain boundary segregation in the 316 series of model austenitic stainless steels was studied as part of the grain boundary composition engineering path. The alloys were heat-treated at temperatures ranging from 1,100°C to 1,300°C and quenched using four different cooling paths (furnace cool, air cool, water quench, and ice brine quench) to evaluate the effect of annealing temperature and cooling rate on pre-irradiation grain boundary chemistry. Subsequent RIS behavior following irradiation with high-energy protons was characterized to understand the influence of alloying additions and pre-irradiation grain boundary chemistry in irradiation-induced elemental enrichment and depletion profiles. The study reveals that faster cooling rates provided by water and salt-brine

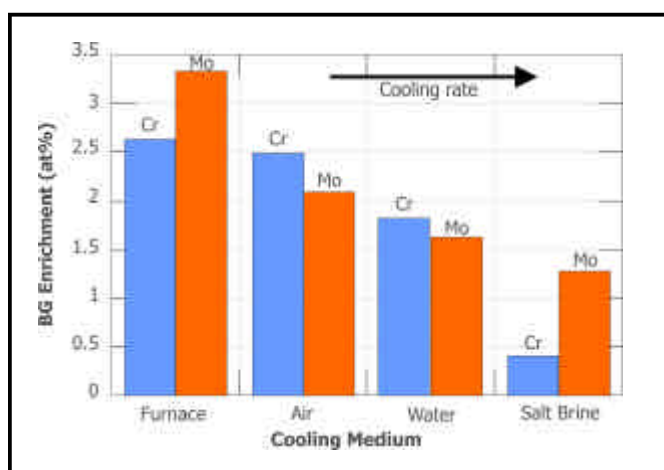


Figure 1. The figure shows the effect of cooling rate on the extent of grain boundary elemental enrichment in Fe-16Cr-13Ni + Mo + P annealed at 1,200°C for 1 hour.

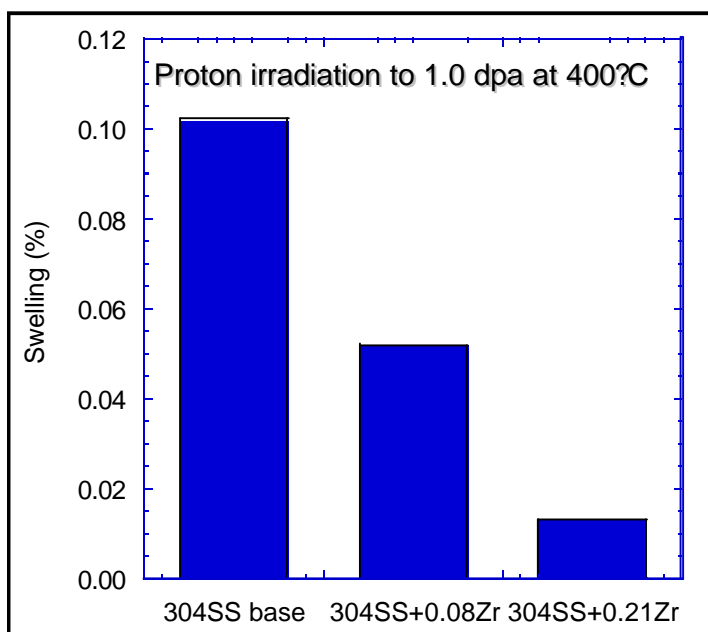


Figure 2. Increasing the Zr content in 304 stainless steel decreases the amount of void swelling

quenching resulted in moderate Cr enrichment. However, slower cooling rates provided by both air and furnace cooling led to more substantial grain boundary enrichment of Cr, and Mo, and depletion of Ni and Fe.

Figure 1 illustrates the change in Cr and Mo enrichment as a function of cooling rate. Lower annealing temperatures also tended to enhance the degree of boundary enrichment. Subsequent proton irradiation of the Fe-16Cr-13Ni + Mo alloy following heat treatments to enrich the grain boundary resulted in the formation of a W-shaped Cr segregation profile and a reduction in the extent of Cr depletion.

Formation of vacancy concentrations during higher temperature annealing and their subsequent migration to sinks during cooling is believed to be the primary process leading to the enrichment of solute species at grain boundaries. Grain boundaries act as sinks for vacancies during cooldown, and the vacancies can drag the solute and thus enrich the boundaries. Models that have been used to describe and explain this include terms for the diffusion of vacancies and vacancy solute complexes to the grain boundary and an associated back-diffusion of free solutes that limits the overall amount of segregation. However, current models do not adequately predict the subsequent segregation behavior during irradiation and the result of this study may provide additional insight into these processes.

In the third year, the radiation response in the 304 + Zr alloys and the 316 + grain boundary composition engineering samples were analyzed.

Following proton radiation, hardness was measured and microstructures were characterized. The addition of Zr decreased the hardening, reduced the swelling (figure 2), reduced the density of radiation-induced void and dislocation loops, and increased the radiation-induced grain boundary segregation. The Zr additions appear to be greater improvement in radiation resistance than the increases in nickel concentration pursued in year 1. Both treatments reduced the swelling, but the Zr-doped alloys did so with out an associated increase in hardening. The 316 plus grain boundary composition engineering delayed the Cr depletion that occurs under irradiation as compared to the non-treated samples. This treatment alone does not provide radiation resistance but may be combined with other treatments to create a more optimal situation.

Planned Activities

The NERI project has been completed.

NUCLEAR ENERGY RESEARCH INITIATIVE

An Investigation of the Mechanism of IGA/SCC of Alloy 600 in Corrosion-Accelerating Heated Crevice Environments

Primary Investigator: Jesse B. Lumsden, Rockwell Science Center

Project Number: 99-202

Project Start Date: August 1999

Project End Date: March 2003

Research Objectives

Most corrosion damage in nuclear steam generators has occurred in tubes forming the tube/tube support plate (T/TSP) crevices. Tubing in this location has experienced damage by pitting, wastage, and intergranular attack/stress corrosion cracking (IGA/SCC), caused by secondary water impurities that have concentrated in these deposit-filled crevices by a thermo-hydraulic mechanism. Crevice chemistries in an operating steam generator cannot be measured directly because of their inaccessibility. In practice, computer codes, which are based upon hypothesized chemical reactions and thermal hydraulic mechanisms, are used to predict crevice chemistry. In most cases the codes have not been benchmarked. Remedial measures for IGA/SCC in the form of water chemistry guidelines have been implemented aimed at controlling crevice chemistries. The guidelines have been formulated based on SCC tests using static autoclaves containing solutions, assumed to duplicate those found in crevices.

The objective of the Rockwell program is to provide an experimental base to benchmark crevice chemistry models, to benchmark crevice chemistry control measures designed to mitigate IGA/SCC, and to model IGA/SCC processes. The objective includes identifying important variables, including the relationship between bulk water chemistry and corrosion accelerating chemistries in a crevice. One important result will be the identification of water chemistry control measures needed to mitigate secondary side IGA/SCC in steam generator tubes. A second result will be a system, operating as a side-arm boiler, which can be used to monitor nuclear steam generator crevice chemistries and crevice chemistry conditions causing IGA/SCC.

Research Progress

The key element in the approach is a heated crevice apparatus constructed under the NERI program. This is an instrumented replica of a steam generator tube/TSP crevice and operates at simulated steam generator thermal conditions. The pressure in the autoclave containing the crevice is adjusted to give a boiling point of 280°C for the constantly refreshed feedwater. A cartridge heater inside the tube supplies a 40°C superheat, simulating the thermal conditions of the primary water. The apparatus is instrumented to monitor the electrochemical potential (ECP) of the free span, the ECP in the crevice, and the temperature in the tube wall at different elevations in the crevice. The tube is pressurized with He to provide a hoop stress. The additional capability to measure electrochemical noise (EN) monitors IGA/SCC and other corrosion processes on the tube. A schematic of the instrumented crevice and the steam generator tube/TSP replicated is shown in Figure 1. The ZRA is a zero resistance ammeter, which measures the direct current and current fluctuations between the tube and the TSP.

Several advances have been made since the initiation of this project. Using feedwater with sodium hydroxide, work in this program established that the corrosion damage to the tube in the heated crevice duplicates that observed in tubes forming the tube/TSP crevice in operating nuclear steam generators, believed to have caustic crevice solutions. This suggests that the same mechanism causes caustic IGA/SCC in steam generators and in the accelerated conditions of the heated crevice. It was also demonstrated that the relationships between ECP, crevice chemistry pH, and SCC susceptibility follow the thermodynamic/passive film stability methodology. This is of importance because computer codes for crevice

chemistry and predictive models rest on the assumption that equilibrium thermodynamics can be applied. The results in this program have established that EN detects the initiation of SCC and monitors crack propagation in Alloy 600. Finally, all results are consistent with the oxide film rupture/anodic dissolution model for IGA/SCC. An understanding of the mechanism of IGA/SCC is necessary for confidence in the success of measures implemented to control and mitigate IGA/SCC.

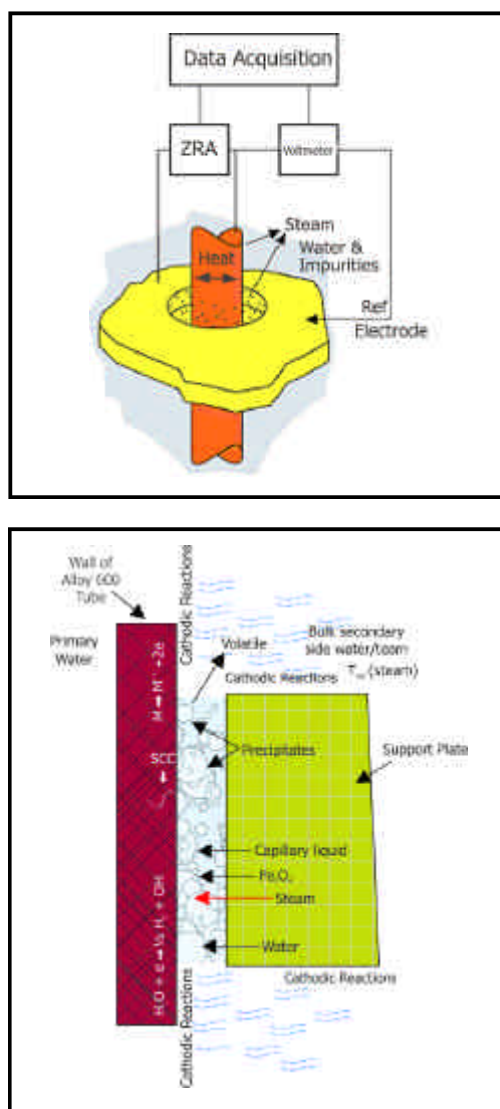


Figure 1. The schematic illustrates (top) the instrumented heated crevice and (bottom) a tube/TSP crevice in an operating pressurized water reactor (PWR) steam generator.

High alkalinity in caustic tube/TSP crevice chemistries was one of the first causes of IGA/SCC in Alloy 600 steam generator tubes in modern operating plants. Accordingly, initial work with the heated crevice investigated caustic IGA/SCC using deaerated feedwater with 40 ppm NaOH. The crevice was packed (22 percent porosity) with

magnetite powder, simulating the magnetite deposits and precipitates in the tube/TSP crevices of operating plants. Solution extraction showed that a steady-state concentration of approximately 30 percent NaOH was reached in the crevice after the tube heater was on for approximately 20 hours. These test conditions produced multiple axial cracks, one of which propagated through the wall in four to eight weeks. A destructive examination showed that the cracks were totally intergranular. The crack distribution and morphology are like that found in tubes removed from operating steam generators. An Auger electron spectroscopy analysis of areas on the fracture face showed that the surface was rich in Ni, which is in accordance with thermodynamic predictions for high pH environments. Both Ni or NiO are thermodynamically stable at high pHs, while only soluble species of the alloying metals, Cr and Fe, are thermodynamically stable at caustic conditions. Conditions of high pH lead to the selective dissolution of Cr and Fe. The same surface composition has been found on fracture faces in tubes, forming tube/TSP crevices, removed from operating steam generators believed to have had caustic crevices.

Computer codes describing crevice chemistry and models for IGA/SCC in Alloy 600 steam generator tubes are based on the assumption that equilibrium thermodynamics can be applied. One of these codes, MULTEQ, was used to determine the pH in the heated crevice using the chemistry of the extracted solution. An important result was that the pH determined by MULTEQ agreed with a calculation of the pH derived from the crevice ECP, using an expression derived from equilibrium thermodynamics. Since the results from the two approaches were equivalent, it suggests that the assumptions used in the computer code apply correctly to the conditions in steam generator crevices. Thermodynamics has been used to form a framework for a predictive model for IGA/SCC susceptibility of Alloy 600. This model hypothesizes that the film rupture/anodic dissolution mechanism is responsible for caustic cracking and that IGA/SCC occurs in a zone of pHs and ECPs. The measured value of the crevice ECP when SCC occurred in the heated crevice was well within this zone, supporting this thermodynamic-film instability model. Aggressive impurities in the magnetite deposits and feedwater shifted the "cracking zone" to lower potential values.

The EN, the random pulses of current and ECP generated during corrosion processes, detects the initiation and propagation of cracks resulting from IGA/SCC. The EN signature during SCC results from the

creation of new surface area when a crack is initiated or advances. A surge in current occurs as the new surface undergoes the electrochemical processes of dissolution and oxide film formation. The current drops rapidly as the new surface becomes covered with protective oxide. The intensity and frequency of the current and potential pulses are related to crack growth rate. Figure 2a shows typical current and potential noise pulses. Figure 2b shows the standard deviation of the current noise from a tube that developed a through-wall crack in 1,300 hours of superheat using the 40 ppm NaOH feedwater. The standard deviation is in the microampere range during the first 400 hours of the test, suggesting that this is the crack-initiation period. Crack propagation occurs between 900 hours and 1,300 hours of superheating.

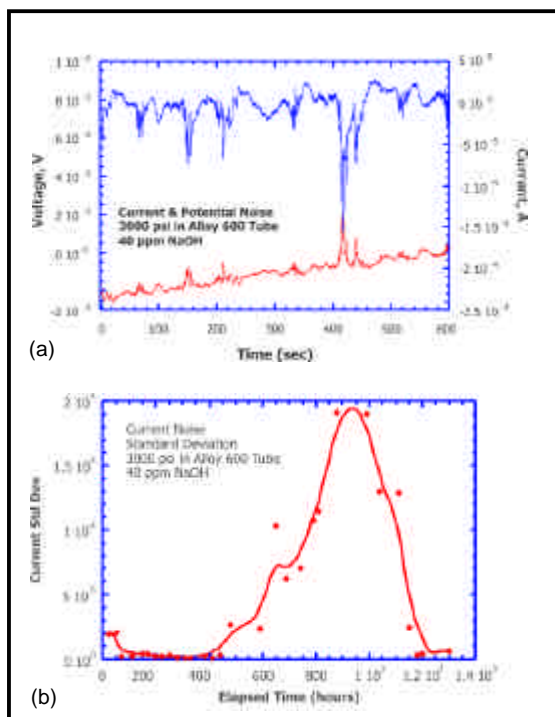


Figure 2. Graph (a) illustrates typical current and potential fluctuations during SCC, and graph (b) plots the standard deviation of the current noise during caustic SCC.

Planned Activities

The present strategy for mitigating IGA/SCC is based on the assumption that the crack initiation and propagation rate in Alloy 600 steam generator tubes, forming the tube/TSP crevices, depend only on pH and the ECP. Planned work will continue to examine the effectiveness of the present practice of adding hydrazine to the feedwater to inhibit the initiation and propagation of IGA/SCC. The hypothesized rationale for adding hydrazine is that it lowers the ECP of the crevice chemistry to a regime where IGA/SCC does not occur. Preliminary results indicate that hydrazine concentrates in the crevice, and lowers the ECP. However, the ECP values are not sufficiently low to prevent IGA/SCC. The effect of hydrazine concentration in the feedwater and pH have not yet been assessed. The pH effects will be evaluated by controlling the Na^+/Cl^- molar ratio in the feedwater. Computer codes show that the pH in the tube/TSP crevice decreases as the Na^+/Cl^- molar ratio in the feedwater decreases. Crevice chemistry and pH will be determined by chemical analysis of solutions extracted from the crevice. The measured ECP of the freespan and crevice also provide a measure of the pH of the crevice solution. The crevice chemistry results will be used to benchmark the computer codes used by utilities to calculate crevice chemistry and crevice pH. The results of this activity will also provide a preliminary indication of effectiveness of "molar ratio control" as a measure to mitigate IGA/SCC.

Signal analysis and other data analysis procedures will be developed for the EN technique. The analysis will model the transition from microcracks to macrocracks and crack propagation processes. This will enable monitoring of the steam generator crevice for the initiation and severity of IGA/SCC.

NUCLEAR ENERGY RESEARCH INITIATIVE

Interfacial Transport Phenomena and Stability in Molten Metal-Water Systems

Primary Investigator: M. Corradini, University of Wisconsin-Madison (UW)

Collaborators: Argonne National Laboratory (ANL)

Project Number: 99-233

Project Start Date: August 1999

Project End Date: September 2002

Research Objectives

A concept being considered for steam generation in innovative nuclear reactor applications involves water coming into direct contact with a circulating molten metal. The vigorous agitation of the two fluids, the direct liquid-liquid contact, and the consequent large interfacial area give rise to very high heat transfer coefficients and rapid steam generation. For an optimal design of such direct-contact heat exchange and vaporization systems, more detailed knowledge is needed relative to the various flow regimes, interfacial transport heat transfer coefficients, and operational stability under reactor-relevant operating conditions. This research project is studying the transport phenomena involved with the injection of water into molten metals (e.g., lead alloys), with the following objectives:

- Design, fabricate, and operate experimental apparatuses that investigate molten metal-water interactions under prototypic thermal-hydraulic conditions,
- Measure the integral behavior of such interactions to determine the flow regime behavior for a range of conditions and stability of these flow regimes,
- Measure the local interfacial mass and heat transfer behavior to ascertain the interfacial area concentration and heat transport length and time scales, and
- Analyze test results to determine an envelope of operating conditions that yields optimal energy transfer between molten metal and water and maximizes stability.

Research Progress

A comprehensive review of pertinent past

experimental investigations has been completed, and new experimental data gained by using different fluid combinations has been compared to some of the past experiments. Two pre-doctoral students and several undergraduate students at the University of Wisconsin - Madison (UW) and two visiting students at Argonne National Laboratory (ANL), working with several scientists and staff at the laboratory, have been instrumental in the fabrication of two large complimentary experimental apparatuses (one at ANL and one at UW). These devices, one of which is illustrated in Figure 1, facilitate the direct contact of water with molten liquid metals, making it possible to carry out detailed studies of the heat transfer and void fraction.



Figure 1. Photograph of liquid metal direct contact heat exchanger facility at the University of Wisconsin - Madison. Tests are conducted with 70 cm of liquid metal in the test section and water injection from 1-10g/s. The facility is capable of running at pressures up to 10bar with liquid metal temperatures at 500°C.

While the two facilities share a common goal, they were designed to provide mutually complementary information. The ANL experiments focus on the heat

transfer and flow stability behavior of water injected into molten metal and provide measurements on the evaporation zone length and associated volumetric heat transfer coefficients. The UW experiments focus on two-dimensional mixing behavior and provide real-time X-ray imaging of the multiphase structure of vaporizing water in the molten metal, and have been able to obtain the first of a kind estimates of local average heat transfer coefficients for the compact heat exchanger.

Current experimental results have been discussed during weekly conference calls and several visits among laboratory researchers, resulting in an increased understanding of the physics involved in the direct contact heat transfer between a continuous phase hot liquid at temperatures well above the saturation point of a dispersal injected second liquid. Figure 2 depicts an example of a single frame of high-speed X-ray movies of the void distribution that were obtained with a high-energy X-ray system. The real time X-ray images of this flow allowed the first of its kind measurement of the bubble production time, the bubble rise velocity, and the vaporization rate of water being injected into a high-temperature ($T < 400^\circ\text{C}$) liquid metal pool. These measurements also allowed an estimate of the average local heat transfer coefficient for the vaporization of water in the region just above the nozzle for several different system pressures, injection temperatures, and injection flow rates (Figure 3).

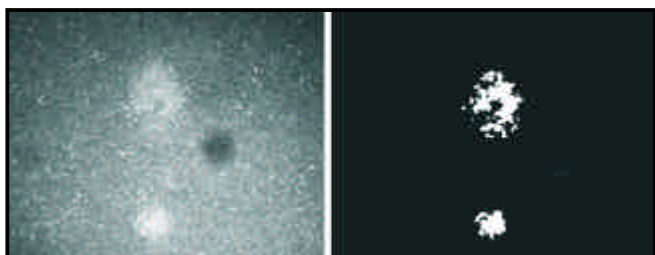


Figure 2. Single frame image of a high-speed movie taken at 100/fps shows water being injected into a liquid metal pool at 500°C . The left image shows a raw image of the bubble formation and evaporation of the water droplets. The right image show the individual bubbles after some image processing. These images can then be analyzed with the aid of a calibration file to determine the local void fraction. From the change in the void fraction the local heat transfer coefficient can be estimated.

The research results from ANL and the UW will constitute a significant database of volumetric heat transfer coefficients and void distribution data associated with direct contact heat transfer, which will aid in the design of advanced heat exchangers for future power

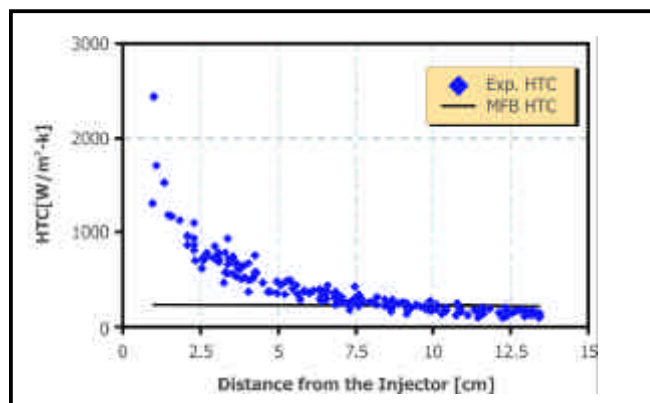


Figure 3. Local average heat transfer coefficients for injection of water into a liquid lead pool at a rate of 1.7g/s at 3.17 bar . The plot shows the average local heat transfer coefficient as a function distance above the water injection nozzle. Above a height of approximately 15 cm , the individual bubbles break up and it is no longer possible to estimate the local heat transfer coefficient. As can be seen, the average heat transfer coefficient approaches the minimum film boiling heat transfer limit (MFB).

reactor designs. The complete set of data from the 1-D and 2-D experiments is currently being assembled for publication in the final research report. The results can be summarized as follows:

- (1) Both experiments have obtained similar measurements of the volumetric heat transfer coefficients (in the range of $10\text{ to }20\text{ kW/m}^3$).
- (2) This heat transfer rate seems to occur when the injected water is in film boiling within the molten metal pool.
- (3) Flow oscillations have been observed at the lower ambient pressures ($1\text{ to }2\text{ bars}$) for water injection into the molten metal pool and can be suppressed as the system pressure is increased and to a lesser extent if the water flow is decreased or its temperature approaches saturation.
- (4) Dynamic X-ray imaging and associated image reconstruction has allowed measurement of the local void fraction and estimates of the associated local heat transfer coefficients (Figures 2 and 3). These results indicate that the flow regime is bubbly flow with a transition to churn flow at lower pressures. In addition, the local heat transfer coefficient is similar to what may be expected during film boiling heat transfer.

Planned Activities

The NERI project has been completed.

NUCLEAR ENERGY RESEARCH INITIATIVE

Fundamental Thermal Fluid Physics of High Temperature Flows in Advanced Reactor Systems

Primary Investigator: Donald M. McEligot, Idaho National Engineering and Environmental Laboratory (INEEL)

Collaborators: Iowa State University; University of Maryland; General Atomics; University of Manchester, England; University of Montenegro, Yugoslavia; Kyoto University, Japan; Tokyo University of Science, Japan; Commissariat à l'Energie Atomique (CEA), France

Project Number: 99-254

Project Start Date: August 1999

Project End Date: December 2002

Research Objectives

This project is a collaborative effort among researchers from laboratories, universities, and industry that couples computational and experimental studies while addressing fundamental science and engineering issues related to new and advanced reactor designs to improve the performance, efficiency, reliability, and enhanced safety of the new reactors, while also reducing their cost and waste levels. This research will provide knowledge in basic thermal fluid science to develop an increased understanding of the behavior of fluid systems at high temperatures, in the application and improvement of modern computation and modeling methods, and in the incorporation of enhanced safety features for nuclear plants. The project promotes, maintains, and extends the nuclear science and engineering base to meet future technical challenges in design and operation of high efficiency and low output reactors, and nuclear plant safety.

INEEL's unique Matched-Index-of-Refraction (MIR) flow system, the world's largest facility of this type, is being applied to obtain, for the first time, fundamental data on flows through complex geometries important in the design and safety analyses of advanced reactors. Successful completion of the study will provide the following new basic science and engineering knowledge:

- Time-resolved data plus flow visualization of turbulent and laminarizing phenomena in accelerated flow around obstructions (spacer ribs) in annuli.
- Application of Direct Numerical Simulation (DNS) and Large Eddy Simulation (LES) for the first time to

complex turbulent flows with gas property variation occurring in advanced reactors.

- Fundamental data of internal turbulence distributions for assessment and guidance of Computational Thermal Fluid Dynamic (CFD) codes proposed for advanced gas cooled reactor applications.

Research Progress

Progress has been on the six tasks:

Heat transfer and fluid flow in advanced reactors: Six areas of thermal hydraulic phenomena have been identified in which the application of CFD techniques can improve the safety of advanced gas cooled reactors. Selection of commercially available CFD codes capable of simulating flows through complicated geometries with large variations of fluid properties has been initiated.

Complex flow measurements: Experimental models were developed for laser Doppler velocimeter (LDV) measurements in the MIR flow system to examine flow in complex core geometries (ribbed annular cooling channels and control rod configurations) and in the transition from cooling channels to formation of jets issuing into a plenum. The initial model was a ribbed annulus forming an annular jet exhausting into the MIR flow system. LDV measurements with this model were completed and were compared to predictions from a commercial CFD code. A second model—a quartz and plastic model that was shown in the 2001 Annual Report—has been fabricated and was assembled in a mockup of the MIR test section. Measurements by LDV and flow visualization have been completed and documented; they are now being analyzed.

DNS development: DNS of laminarizing gas flow and sub-turbulent gas flows have been completed. The turbulent case has been initiated.

LES development: LES results have been obtained for vertical upward flow of air in a channel heated on one side and cooled on another; such a channel flow corresponds closely to the flow in an annular passage with a large radius ratio. This work is the first known LES study of a vertical flow accounting for buoyancy and variations in fluid properties. Work continues on LES codes for heated pipes (Figure 1) and annuli with gas property variation and buoyancy effects. Simulation of flows in annuli with spacer ribs has been initiated. Predictions are in process for comparison to mixed convection measurements in a large rectangular channel at CEA in Grenoble.

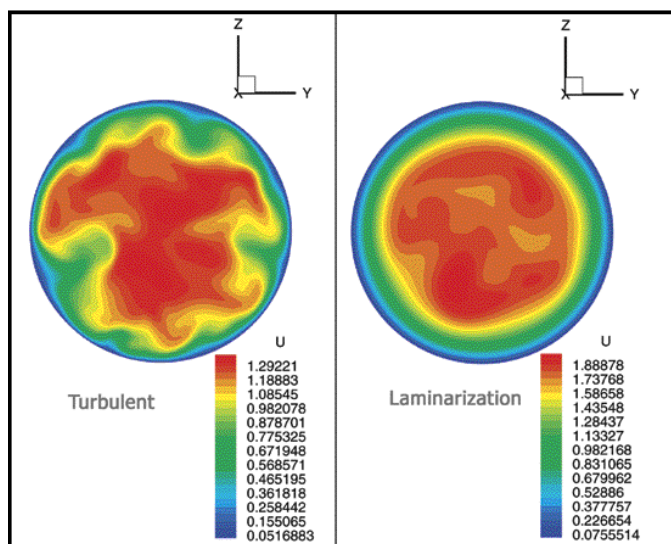


Figure 1. The figure shows large eddy simulations (LES) of strongly-heated gas flow in a vertical tube with buoyancy effects and fluid property variation. Streamwise velocity contours are shown (left = turbulent flow; right = same flow at higher heating rate, causing apparent laminarization, i.e., reduction in turbulent transport).

Miniaturized multi-sensor probe development: Several probes with three and four sensors were developed for application in gases over a velocity range of 0.5 to 15 m/s at temperatures from room temperature to about 1,000K. Three probes were fabricated with three sensors each (one cold-wire, two hot-wires), fitting within a volume of about one mm in diameter. A detailed examination has been conducted of a final probe capable of simultaneous measurement of two velocity components and of temperature in a heated turbulent gas flow, and this probe has been employed in a heated turbulent gas flow in a pipe.

Mixed convection: Data have been obtained to examine the effects of buoyancy forces on heated vertical flows in a pipe, annuli, and a wide rectangular channel. Measurements include mean velocity, temperature, and turbulence profiles as well as wall heat transfer coefficients. These results have been compared to predictions of a research code using a popular turbulence model.

Planned Activities

In the area of LES development, code development will continue and data comparisons will be made. Calibration procedures and algorithms will be compared and improved, particularly for low velocities. Efforts in mixed convection will include completion of the analysis and documentation of the effects of buoyancy on the turbulent flow of water in a vertical annulus with a heated core. The final technical report will be completed, presenting the key results of all tasks.

NUCLEAR ENERGY RESEARCH INITIATIVE

An Innovative Reactor Analysis Methodology Based on a Quasidiffusion Nodal Core Model

Primary Investigator: Dmitriy Y. Anistratov, North Carolina State University

Project Number: 99-269

Collaborators: Texas A&M University; Oregon State University; Studsvik Scanpower, Inc.

Project Start Date: August 1999

Project End Date: December 2002

Research Objectives

The present generation of reactor analysis methods uses few-group nodal diffusion approximations to calculate full-core eigenvalues and power distributions. The cross sections, diffusion coefficients, and discontinuity factors (collectively called "group constants") in the nodal diffusion equations are parameterized as functions of many variables, ranging from the obvious (temperature, boron concentration, and so forth) to the more obscure (spectral index, moderator temperature history, and so forth). These group constants, and their variations as functions of the many variables, are calculated by assembly-level transport codes.

The current methodology has two primary weaknesses that this project will address. The first weakness is the diffusion approximation in the full-core calculation; this can be significantly inaccurate at interfaces between different assemblies. This project will use the nodal diffusion framework to implement nodal quasidiffusion equations, which can capture transport effects to an arbitrary degree of accuracy. The second weakness is in the parameterization of the group constants; current models do not always perform well, especially at interfaces between unlike assemblies. Researchers will develop a theoretical foundation for current models and use that theory to devise improved models. The new models will be extended to tabulate information that the nodal quasidiffusion equations can use to capture transport effects in full-core calculations.

Research Progress

Progress made on various tasks will be discussed in turn.

Homogenization Methodology for the Low-Order Equations of the Quasidiffusion (QD) Method: A coarse-mesh

discretization of the low-order QD (LOQD) equations (Gol'din 1964) was developed that is consistent with the given fine-mesh differencing method for the LOQD equations. It is consistent in the sense that it preserves average values of the fine-mesh scalar flux over the given coarse cells as well as reaction rates, the first and second spatial Legendre moments of the fine-mesh scalar flux over coarse intervals, currents at edges of coarse cells, and the fine-mesh multiplication factor (Anistratov 2002). All these facts are rigorous mathematical results. The definition of discontinuity factors has been derived. The resulting discretization scheme enables one to approximate accurately the large-scale behavior of the transport solution within assemblies. The results from the test problems are extremely encouraging: the coarse-mesh scalar fluxes almost perfectly match every fine-mesh pin-cell average flux, in both the fast and thermal groups.

The developed method can be applied to a general transport method as well, if this method preserves the particle balance. If a fine-mesh solution is obtained directly from a transport differencing method, and it is used to calculate spatially averaged cross sections and special functionals defined in the method, the resulting coarse-mesh solution of the LOQD equations will be consistent with the given transport method. The reason is that the coarse-mesh scheme was derived by algebraically consistent discretization based on the discrete particle balance equation and, thus, this scheme works also for any transport method whose solution satisfies the discrete balance equation.

The developed coarse-mesh algorithm can be coupled with other parts of a complete reactor analysis methodology (e.g., generation of tables of constants, interpolation using tables, pin-power reconstruction).

Improved Boundary Conditions for Assembly-Level Transport Codes: An extension of present-day reactor-

analysis methodology was developed that systematically accounts for the effects that different neighbors have on a given assembly's few-group constants (Clarno and Adams 2002). The new technique centers on energy- and angle-dependent albedos that simulate the effect of the unlike neighbors. Each set of albedos defines a branch case and therefore fits into the framework of present-day methodology. The parameter varied in each new branch case is the fractional difference in the neighbor's concentration of an isotope or mixture. (The base case corresponds to a zero difference in all concentrations—an identical neighbor—which produces the usual reflecting boundary condition.) The key simplification is that the albedos are generated by a one-dimensional transport calculation with an homogenized assembly and homogenized neighbor.

The albedo produced from 1D homogenized (1DH) calculations was found to do an extremely good job of capturing the effects of different neighbors in the rather restricted case of lattices that are uniform in one direction (in which the only large-scale variation is in the other direction). In fully 2D problems, the 1DH albedos are accurate near the center of an interface but in general lose accuracy at corners. This loss of accuracy in the albedo produces large errors in corner-pin powers in the worst cases. Very simple modifications to the 1DH albedos have been found to dramatically reduce these large errors. This encouraging result has led the team to pursue systematic (but simple) modifications that are theoretically sound and that produce very accurate results.

The team's complete methodology relies on albedos to estimate the changes in few-group parameters that are induced by differences in a neighboring assembly's composition. Another part of the methodology is to assume superposition and thus build the change in a parameter by summing the partial changes from a variety of differences in a neighbor's composition.

Numerical Method for Solving 2D QD Low-Order

Equations: The polynomial-analytic nodal method of Palmtag (1997) was successfully adapted to the solution of the QDLO equations, and the methodology was tested on problems with constant nodal properties (cross sections and Eddington tensor). The QDLO equations are solved for several diffusion test problems (diagonal Eddington tensor with diagonal entries equal to $1/3$), and "transport" problems (Eddington tensor with diagonal entries different from one-third and zero or positive off-diagonal

components). Several single-node test problems were solved and have reproduced known analytic solutions. A series of two-node MOX-UO₂ interface diffusion problems were also solved, and results were compared with reference values and to those calculated by Palmtag (1997). In a representative problem [UO₂ (3 percent enriched)-MOX (12 percent enriched)], the fast flux is higher in the MOX assembly, due to its higher fission cross sections. The steepest variation is observed near the surface between the two assemblies, and the flux flattens as the reflecting boundaries are approached. The thermal flux varies strongly at the surface between nodes because thermal absorption is greater in the UO₂ assembly than in the MOX assembly. A variety of multi-node (2x2, 3x3 and 4x4) configurations were also solved, and the diffusion results compare favorably with those previously published in the literature.

The transport problems that were solved involve Eddington tensor data in a range observed in homogenized UO₂ and MOX assemblies. The increase in values of E increases leakage and therefore decreases k . To more accurately account for transport effects at interfaces between assemblies, the spatial dependence of the homogenized cross sections and Eddington tensor must be incorporated. Equations were derived for a local "correction" to the fluxes generated by the polynomial-analytic nodal method. These equations are designed to yield a zero correction if the diffusion equation adequately represents the physics of the node. If transport effects are present, these finite volume-based correction equations will capture it, to leading-order.

Planned Activities

The team believes the new methodology is promising, and plans are to continue to refine it, to couple all pieces of a full reactor-analysis system together, and to test the coupled system. This will include the homogenization procedure for 2D assembly-level calculations; method of group constants functionalization using assembly transport solution of 2D multigroup eigenvalue problem with albedo boundary conditions; and numerical method for solving equations of multidimensional coarse-mesh effective few-group nodal QD model, using tables of data parameterized with respect to a set of parameters. The full new methodology must then be compared against the existing state of the art.

NUCLEAR ENERGY RESEARCH INITIATIVE

Radiation-Induced Chemistry in High Temperature and Pressure Water and Its Role in Corrosion

Primary Investigator: David M. Bartels, Argonne National Laboratory

Project Number: 99-276

Collaborators: Atomic Energy of Canada LTD - Chalk River Laboratories

Project Start Date: August 1999

Project End Date: September 2002

Research Objectives

Commercial nuclear reactors essentially provide a source of heat that is used to drive a "heat engine" (turbine) to create electricity. A fundamental result of thermodynamics is that the higher the temperature at which any heat engine is operated, the greater its efficiency. Consequently, one obvious way to increase the operating efficiency and profitability for future nuclear power plants is to heat the water of the primary cooling loop to higher temperatures. Current pressurized water reactors (PWRs) run at roughly 300°C and 100 atmospheres of pressure. Designs under consideration would operate at 450°C and 250 atmospheres, i.e., well beyond the critical point of water. This would improve the thermodynamic efficiency by about 30 percent. A major unanswered question is, however, "What changes occur in the radiation-induced chemistry in water as the temperature and pressure are raised beyond the critical point, and what does this imply for the limiting corrosion processes in the materials of the primary cooling loop?"

The direct measurement of the chemistry in reactor cores is extremely difficult, if not impossible. The extreme conditions of high temperature, pressure, and radiation fields are not compatible with normal chemical instrumentation. There are also problems of access to fuel channels in the reactor core. For these reasons, theoretical calculations and chemical models have been used extensively by all reactor vendors and many operators, to model the detailed radiation chemistry of the water in the core and the consequences for materials. The results of these calculations and models can be no more accurate than the fundamental information fed into them, and serious discrepancies exist between current models and reactor experiments. The object of this research program is to generate the necessary radiation chemistry data (yields and reaction rates) needed to accurately model the

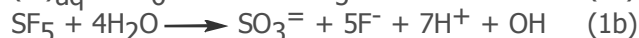
chemistry in both existing water-cooled reactors, and the higher temperature reactors proposed for the future. This will allow engineers to define the optimal chemical conditions conducive to long life for the primary heat transport system.

Research Progress

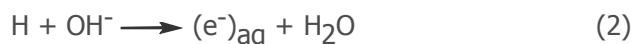
It is impossible in the space of a few pages to even briefly describe all of the results attained on reaction rate measurements in hydrothermal and supercritical water over the past two years. Instead, more details will be provided about what is likely the most important experiments carried out so far. Initial work involved building and testing a cell with which to carry out optical measurements on supercritical water. A comprehensive study of the solvated electron absorption spectrum was carried out, because that is the largest optical absorption available to probe the kinetics of the system. A study was conducted of the reaction of O₂ with solvated electrons, as described in the first year report. The kinetics of SF₆⁻ saturated solutions were measured as described below. The reaction rate of hydrated electrons with perchloric acid was briefly studied, as was the reaction with sodium nitrite and sodium nitrate scavengers. An apparatus was built for high pressure saturation of water with H₂ gas. Using this apparatus, measurements of the self-recombination of hydrated electrons were carried out in 100-bar-H₂-saturated alkaline water. An extensive series of measurements of nitrobenzene scavenging was carried out; both the reaction with hydrated electrons and the reaction with OH radical were studied. Using the hydroxynitrobenzyl radical absorption as a probe, the reaction rate of OH with H₂ has now been measured up to 350°C.

The reaction rate of solvated electrons with SF₆ was investigated, because SF₆ is to be used to measure the

radiolytic yields of solvated electrons. The reaction(s) can be written



The reaction is very specific for hydrated electrons, and tests have shown there is no decomposition of the SF_6 under supercritical water conditions. The fluoride ion product can be conveniently measured with ion chromatography. Because acid is a product of the hydrolysis reaction (1b), it was thought prudent to make measurements in alkaline solution to prevent any reaction of electrons with the product acid. In neutral solution, addition of SF_6 shortened the electron lifetime, and the signal quickly went to baseline. In alkaline solution, addition of the SF_6 accelerates the electron decay at short times, but the signal does not decay to baseline. The signal decays with a second exponential time constant which is independent of the SF_6 concentration, but proportional to the hydroxide concentration. The long decay component results from the delayed formation of electrons in the reaction



The rate constants for both reaction (1a) and (2) can be extracted from the biexponential kinetics as a function of temperature and pressure (density). The rate constants determined above the critical temperature at 380°C are plotted against density in Figure 1, along with the rate constants for electron reaction with O_2 . It is apparent that all three reactions have exactly the same dependence on the density, even though reaction (2) is an order of

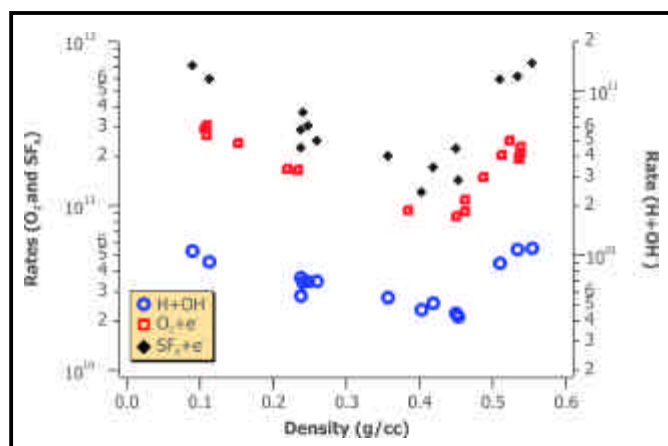


Figure 1. The graphic shows reaction rates for three reactions in supercritical water at 380°C, as a function of the water density. A minimum is seen at about 0.45 gm/cc .

magnitude slower. The only apparent similarity in all three reactions is that a hydrophobic molecule or atom (O_2 , SF_6 , or H) reacts with an anion. It is postulated that this results from a potential of mean force that develops between any hydrophobic species and any charged species in the compressible fluid at intermediate densities. It becomes clear that the radiation induced chemistry in any supercritical-water-cooled-reactor may be very different at the inlet and the outlet of the core.

The detection of reaction (2) in these experiments was a surprise because at lower temperatures the yield of H atom is much smaller than that of electrons. In Figure 2 the ratio $G(H)/G(e^-)$ of the initial radiolytic yields of H atoms and electrons is plotted against the density of the water in various temperature regimes. It is clear that as the density decreases, the H atom becomes favored over the solvated electron. This is ascribed in large part to very fast recombinations of electrons and protons (giving H) at the lower densities, where the enormous reduction in dielectric constant enhances the coulombic attraction. This experimental result shows that H atom chemistry will be much more important in a supercritical water reactor than is the case for PWR water chemistry.

Nitrobenzene was studied to provide a light-absorbing competition partner for other OH radical reactions. The most important of these is the reaction



of OH with H_2 , which gives a H atom and water as product. The high pressure H_2 -saturator apparatus was used to mix H_2 -saturated water with variable amounts of O_2 -saturated nitrobenzene solution. Adding the H_2

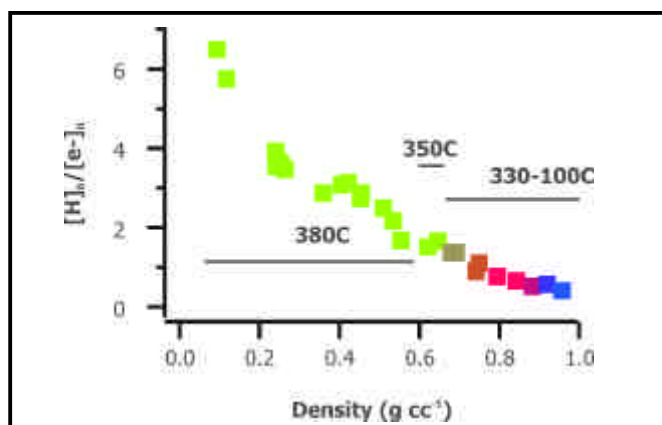


Figure 2. The figure illustrates the ratio of initial concentrations of H atoms and solvated electrons, as a function of the water density in different temperature regimes.

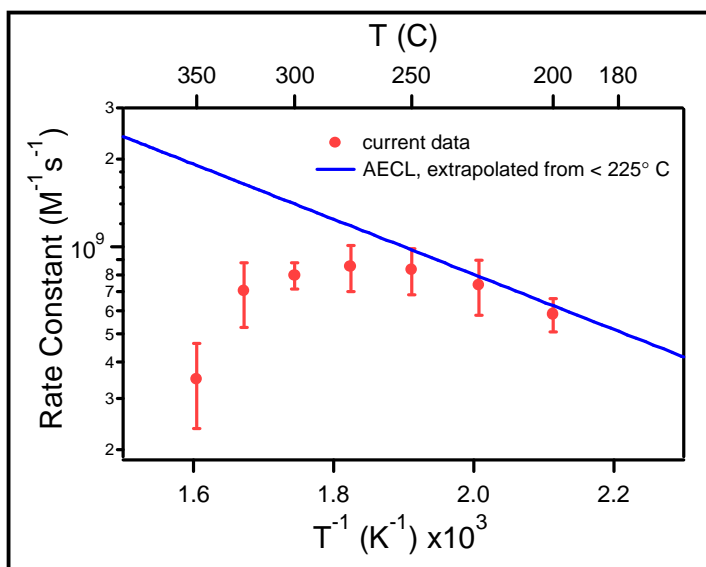


Figure 3. The graph is an Arrhenius plot for the reaction of OH with H₂.

intercepts the OH radicals that would otherwise react with nitrobenzene. From straightforward analysis of the absorption growth at 400nm, the rate of the competing reaction can be deduced. The rate constant for reaction (3) from slightly above room temperature to 350°C has now been measured. An Arrhenius plot is shown in Figure 3. The measurements are in agreement with previous work below 250°C. Researchers were astonished to discover that the rate constant for H₂ + OH reaches a maximum near 275°C, and then decreases at higher temperature. Unfortunately, the reaction becomes too slow above 350°C for the use of nitrobenzene as the absorbing competition partner. Another scavenger should permit the measurement in supercritical water.

Hydrogen is added to reactor cooling water to inhibit the radiolytic formation of oxidizing species such as O₂ and hydrogen peroxide, and to prevent the net radiolytic decomposition of water. Reaction (3) is the key step,

because the oxidizing OH radical is converted to the reducing H atom. The amount of hydrogen that is found necessary to inhibit the formation of oxidizers in reactor tests (the critical hydrogen concentration or CHC) is considerably greater than the amount that previous simulations would suggest is necessary. The new reaction-rate result (a lower reaction rate than expected) will explain much of the difference between empirical reactor tests and the predicted CHC. The primary issue is whether the reaction is sufficiently fast to suppress radiolysis in a supercritical water-cooled reactor, with reasonably low H₂ overpressure. In all probability this chemistry will still work in supercritical water, but no definitive answer can be given without further experiments.

Planned Activities

With the end of the funding for this project, it is clear that insufficient data was obtained for a comprehensive model of supercritical water radiolysis. As data for electron recombination is analyzed, a greatly improved model of radiation chemistry in liquid water up to 350°C is expected, which will be of great utility in current PWR calculations. Still missing from the water radiolysis model for reactor chemistry is sufficient information about the chemical yields of neutron radiolysis, which can amount to 30 percent of the total radiation deposited in water. The objectives of a newly funded NERI project are to gather this information, and extend the reaction rate measurements of the current project.

The NERI project has been completed.

NUCLEAR ENERGY RESEARCH INITIATIVE

Novel Concepts for Damage-Resistant Alloys in Next Generation Nuclear Power Systems

Primary Investigators: Stephen M. Bruemmer and E.P. Simonen, Pacific Northwest National Laboratory (PNNL)

Collaborators: General Electric Global Research & Development (GEGRD); University of Michigan (UM)

Project Number: 99-280

Project Start Date: August 1999

Project End Date: September 2002

Research Objective

The objective of the NERI research is to develop the scientific basis for a new class of radiation-resistant materials to meet the needs for higher performance and extended life in next generation power reactors. New structural materials are being designed to delay or eliminate the detrimental radiation-induced changes that occur in austenitic alloys. These may include a significant increase in strength and loss in ductility (<10 dpa), environment-induced cracking (<10 dpa), swelling (<50 dpa), and embrittlement (<100 dpa). Non-traditional approaches are employed to ameliorate the root causes of materials degradation in current light water reactor systems. Changes in materials design are based on mechanistic understanding of radiation damage processes and environmental degradation, and the extensive experience of the principal investigators with core component response. This work is integrated with fundamental research at PNNL and with focused international projects at PNNL, GEGRD, and UM, led by the Electric Power Research Institute (EPRI). This leveraged approach will help facilitate the revolutionary advances envisioned within NERI. The multi-faceted study of basic and applied science is expected to provide a mechanistic understanding of next generation materials and promote their development. The research strategy capitalizes on the unique national laboratory, industry, and university capabilities that are available for studying radiation damage and an environmental cracking response.

Research Progress

The highlight of the research is the discovery of an alloy that is resistant to radiation damage based on additions of hafnium (Hf) solute to a low-carbon 316SS. Characteristics and properties of the alloy are illustrated in Figure 1. This damage resistance is supported by

characterization of radiation-induced microstructures and microchemistries along with measurements of environmental cracking. Research progress was achieved through a coordinated collaboration among a national laboratory (PNNL - nickel-ion irradiation and characterization); a university (UM - proton irradiation, characterization, and stress corrosion testing); and industry (GEGRD - crack-growth-rate testing in non-irradiated stainless steels tailored to emulate radiation-hardened microstructures). The addition of the oversized element Hf to a low-carbon 316SS reduced the detrimental impact of radiation in contrast to the addition of the

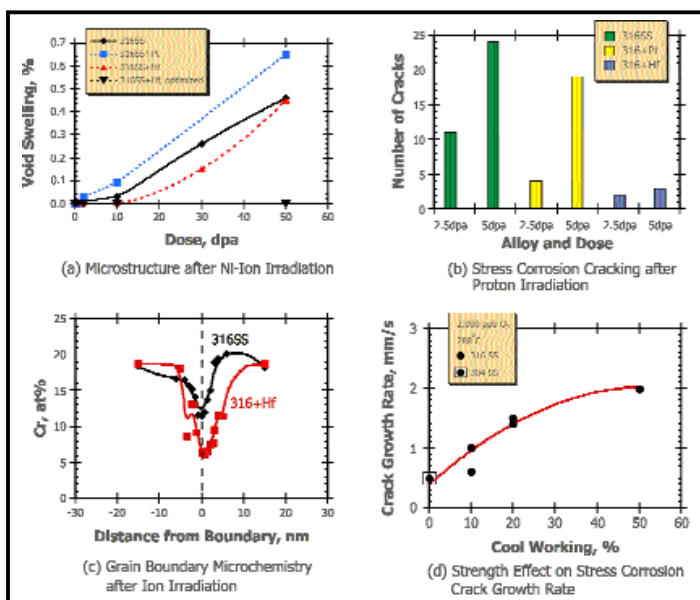


Figure 1. The beneficial effects on the characteristics and properties of an alloy when Hf is added to a low-carbon 316SS are shown for (a) void swelling after Ni-ion irradiations, (b) stress corrosion cracking of proton-irradiated alloys, and (c) radiation-induced Cr depletion after high-dose Ni-ion irradiation. These results suggest that the important influence of Hf is on radiation-induced microstructure. The beneficial effect on matrix microstructure is consistent with the (d) strength effect on SCC-growth-rate tests. Hf addition retarded the void swelling shown in (a) and retarded loop formation and hence radiation strengthening.

element platinum (Pt), which had no beneficial effects. This reinforces the belief that solute atom size and chemical reactivity are important for enhancing recombination of radiation defects and minimizing damage evolution. Hafnium additions were most effective after specific thermomechanical treatments to maximize the solute content in solution. The presence of Hf in the stainless steel altered microstructure evolution (dislocation loops and voids), altered grain boundary segregation at low doses, and improved resistance to stress corrosion cracking (SCC). Because cracking susceptibility is associated with several material characteristics, separate experiments on non-irradiated stainless steels explored the effects of matrix strength and grain boundary composition on SCC. This work has quantitatively demonstrated the critical importance of matrix strength on crack growth for the first time.

The concept of using oversized solutes to promote catalyzed defect recombination is a major thrust of this NERI project. The successful demonstration of damage resistance in the optimized Hf-doped alloy demonstrates promise for developing damage-resistant alloys for future-generation nuclear reactors. Void formation was delayed in the optimized Hf-doped alloy to radiation doses more than twenty times higher than in the base stainless steel. Resistance to irradiation-assisted SCC measured for proton-irradiated samples was also dramatically improved in the Hf-doped alloy. A key next step for assessing this damage-resistant alloy is to evaluate material performance after relevant neutron irradiations. Negotiations were successful with the international Cooperative IASCC Research project to add samples to an irradiation program underway in Russia. Samples from these initial alloys were prepared and are being irradiated to various doses up to ~70 dpa at 330°C.

The collaborative NERI experiments conducted at the three cooperating institutions indicate that radiation effects on strength are more important than radiation effects on grain boundary composition. Radiation-induced strengthening is strongly correlated with susceptibility of

stainless steels to IASCC. Strength effects on environmental cracking susceptibility were elucidated on non-irradiated stainless steels after working to systematically increase matrix strength levels. Crack-growth rate increased with strength level for both oxidizing (similar to boiling water reactors) and non-oxidizing (similar to pressurized water reactors) environments. These results suggest that the suppression of radiation-induced grain boundary segregation alone will not assure that an alloy will be resistant to SCC.

The second concept for developing damage-resistant alloys is the use of fine-scale multiphase alloys to mitigate detrimental microstructure evolution during irradiation. Three alloys have been tailored for evaluation of precipitate stability influences on damage evolution. The first alloy was a nickel-base alloy (alloy 718) that was characterized at high irradiation doses for the first time. Microstructural evolution (nanoscale hardening phases and loop/void structures) was examined. The γ'' phase begins to dissolve at low dose and disappeared altogether at moderate-to-high doses. The γ' phase dissolved and re-precipitated, but remained at a small size even to doses of 50 dpa. The experiment demonstrated the benefit of this nanoscale high-density phase to alter loop and void formation and control stability of high-dose irradiated properties. Two precipitation-hardened, Fe-base alloys (PH 17-7 and PH 17-4) were also studied to further evaluate complex second-phase structures on the evolution of radiation damage. One final aspect of evaluating complex multiphase alloys was examined in high-temperature crack-growth tests on specially processed stainless steels. High densities of second-phase carbides at grain boundaries were found to significantly decrease the susceptibility to intergranular SCC. Results demonstrate that proper tailoring of multiphase structures can improve both radiation and environmental damage resistance in stainless alloys.

Planned Activities

The NERI project has been completed.

NUCLEAR ENERGY RESEARCH INITIATIVE

Advanced Ceramic Composites for High-Temperature Fission Reactors

Primary Investigator: R.H. Jones, Pacific Northwest National Laboratory

Project Number: 99-281

Project Start Date: August 1999

Project End Date: September 2002

Research Objectives

The objective of this research is to develop the understanding needed to produce radiation-resistant SiC/SiC composites for advanced fission reactor applications. The structural and thermal performance of SiC/SiC composites in a neutron radiation field depend primarily on the radiation-induced defects and internal stresses resulting from this displacement damage. The objective of this research is to develop comprehensive models of the thermal conductivity, fiber/matrix interface stress, and mechanical properties of SiC/SiC composites as a function of neutron fluence, temperature, and composite microstructure. These models will be used to identify optimized composite structures that result in the maximum thermal conductivity and mechanical properties in a fission neutron field.

Research Progress

A newly developed model was used to predict the effects of component (fiber, matrix and interface) parameters and radiation on the overall transverse (through-thickness) thermal conductivity of 2D-SiC/SiC composites. To achieve high overall transverse thermal conductivity, both the matrix and fiber components must have a relatively high thermal conductivity. Furthermore, model predictions indicate that further conductivity enhancement is possible by improving the fiber/matrix (f/m) interface conductance. For instance, while using current interface technology the overall thermal conductivity of a commercially available SiC/SiC composite made with Hi-Nicalon fiber could be about doubled by replacing the Hi-Nicalon with an advanced SiC fiber with higher thermal conductivity (Figure 1, case b). However, by also improving the f/m interface conductance over that available with current design the composite thermal conductivity potentially could be increased by another 25% (case a), i.e., to values exceeding that of stainless steel. For instance, an

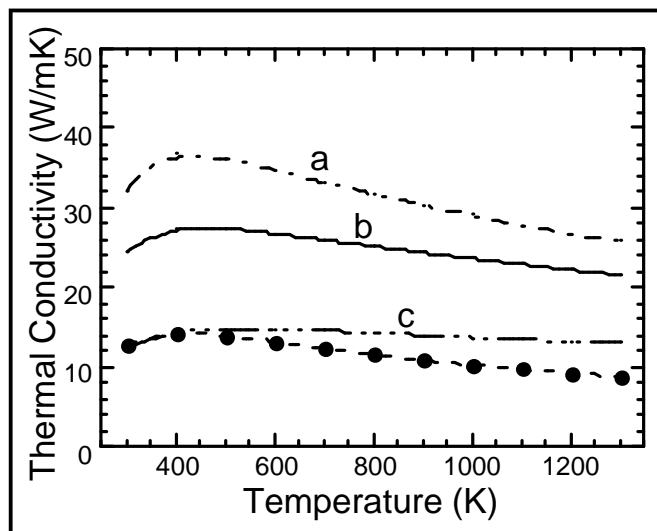


Figure 1. Model predictions of the transverse thermal conductivity for 2D-SiC/SiC composite made with advanced fiber and (a) an advanced f/m interface, (b) current interface technology, and (c) a degraded f/m interface. For comparison, the data points indicate the thermal conductivity for the Hi-Nicalon composite.

oriented graphitic carbon interface might provide such an improvement in interface conductance. However, the thermal conductivity of a composite made with advanced SiC fiber also is more sensitive to degradation effects at the interface. As an example, if only the interface conductance were reduced by a factor of ten (as might happen due to irradiation or other environmental effects) while maintaining the condition of the fiber and matrix components the overall thermal conductivity of the composite with advanced fiber would be reduced by at least 40% (case c). Nevertheless, for such a case the overall thermal conductivity is still about the same as that for the Hi-Nicalon SiC/SiC composite, as indicated in the figure.

A dynamic crack-growth model has been utilized to predict effects of irradiation on the crack growth. Fibers function as bridges that apply closure forces across the crack, which retard crack growth. Thermal- and irradiation-enhanced creep of the fibers reduces the closure force and

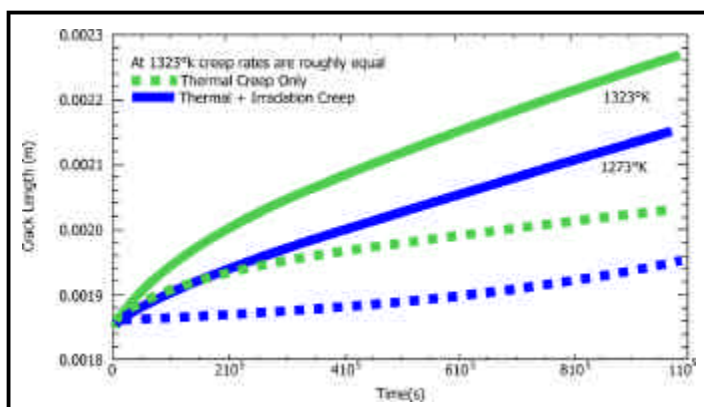


Figure 2. The graph indicates the model result in terms of crack length as a function of time for the indicated test temperatures.

an acceleration in the crack velocity. Experimental data on thermal and irradiation creep of SiC fibers was utilized in the model with the result that thermal creep dominates the growth effects at temperatures above 1,000°C and irradiation creep dominates at temperatures below 1,000°C (Figure 2).

A review of the literature on thermal fatigue and thermal shock of SiC/SiC composites has been completed. Transient thermal conditions will occur in a fission reactor from both the system duty cycle and an accidental loss of coolant. Shut-down of the system will cause some stress build-up in the material with the magnitude being dependent on the cooling rate and thermal gradients. Start-up will also induce stress of the opposite sign to that produced by shut-down and may relax the cool-down stresses. Coolant loss will induce a rapid heating and subsequent rapid stress change. The limited, existing data suggests that continuous fiber ceramic matrix composites such as SiC/SiC exhibit very good thermal shock characteristics, but most data was obtained for $-\Delta T$ conditions as a result of quenching from an elevated temperature. Thermal shock in a fission reactor will result from loss of coolant and will result in a $+\Delta T$. One study was reported for SiC/SiC composites given a $+\Delta T$ with no loss in strength following 25 cycles at a heating rate of 1,700°C/s. Monolithic SiC failed in 1.5 cycles at a heating rate of 1,400°C/s. Thermal fatigue test results also suggest that SiC/SiC composites will exhibit little or no degradation for hundreds of cycles.

The 3-cylinder model was used to calculate the radial, axial, and hoop stresses in the composite components as a function of irradiation dose. An initial residual thermal stress was present due to a ΔT of -100°C from a nominal synthesis temperature of 1,100°C and an irradiation temperature of 1,000°C. Since previous experimental results indicated that complete fiber-matrix debonding

occurred after exposure to low doses at 1000°C for Hi-Nicalon fiber composites, the study monitored the dose dependence of σ_{rr} at $r = r_4$, the fiber/coating interface. Values of the various domain radii were chosen to match microstructural information for CVI SiC/SiC composites. Total doses were limited to less than 10 displacements per atom (dpa) due to limitations in the swelling data for the various materials.

Large radial stresses are observed to build up at the Hi-Nicalon fiber/carbon coating interface regardless of the properties of the coating, Figure 3. The response of the composite is principally due to the fiber shrinkage during irradiation as the fiber densifies. This is predicted to lead to fiber/matrix debonding at the fiber-coating interface at relatively low doses, which corresponds to the experimental data for this material. Although there is little information on the strength of the interface in radial tension, the model predicts that these stresses approach 1 GPa for a dose of about 1 dpa, which probably exceeds the interface strength. The most important finding is that the radiation-induced shrinkage of Hi-Nicalon leads to fiber/matrix debonding at low neutron doses and, therefore, Hi-Nicalon fibers are unsuited for use as a continuous fiber in SiC/SiC composites exposed to such a radiation field.

Stresses are much smaller for the cases involving the Type-S fiber compared to the Hi-Nicalon fiber. The fiber and the SiC matrix respond identically and there is no differential swelling to contend with for this composite material. Now the response of the composite is principally

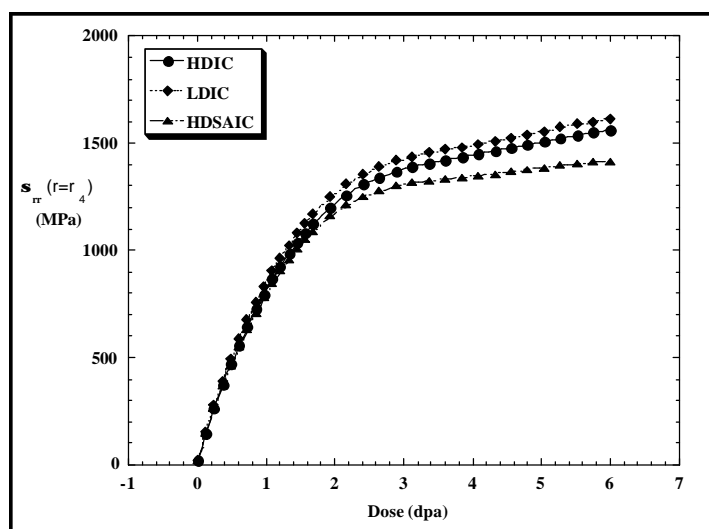


Figure 3. Comparison of three carbon coatings, high-density carbon (HDIC), low-density carbon (LDIC), and high-density slightly anisotropic carbon (HDSAIC) on Hi-Nicalon fibers, showing the radial stresses (σ_{rr}) at the fiber/coating interface. The model predicts a minor influence of the coating properties on the radial stress.

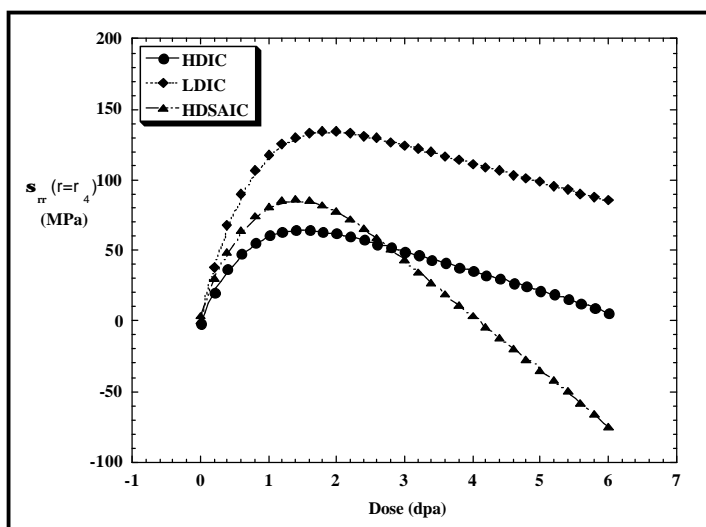


Figure 4. Comparison of three carbon coatings, high-density isotropic carbon, low-isotropic carbon, and high-density slightly anisotropic carbon, on Type-S fibers, showing the radial stresses (σ_{rr}) at the fiber/coating interface. The model predicts a significant influence of the coating properties on the radial stress in the system.

due to the radiation response of the carbon coating. Small values of the radial stress at the fiber/coating interface are predicted to lead to retention of fiber/matrix bonding up to significant neutron doses, which corresponds to the experimental data for this material. The most significant finding for the Type-S fiber cases is that the HDIC carbon coating yields the smallest value of the radial stresses in the system, with a peak stress of about 65 MPa predicted after a dose of about 1.5 dpa, Figure 4. The radial stress is then predicted to decrease slowly, with an increasing dose corresponding to the "turn-around" in the HDIC swelling curve. The LDIC material shrinks more than the HDIC and the peak radial stress is predicted to be about 140 MPa. The HDSAIC swells more than either HDIC or LDIC and puts the system into radial compression at the fiber/coating interface. A concern for this coating material is that continued radiation exposure may cause high compressive stresses and interface failure modes that have not yet been observed may be initiated.

Neutron irradiation-induced transmutations result in the presence of both radioactive and stable transmutant elements in the irradiated material. In general, as the neutron irradiation proceeds, the composition of the irradiated material can change due to the addition (or depletion) of solutes and impurities through radiation-induced transmutations, and it can also become radioactive. Activation and transmutation calculations were performed for SiC in the MPBR neutron spectrum. Results for transmutations are shown in Table 1. Calculations were performed for pure SiC irradiated for 10 efpy (4.4 dpa) in MPBR. During that exposure, small concentrations of five

elements were produced by transmutation. The concentrations of transmutants are listed in atomic parts per million (appm), and the rate of transmutation relative to damage (appm/dpa) is also shown. For comparison, the transmutation rates per dpa for SiC in HFIR-PTP are also shown, and are very similar to those for MPBR.

Induced radioactivity is generally extremely low for SiC in any neutron environment. In MPBR, after 10 efpy of irradiation and 4 days of cooling, SiC has a residual decay rate of about 4×10^{-4} Ci/g. This activity is due primarily to ^{32}P , which is a beta emitter. The gamma dose rate at this time is 3×10^{-11} R/h/cm³ at 1 m due to several short-lived gamma emitters. After cooling a year, the decay rate is 1×10^{-6} Ci/g dominated by ^{14}C , while the gamma dose rate is 5×10^{-14} R/h/cm³ at 1 m, due to the long-lived ^{26}Al produced from Si by a two-step reaction.

As reported earlier, dpa cross sections for SiC as a function of neutron energy have been developed under this project as reported earlier. With these cross sections, the dpa for SiC irradiated in a particular facility can be determined by integrating the DPA cross sections with the neutron energy spectrum of the facility. This procedure has been used to

Element	MPBR		HFIR-PTP
	Concentration (appm)	appm/dpa	appm/dpa
P	36	8.2	6.1
H	8.0	1.8	3.3
He	5.8	1.3	2.5
Mg	3.6	0.8	1.5
Be	1.5	0.3	1.4

Table 1. Concentrations of elements in SiC produced by neutron irradiation induced transmutations after irradiation in the MPBR for 10 full power years (4.4 dpa). The transmutation per dpa is compared with that for SiC in HFIR-PTP.

Reactor	Position	DPA/efpy	
		Fe	SiC
MPBR	core/He coolant	0.46	0.44
BWR	midplane	2.8	2.4
PWR	midplane	3.7	3.1
HFR	C5	12	11
ATR	midplane	14	12
EBR-2	midplane	25	27
HFIR	PTP mid	33	28
FFTF-MOTA	midplane	43	53

Table 2. Displacement damage rates in dpa per effective full power year (DPA/efpy) for SiC in several fuel and materials test reactors, commercial reactors, and a pebble bed reactor design. Values for pure Fe are shown for comparison to typical metals (listed in order of increasing values for SiC).

generate spectrally averaged displacement cross sections for SiC in a number of reactors that are or have been used for radiation damage testing of structural nuclear materials, in typical commercial reactors, and in the Modular Pebble Bed Reactor (MPBR). Calculations of DPA damage rates were also made, and the results are listed in Table 2 for several reactor positions. The damage rate for MPBR is less than one-fifth of that for the commercial pressurized water reactor (PWR) and boiling water reactor

(BWR). Test reactors have damage rates more than an order of magnitude greater than the 0.44 dpa/efpy for MPBR, so they could quickly irradiate test materials to MPBR lifetime doses.

Planned Activities

The NERI project has been completed.

NUCLEAR ENERGY RESEARCH INITIATIVE

Isomer Research: Energy Release Validation, Production, and Applications

Primary Investigator: John A. Becker, Lawrence Livermore National Laboratory (LLNL)

Project Number: 00-123

Collaborators: Los Alamos National Laboratory (LANL); Argonne National Laboratory (ANL)

Project Start Date: April 2000

Project End Date: September 2003

Research Objectives

The goal of this applied nuclear isomer research program is the search for, discovery of, and practical application of a new type of high energy density material (HEDM). Nuclear isomers could yield an energy source with a specific energy as much as a hundred thousand times as great as that of chemical fuels. There would be enormous payoffs to the Department of Energy and to the country as a whole if such energy sources could be identified and adapted to a range of civilian and defense applications. Despite the potential payoff, efforts in applied isomer research have been rather limited and sporadic. Basic research on nuclear isomers dates back to their discovery in 1935 with an occasional hint of further progress since then to tantalize interest in HEDM. In most cases, these hints were refuted following careful examination by other groups.

The isomer research area is rich with possibilities and several areas were prioritized as likely to be the most rewarding and fruitful for initial experimental and theoretical investigation. These areas bear directly on important issues: Can the energy stored in nuclear isomers be released on demand? Is the size of the atomic-nuclear mixing matrix element large enough to be useful? Under what circumstances? Can quantal collective release of isomeric energy be initiated from a Mössbauer crystal? What is the precise energy of the 3.5 eV level in ^{229m}Th ?

Specific experiments have been targeted to provide some answers:

- X-ray induced decay of isomeric Hf ($^{178m2}\text{Hf}$) with a sensitivity 10^5 times that of recent work
- NEET: A measurement of the atomic-nuclear mixing matrix element in ^{189}Os

- Stimulated emission in isomeric Te (^{125m}Te)
- Superradiance in isomeric Nb (^{93m}Nb)
- Energy and lifetime of the ^{229m}Th isomeric level at 3.5 eV
- TEEN: Nuclear isomer energy release in isomeric Hf $^{178m2}\text{Hf}$

Research Progress

Triggered decay of a nuclear isomer is clearly one requirement for usefulness of isomers as an energy source. Research in the past two-years focused on the question, "What is the cross section for keV X-ray induced decay of the 31-y isomer in the nucleus ^{178}Hf with nuclear excitation energy 2.4 MeV?" The question is relevant because induced decay had been reported in isomeric Hf ^{178}Hf with an integrated cross section of 10^{-21} cm²-keV, orders of magnitude greater than nuclear cross sections (Collins et al., 1999, Phys. Rev. Lett. 82, 695, and Collins et al., 2002, Europhys. Lett. 57, 677). This team (Ahmad et al., 2001, Phys. Rev. Lett. 87, 072503) has reported an upper limit approximately 5 orders of magnitude below that of Collins (1999) for $E_x > 20$ keV (see Figure 1). The 2002 report of Collins et al., claims that the induced decay occurs at lower X-ray energies than they previously reported (near 10 keV). This work was done at the Japanese 3rd Generation Synchrotron light source, SPring-8.

The collaborative team from ANL, LANL, and LLNL believes this result is also specious. They designed and fielded a second experiment at the ANL Advanced Photon Source (APS) in 2002 with an experimental arrangement optimized for low energy X-ray bombardment, but still taking advantage of the intense "white" beam as opposed to utilizing an monochromatic beam. This arrangement permits more photons incident on the target than in an

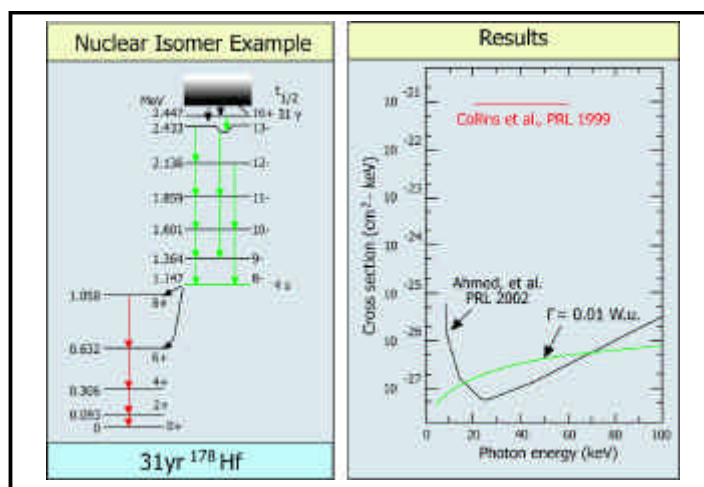


Figure 1. The graphs illustrate the decay scheme of 31-y isomeric Hf-178. The cross-section results of Ahmad et al. (2002) and Collins et al. (2001) are shown on the right-hand side. The green line shows the cross section expected for E1 absorption to a level at E_{photon} with strength 0.01 W.u. as a function of E_{photon} . The strength of the photon absorption (0.01 times a single particle unit) represents a reasonable upper limit to the transition strength based on nuclear

experiment with a quasi-monoenergetic beam, without "holes" in the incident X-ray flux. Thin Hf targets enriched in the 31-y isomer mounted on Be disks were used in the experiment. On-line analysis suggests that the cross section $\sigma_{\text{X-ray}}$ for induced X-ray emission is less than $10^{-27} \text{ cm}^2/\text{keV}$ at the 5σ limit for $E_{\text{X}} > 6.5 \text{ keV}$. This result is orders of magnitude below claims made any positive published claims.

Planned Activities

Work will move on from the isomeric Hf issue to attack the physics of nuclear isomers relevant to their use as an energy source. The particular focus will be on the following areas:

- Documentation of the experiments on the X-ray induced enhanced decay of isomeric ^{178}Hf , with a focus on low incident X-ray energies. Controversial experimental reports continue to circulate in the literature and in the community of scientists working in isomer physics (see above).
- NEET, Nuclear Excitation by Electronic Transition, in ^{189}Os . The process has been demonstrated in ^{197}Au , in a recent synchrotron experiment in Japan. The matrix element is similar to the (inverse) internal conversion matrix element. Important conditions for NEET to compete with real photon emission will include an energy overlap of the atomic and nuclear states, and a common multipolarity of the atomic and nuclear transitions. An experiment is being

developed to prepare ionized atomic ^{189}Os by bombardment with a variable energy electron beam in an electron beam ion trap (EBIT) and to pump a nuclear state in ^{189}Os at 216.6 keV. The energy of the electron beam is carefully controlled and tuned so that the sum of the energies of the bombarding electron beam and the L-shell ionized ^{189}Os (a free-bound transition) add up to the excitation of the nuclear ^{189}Os level at 216.6 keV. Trapped ions are periodically gathered up and counted. The signal is the energy and decay rate of the $J^{\Pi}=9/2^-$, $E_{\text{X}}=30.814 \text{ keV}$, $t_{1/2}=5.7 \text{ h}$ state, populated in the decay of the 216.6-keV nuclear state. The experiment is sited at LLNL's EBIT facility.

- Stimulated emission of isomeric ^{125m}Te . Large quantities of isomeric ^{125m}Te enable an experiment to demonstrate stimulated emission of photons from nuclear isomers. The signal is the enhancement of time-correlated photons observed in a solid state detector located on the axis of a rod-shaped Mössbauer source. The Khlopin Radium Institute in St. Petersburg, Russia, has developed a program (under ISTC auspices) to extract ^{125}Sb from spent nuclear fuel as a generator of 20 percent ^{125m}Te . The content of ^{125}Sb in 20 to 50 GW-day fuel after a four-to six-year cooldown is 3 curies per kilogram of uranium. This is a larger source of isomeric ^{125m}Te than previously available. A 0.5-cm long source of magnesium tellurate containing 20 percent ^{125m}Te would produce a stimulated gamma ray at the rate of $3.9 \times 10^{-3}/\text{sec}$, observable over accidental coincidence rate $8 \times 10^{-4}/\text{sec}$. If successful, this would be the first observation of stimulated emission of gamma rays. In order to achieve gain, Borrmann channeling or some other effect requiring single crystals would be necessary to reduce the attenuation of 109-keV gamma rays. The Khlopin Radium Institute has been contacted to determine the availability and schedule the acquisition of ^{125m}Te . Once the source is acquired, a magnesium tellurate Mössbauer source will be made, and the experiment fielded. The needed apparatus to observe time-correlated photon emission exists in the laboratory at Los Alamos and can be set up within a few months.
- Superradiance in isomeric ^{93m}Nb . Superradiance is an effect discovered by Robert Dicke in the 1950's that results in an enormous broadening of the photon channel through the cooperation of an ensemble of quantum excited states. The possibility of nuclear

superradiance was recognized for Mössbauer crystals in the 1960s. One of the most likely candidates for exhibiting nuclear superradiance is ^{93m}Nb . The observation of enhanced photon emission would be the first evidence of the broadening of the photon channel width necessary to exploit the stored nuclear energy in a nuclear isomer. Molybdenum isotope production targets in the Medical Isotope Program are a source of ^{93m}Nb at LANSCE. Approximately, 300 grams of molybdenum was processed last year to extract 0.5 milligrams of niobium. This brings the total inventory at LANL to 3 milligrams. The inventory of ^{93m}Nb is now 0.2 milligrams. An attempt will be made to create a single crystal containing a high enrichment of ^{93m}Nb from the present stock. The synthesis of potassium heptafluoronioate crystals is being attempted from

Nb-HF-KF aqueous solution. This method is being examined as a possible method for producing single crystals containing ^{93m}Nb . A search will be made for enhanced photon emission along nuclear Bragg angles following successful crystal growth.

- ^{229}Th ground state doublet (3.5 eV). What is the energy of the first excited state of ^{229}Th near 3.5 eV? The uncommonly low energy of the ground state doublet would allow a laboratory isomer that could be manipulated by a laser. There are also potential applications as a radionuclide thermal source (RTG). Researchers at LLNL and LANL are working with colleagues at ANL to establish the feasibility of such an experiment, taking advantage of unique facilities at ANL.

NUCLEAR ENERGY RESEARCH INITIATIVE

Random Grain Boundary Network Connectivity as a Predictive Tool for Intergranular Stress-Corrosion Cracking

Primary Investigator: Mukul Kumar, Lawrence Livermore National Laboratory

Project Number: 01-084

Collaborators: University of Michigan; General Electric Corporate Research & Development

Project Start Date: October 2001

Project End Date: September 2004

Research Objectives

Intergranular stress corrosion cracking (IGSCC) is one of the most pervasive degradation modes in current light water reactor systems and is likely to be a limiting factor in advanced systems as well. In structural materials, IGSCC arising from the combined action of a tensile stress, a "susceptible" material, and an "aggressive" environment has been recognized for many years and the mechanisms widely investigated. Recent work has demonstrated that by sequential thermomechanical processing, properties such as corrosion, IGSCC, and creep of materials can be dramatically improved. The improvements have been correlated with the fraction of so-called "special" grain boundaries in the microstructure. A multi-institutional team comprising researchers from Lawrence Livermore National Laboratory (LLNL), University of Michigan (UM), and General Electric Corporate Research & Development (GECRD) propose an alternative explanation for these observations: that the effect of grain boundary engineering is to break the connectivity of the random grain boundary network through the introduction of low-energy, degradation-resistant twins and twin variants. A collaborative science and technology research project is being carried out that is aimed at verifying the mechanism by which sequential thermomechanical processing ameliorates IGSCC of alloys relevant to nuclear reactor applications, and prescribing processing parameters that can be used in the manufacture of IGSCC-resistant structures.

In this work, methods are being developed to quantify the interconnectivity of the random grain boundary network and measure the interconnectivity of a series of materials where it has been systematically altered. Property measurements are then performed on the materials, their performance ranking compared with the boundary network measurements, and the materials

characterized to correlate actual crack paths with the measurements of the random grain boundary network.

With this data, the methods that have been chosen to describe the random grain boundary network will be evaluated and improved. The characterization method will be tested by evaluating the interconnectivity of the random grain boundary network in a series of as-received materials, their expected performance ranked, and that result compared with property measurements.

The major accomplishments of this project are expected to be (1) the determination that the random boundary network connectivity (RBNC) is a major driver of IGSCC in low to medium stacking fault energy austenitic alloys, (2) the development of a predictive tool for ranking IGSCC performance of these alloys, and (3) the establishment of thermomechanical processing parameters to be applied in the manufacture of IGSCC resistant materials. The outcome of the project will be identification of a mitigation strategy for IGSCC in current Light Water Reactor (LWR) conditions that can then enable the development of economically and operationally competitive water-cooled advanced reactor systems.

Research Progress

The experimental test material, Inconel 600 of nominal composition Ni-16Cr-9Fe (by weight percent) was subjected to cycles of sequential thermomechanical processing. Each processing cycle consisted of rolling at room temperature to a reduction in thickness of 25 percent, annealing at 1,025°C for 18 minutes (following a 42-minute heating ramp), and water quenching. This cycle was repeated up to four times, so specimens were analyzed in a total of five processing conditions (including the as-received state).

Specimens for electron back-scatter diffraction (EBSD) were sectioned to analyze the microstructure at the center of the rolled and annealed sheets, in order to avoid artifacts associated with the specimen surfaces. Metallographically prepared specimens were examined in a Hitachi S2700 or Philips XL30S scanning electron microscope, both with an automated EBSD attachment from TSL, Inc. (Draper, Utah). Orientation information was acquired on a hexagonal grid, with total scan areas in the range 1.1×10^5 to $2.5 \times 10^6 \mu\text{m}^2$, using a step size in the range 0.5-5 μm .

The analysis of EBSD data was carried out using custom algorithms written using Interactive Data Language software from Research Systems, Inc. (Boulder, Colorado). Grain boundaries were categorized according to the Brandon criterion, using 2° as a minimum disorientation for a low-angle boundary. Those boundaries with $\Sigma \geq 29$ were considered special, including low angle and coherent twin boundaries. The number fraction (f_n) of special grain boundaries was determined for each specimen from populations of more than 1,000 individual boundaries.

The changes in the grain boundary network structure was quantified using new cluster analysis algorithms developed for this project. The two-dimensional network of grain boundaries determined from EBSD data was analyzed by identifying boundary clusters, each cluster consisting of all the interconnected boundaries of like type. In this work, the focus is on clusters of only random or only special boundaries. Clusters were identified using a depth-first graph-search algorithm. About 632 grains were analyzed for each specimen. Figure 1 shows the mass fraction, m_s , for clusters of size s in Inconel 600, as a function of processing history. The cluster mass is the total (dimensionless) length of boundary contained in the cluster. In percolative systems, cluster masses tend to be distributed across several orders of magnitude, particularly near the percolation threshold. Therefore, the data in Figure 1 has been collected in bins spaced evenly in $\log(s)$; the size s on the x-axes in this figure represents the upper bound of each bin. Physically, Figure 1 indicates what fraction of the total length of boundaries in the specimen is occupied in clusters of size s . For example, Figure 1a pertains to the random boundary clusters in the as-received material, where the majority of boundaries are incorporated into a single large cluster of mass 391 units (i.e., spanning hundreds of grains).

In Figures 1a-e, the effect of grain boundary engineering on random boundary clusters is shown quantitatively. After just one cycle of processing (Figure 1b), the largest interconnected clusters of random boundaries are broken up, and the largest clusters have mass in the range 100-178 units. On each subsequent processing cycle (Figures 1c-e), the random boundary network becomes increasingly fragmented, and larger populations of small clusters emerge. After four processing cycles, all of the clusters have mass below 32 units, more than an order of magnitude smaller than the largest cluster mass in the as-received condition. Although there has been considerable discussion surrounding the connectivity of random grain boundaries during grain boundary engineering, investigators believe that these results are the first direct quantitative measurement of such connectivity and its evolution as a function of processing history. The dramatic fragmentation of the random boundary network documented in Figure 1 may explain the concomitant remarkable improvements observed in material properties after grain boundary engineering.

Figures 1f-i show the mass distributions for clusters of special grain boundaries, and therefore represent the complement to Figures 1a-e for the random boundary clusters. In the as-received state, special clusters are extremely small and isolated (Figure 1f). With each cycle of processing, the connectivity of the special boundaries improves, and after four processing cycles, the largest fraction of boundaries is of mass 100-178 units. Compared with the as-received material, this is an order of magnitude increase in the maximum cluster mass. Thus, the order-of-magnitude decrease in random cluster mass is symmetrically offset by a 10-fold increase in the mass of special clusters.

The foregoing discussion can be simplified by considering simple scalar measures of the cluster mass, such as the maximum cluster mass and the weighted average mass. These two parameters are shown in Figure 2 as a function of the processing cycle number for both random and special clusters. Both the average and maximum cluster mass exhibit similar trends, reflective of the construction of contiguous special boundary networks at the expense of large random boundary clusters, which rapidly break into much smaller clusters during processing. Although the special clusters grow at the same rate that the random clusters fragment, they do not grow to the very large masses that the random clusters exhibit in the as-received state.

The cluster mass changes illustrated in Figure 1 are accompanied by changes in the length scales of the clusters. The decrease in random cluster size and the corresponding increase in special cluster size during sequential thermomechanical processing are shown in Figure 3. The maximum linear cluster dimension, D_{max} , represents a projection of the largest contiguous path of random or special boundaries in the two-dimensional section, while the correlation length ξ is a representation of the average diameter of all clusters measured in a given specimen. As expected from the trends observed in cluster mass (Figures 1, 2), the process of grain boundary engineering leads to a significant reduction in the random boundary cluster size, by about a factor of three.

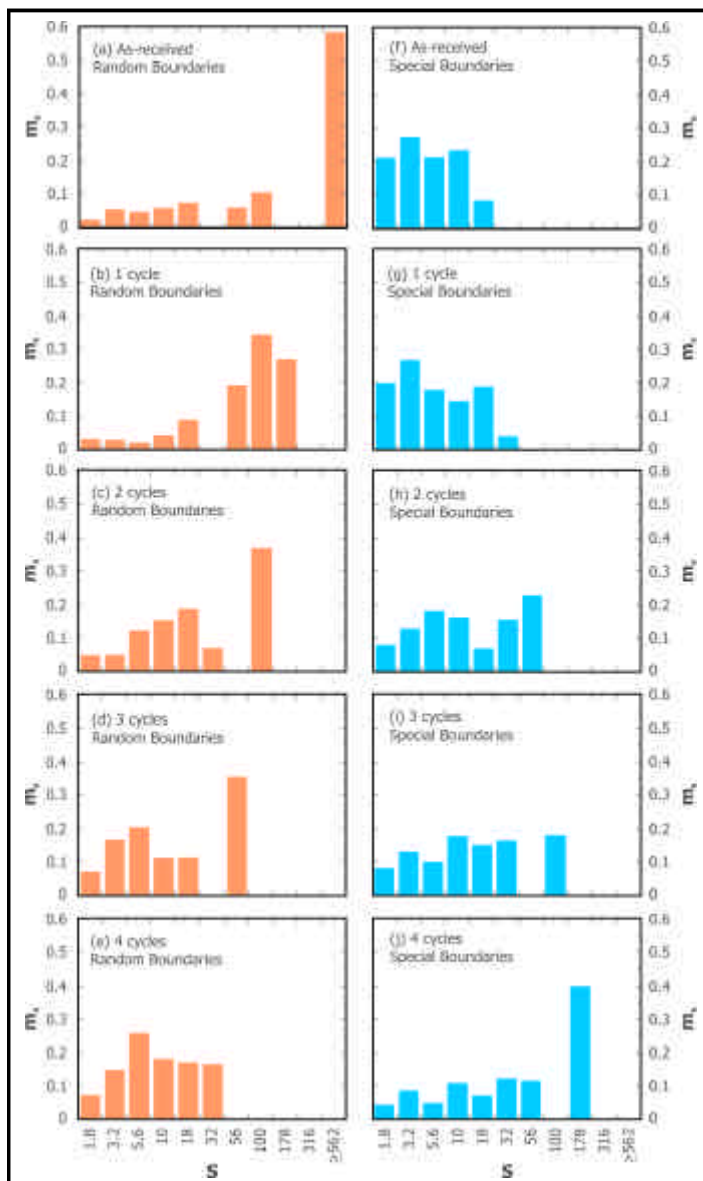


Figure 1. The graphs are a quantitative depiction of the changing grain boundary network topology during grain boundary engineering: (a)-(e) show the cluster mass distributions for only the random boundaries after 0,1,2,3, and 4 cycles of processing, respectively, and (f)-(j) show the complementary mass distributions for the special boundary clusters.

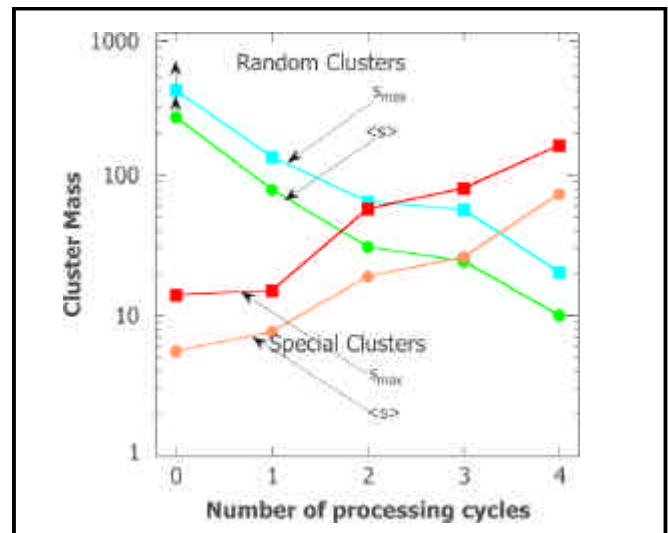


Figure 2. Changes in grain boundary cluster masses are plotted as a function of grain boundary engineering processes. Both the maximum cluster size (s_{max}) and the weighted average mass ($\langle s \rangle$), are shown for random and special clusters. Random clusters for the as-received material extended beyond the scan area, so the data points represent a lower-bound.

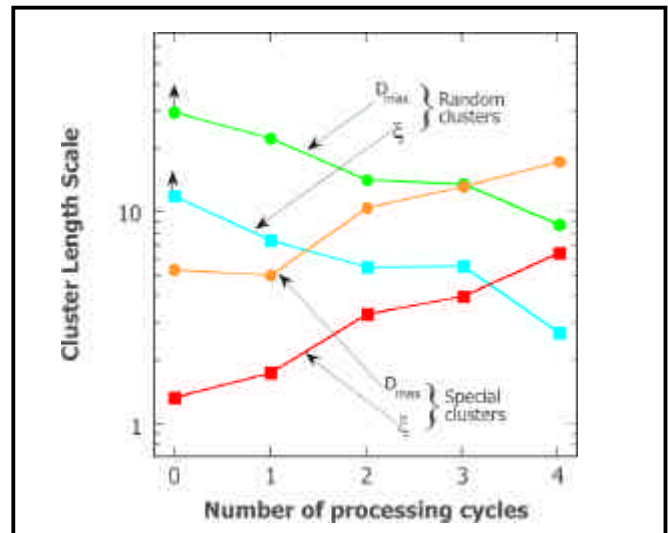


Figure 3. Changes are illustrated in the characteristic length scales of grain boundary clusters during grain boundary engineering, including the maximum cluster dimension (D_{max}) and the correlation length (ξ) for random and special boundary clusters.

The experimental test material, 304 grade stainless steel, was subjected to cycles of sequential thermomechanical processing. Each processing cycle consisted of rolling at room temperature to a reduction of 20 percent and annealing at 1,000°C followed by water quenching. This cycle was repeated up to four times with an annealing time of 60 minutes after the first rolling pass and then for the subsequent cycles these times were sequentially reduced by 10 minutes. The specimens were analyzed in the as-received state, and after two and four processing cycles. A further heat treatment was done after

the fourth cycle for an hour at 1,000°C to get a grain size comparable to the as-received condition, but this had no effect on the other microstructural parameters.

Specimens for electron back-scatter diffraction (EBSD) were sectioned to analyze the microstructure at the center of the rolled and annealed sheets, in order to avoid artifacts associated with the specimen surfaces. Metallographically prepared specimens were examined in a Philips XL30S scanning electron microscope with an automated electron backscatter diffraction (EBSD) attachment from TSL, Inc. (Draper, Utah).

The analysis of EBSD data was carried out using custom algorithms written using Interactive Data Language software from Research Systems, Inc. (Boulder, Colorado). Grain boundaries were categorized according to the Brandon criterion, using 2 as a minimum disorientation for a low-angle boundary. Those boundaries with 29 were considered special, including low angle and coherent twin boundaries. The number fraction (f_n) of special grain boundaries was determined for each specimen from populations of more than 1,000 individual boundaries.

The results are given below in Figures 4a and 4b. The random grain boundaries in all cases are ones in black and the colored boundaries in the background are crystallographically special boundaries. The as-received condition is to be used as the baseline microstructure, as its properties are well understood. The sample after four cycles of thermomechanical processing and additional heat treatment has a lower fraction of special boundaries as well as a more connected network of random grain boundaries. It is anticipated that this will provide a good comparison in the IGSCC behavior.

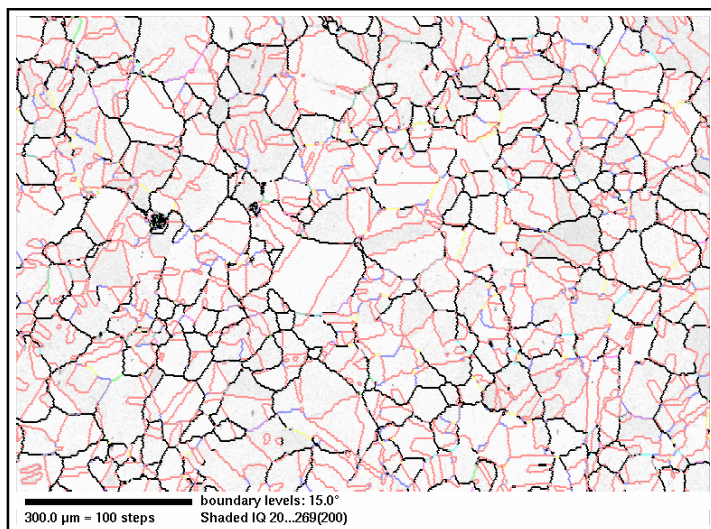


Figure 4a. The as-received condition microstructure is to be used as the baseline. (Special fraction: By length (fL) = 0.65; By frequency (fN) = 0.53.)

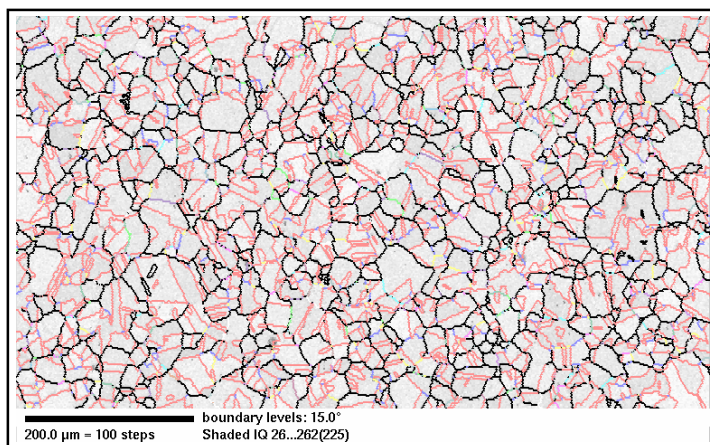


Figure 4b. The microstructure is pictured after 4 cycles of thermomechanical processing. (Special fraction: By length (fL) = 0.53; By frequency (fN) = 0.35.)

Planned Activities

The susceptibility of the microstructure to crack initiation will be assessed using constant extension rate tensile (CERT) testing. CERT tests will be conducted in pressurized water reactor (PWR) primary water (320°C - 360°C, containing a hydrogen overpressure) or in boiling water reactor (BWR) water (288°C - 350°C, with varying corrosion potential and water purity) and a strain rate of $3 \times 10^{-7} \text{ s}^{-1}$. Samples will be periodically removed from the autoclave and examined for intergranular (IG) cracking. The CSL-type of boundaries on which IG cracks appear will be determined by reference to the grain boundary character distribution recorded prior to the IGSCC test. In this way, a strain-dependent map of grain boundary cracking and a tally of the types of grain boundaries that crack will be developed. Crack depth can also be measured using an acetate replica technique.

Following completion of the test, samples will be cross-sectioned and polished, and the grain boundaries along the crack path will be characterized to determine the propensity for cracking of each grain boundary type. The grain boundaries comprising each triple point will also be analyzed.

The Stress Corrosion Cracking (SCC) growth rate response for different microstructures will be compared under different water chemistry conditions. These experiments are performed using fracture mechanics specimens (0.5T or 1T CT specimens) in sophisticated equipment involving precision control and monitoring of water chemistry and corrosion potential; digital servo-control loading systems under computer control; high pressure high temperature autoclave systems with digital temperature controllers; continuous high resolution direct

current potential drop monitoring of crack length; and computer data acquisition and test control.

Tests will be performed at about 25 ksi/in in 288°C high purity water containing 2,000 ppb O₂ or 100 ppb H₂ to represent typical boiling water reactor and pressurized water reactor conditions, respectively. On completion of testing, the specimen will be fatigued apart and evaluated by scanning electron microscopy.

Further plans for FY 2003 include processing of 304 stainless steel and Inconel 600 to optimize the microstructure by increasing the special fraction. These efforts are underway.

Testing to compare the IGSCC behavior will be conducted in the first quarter of FY 2003.

NUCLEAR ENERGY RESEARCH INITIATIVE

Reactor Physics and Criticality Benchmark Evaluations for Advanced Nuclear Fuel

Primary Investigator: William J. Anderson,
Framatome ANP, Inc. (FANP)

Project Number: 01-124

Collaborators: Sandia National Laboratories (SNL);
Oak Ridge National Laboratory (ORNL); University of
Florida (UF)

Project Start Date: September 2001

Project End Date: September 2004

Research Objectives

The objective of this Nuclear Energy Research Initiative (NERI) project is to design, perform, and analyze critical benchmark experiments for validating reactor physics methods and models for fuel enrichments greater than 5-weight (wt) percent ^{235}U . These experiments will also provide additional information for application to the criticality-safety bases for commercial fuel facilities handling greater than 5-wt percent ^{235}U fuel. Because these experiments are to be designed not only as criticality benchmarks but also as reactor physics benchmarks, investigators wish to include measurements of critical boron concentration, burnable absorber worth, relative pin powers, and relative average powers.

Research Progress

The first task of this project was to identify the fuel to be used. Options considered were to use fuel from existing stockpiles, or to fabricate new fuel. In addressing this issue, the project identified a significant stockpile of 6.93-wt percent enriched UO_2 located at Pennsylvania State University. This fuel, the "Pathfinder fuel," consists of 417, unirradiated, 6-fuel rod assemblies. Although the fuel is much longer than the critical facility can use, the fuel is suitable for refabrication into shorter rods. The use of this fuel for this project provides the desired enrichment for these experiments, and eliminates a major stockpile of enriched uranium from Pennsylvania State University's regulated inventory.

Having identified the fuel, the next major task was to identify a suitable shipping container for transporting the fuel from Pennsylvania State University to Sandia National Laboratories. This shipping package needed to be licensed to contain up to 7.0-wt percent-enriched fuel. The container also had to be long enough to accommodate the 82.5-inch long Pathfinder elements. Because no suitable

container was identified with a license to contain up to 7.0-wt percent-enriched fuel, licensing a shipping package became a major challenge.

The first option investigated was the MO-1 shipping package. This was selected because the Department of Energy's Oak Ridge Operations Office had agreed to be shipper of record and already owns two MO-1 shipping packages. However, the MO-1 had to be eliminated as a viable option because it is a "grand-fathered" package that has not been drop tested to current standards.

Attention was then focused on the modified WE-1 shipping package, a Type A shipping package that was recently modified by adding an armor plated steel inner container. The addition of this inner container has made it a Type B shipping package suitable for shipping various higher-enriched uranium fuels. A safety analysis of the WE-1 containing the Pathfinder fuel is underway, which involves the following steps:

- Designing an inner container to hold the Pathfinder fuel in the WE-1
- Performing a criticality safety evaluation to demonstrate that the WE-1 Pathfinder fuel shipment will meet regulatory requirements for criticality safety
- Performing a structural/stress analysis to demonstrate that the WE-1 Pathfinder fuel shipment will meet regulatory requirements
- Submitting a license amendment to the NRC for review

On March 31, 2002, the safety analysis was on schedule for to be submitted to the NRC on May 15, 2002.

Another task in Phase 1 was to design the experiments to be performed at Sandia National Laboratories. The preliminary design configuration involves water-moderated, square-pitched lattices of cylindrical fuel

rods containing enriched UO_2 pellets (approximately 6.93-wt percent ^{235}U). The arrays consist of fully flooded, uniform lattices of aluminum-clad fuel rods.

The Preliminary Design Report, issued in February 2002, describes four suites of fully flooded critical configurations with square-pitch lattices. The experiments consider two pitch values, 0.800 cm and 0.855 cm. Due to the uncertainty of fuel re-fabrication costs, two base designs are documented. These consist of a 3x3 array of 15x15 assemblies, and a cruciform array of 17x17 assemblies. Although the flexibility of the 3x3 array of 15x15 assemblies makes it the preferred design, the cost of constructing 1,836 fuel rods may require that the cruciform array of 17x17 assemblies, which uses 1,596 fuel rods, be used.

In support of future experiments, SNL is preparing a safety basis for the experimental facility, the SPRF/CX. The existing authorization basis (AB) for the SPRF/CX was written to cover the activities associated with the BUC-CX (the BUC-CX is a test of the reactivity effects of fission-product poisons on a critical system). The current experiment differs from the BUC-CX in the following ways:

- (1) The mass of fuel in the current experiment is higher than is authorized for the BUC-CX.
- (2) In the final configuration, the reactivity worth of the soluble poison will be considerably higher than the allowed excess reactivity.
- (3) The experiments involve irradiation to produce sufficient fission products in the fuel to allow the relative fission density to be measured as a function of fuel rod location. The fission products are part of the source term for the accidents considered in the AB. The increased inventory needs to be accounted for in the AB update.
- (4) If experiments at elevated temperatures are to be done, consideration will have to be given to the reactivity effects of the elevated temperatures and the impacts of any cooling that might occur and result in positive reactivity insertion.

The foregoing list suggests several points for consideration in the SPRF/CX AB update, given the test matrix for the current experiment.

The design of the experiments will incorporate the results of a sensitivity/uncertainty (S/U) analysis. The S/U analysis is being performed to determine how well commercial reactor fuel with ^{235}U enrichments greater

than 5-wt percent fit into the area of applicability of existing critical benchmark experiments. Second, the S/U tools are being applied to the proposed experimental design to ensure that it is optimized to provide the best possible coverage for the commercial fuel of interest.

A review of existing critical benchmarks identified a total of 154 experimental configurations with ^{235}U enrichments in the range of 5 to 10 wt percent. Sensitivity data for 125 of these experiments have been generated with the SEN3/KENO analysis sequence. Sensitivity data have also been generated for eight configurations of the proposed experimental design. Critical boron searches were performed for each configuration, and then the sensitivity data were generated for the eight critical configurations.

Part of this project considers the impacts of higher enrichments on fuel fabrication and handling for commercial facilities. Reviews of two of the three major commercial fuel processing and fabrication facilities in the United States indicated that some fuel processing operations are convertible to higher enrichment operation with acceptable cost increases. However, some large batch operations appear to be more challenging with regard to higher enrichments. The primary problem area from a cost standpoint may be the packaging and transportation of UF_6 cylinders.

To date, all the tests to be performed by Framatome ANP, Inc. and ORNL are on schedule, or ahead of schedule. SNL efforts have been delayed due to work on the BUC-CX program. Over the next two quarters, SNL is expected to accelerate its schedule and complete its tasks within the current schedule.

The research subcontract with the University of Florida was not signed until February 2002. Although this placed UF behind schedule on all tasks, work has commenced and UF is expected to complete all tasks on schedule.

Planned Activities

The remainder of Phase 1 includes the following tasks:

- Completion of the sensitivity/uncertainty analysis (ORNL)
- Documentation of the Final Design Report (FANP)
- Analysis of the experiments using industry codes (FANP, ORNL, UF)

- Revisions to the SNL AB (SNL)
- Completion of criticality safety, stress, and containment analysis for the WE-1 (FANP)
- Submittal of the WE-1 license amendment to the NRC (FANP)
- Detailed investigation of UF₆ packaging and transportation considering >5 wt percent enriched UF₆ (UF)
- MCNP scoping calculations to review the sizing of critically safe processing equipment considering >5 wt percent enriched fuel (UF)

NUCLEAR ENERGY RESEARCH INITIATIVE

Fundamental Understanding of Crack Growth in Structural Components of Generation IV Supercritical Light Water Reactors (SC LWR)

Primary Investigator: Iouri Balachov, SRI International

Project Number: 01-130

Collaborators: VTT Manufacturing Technology

Project Start Date: August 2001

Project End Date: September 2004

Research Objectives

The objectives of this project are as follows:

- Increase understanding of the fundamentals of crack growth in structural components of Generation-IV supercritical light water reactors (LWRs) made of stainless steels and nickel base alloys at supercritical temperatures.
- Provide tools for assessing the influence of the operating conditions in power plants with supercritical coolant temperatures on the electrochemistry of different types of corrosion processes taking place in the coolant circuits of supercritical power plants.
- Measure material-specific parameters describing the material's susceptibility to stress corrosion cracking and other forms of environmentally assisted degradation of structural materials at supercritical coolant conditions.
- Use these measurements to interpret the rate-limiting processes in the corrosion phenomena and as input data for lifetime analysis.
- Use the SRI-developed FRASTA (fracture surface topography analysis) technique to obtain information on crack nucleation times and crack growth rates via analysis of conjugate fracture surfaces. Identify candidate remedial actions by which the susceptibility to stress corrosion cracking can be decreased.

A unique combination of two advanced techniques is used for studying material reliability. Controlled Distance Electrochemistry (CDE) allows investigators to determine in relatively short experiments a measurable material parameter that describes the transport of ions or ionic defects in the oxide films. This will be correlated with the susceptibility to cracking, using FRASTA to reconstruct the evolution of crack initiation and growth.

Research Progress

Progress made in examining the fracture surfaces will be discussed.

Crack behavior in the specimens tested in the environment is not easy to interpret, and it is frequently difficult to establish a correlation with loading conditions. A commonly used method of determining the crack length, the DC potential drop measurement, is very useful in providing continuous reading the crack tip position during the test. However, such a method requires careful calibration when applied to a new geometry; it also gives an averaged value through the thickness and through the fracture process zone.

Significant information related to crack behavior can be obtained by examining the fracture surfaces. This section will report the results of applying the SRI-developed fracture surface topography analysis (FRASTA) technique. The FRASTA technique characterizes the topography of conjugate fracture surfaces, juxtaposes conjugate fracture surface profiles on the computer, and assesses the inelastic deformation that occurs at the crack tip during crack extension by manipulating the spacing between the conjugate surfaces. Using the inelastic deformation on the fracture surface, it is possible to reconstruct the crack growth history and microfracture processes and present the results graphically.

The fracture surface topography was characterized by SRI's FRASTAscope, which consists of a confocal-optics scanning laser microscope, a computer-controlled precision x-y stage, and computer software to control the system and create the topography data files.

The FRASTA technique was applied to one of the samples, a single-edge-notch and wedge-loaded disc specimen. This specimen was fatigue pre-cracked and

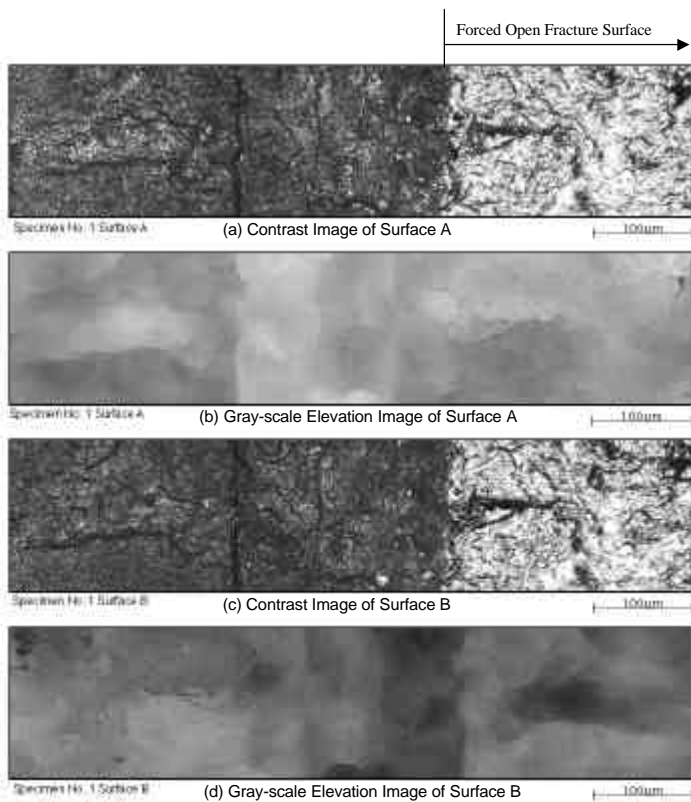


Figure 1. The graphics show contrast and gray scale topography images of conjugate surfaces.

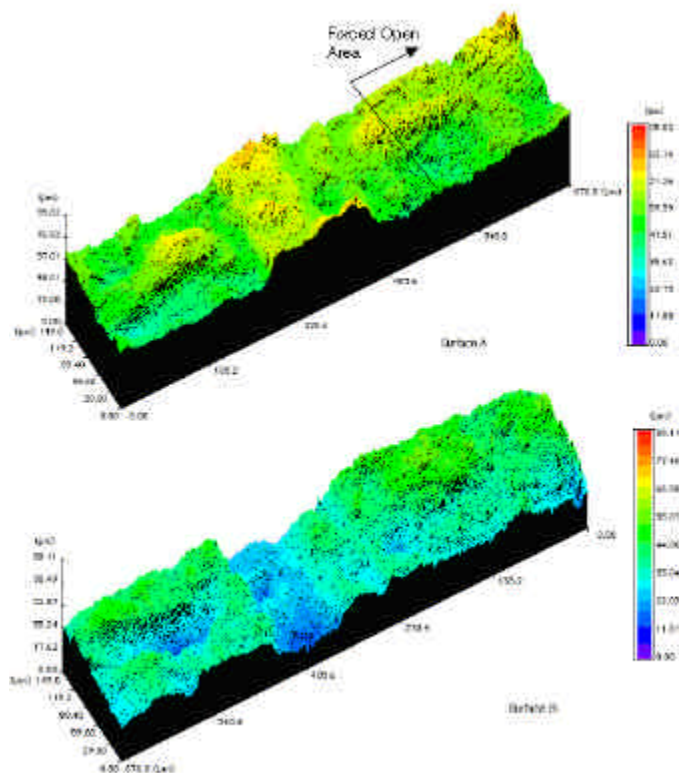


Figure 2. The images provide a perspective view of fracture surfaces.

wedge-loaded at room temperature, then placed in an autoclave to expose it to a supercritical water environment. After several interrupted exposures, the specimen was removed from the autoclave and the crack was opened by applying cyclic loading.

Figure 1 shows the contrast and gray-scale topography images of the area covering the end of the fatigue pre-crack, crack growth during the test in the environment, and the beginning of forced opening after the test. In the gray-scale topography images, white areas represent high elevation and dark areas low elevation. Images of Surface B were flipped horizontally for easier comparison with Surface A. The areas exposed to the environment were covered with oxide film and appear dark. Forced-open areas were highly reflective surfaces. In the dark area in the vicinity of a forced-open fracture surface, several vertical markings were observed. It is difficult to determine where the crack growth in the environment started through the visual examination of the SEM fracture surface images. Thus, researchers are interested in using FRASTA analysis to determine the significance of these markings and also the precise location of the transition from the fatigue pre-crack to the growth of the crack in the supercritical environment.

Figure 2 shows a perspective view of the topography of the fracture surfaces. Several steps in elevation mentioned above are more clearly seen. These steps are parallel to the crack front.

The fracture process was reconstructed using the topography information. Some of the results are shown in the fractured area projection plots (FAPPs) of Figure 3. A well-defined crack front is not seen in the FAPPs. One of the reasons for this is that there are some errors in the elevation data; thus, when conjugate surfaces were matched, the crack front became a zone rather than a single line. The magnitude of elevation error in this analysis is not negligible because the surface reflection was relatively poor due to use of oxide film, and the degree of deformation was small.

Although the crack front was not well-defined, there were some trends in the crack front movement through the series of FAPPs. However, the more precise trend in the crack front movement could be characterized by constructing the fractured area (white area) as a function of conjugate surface spacing. The results are shown in Figure 4.

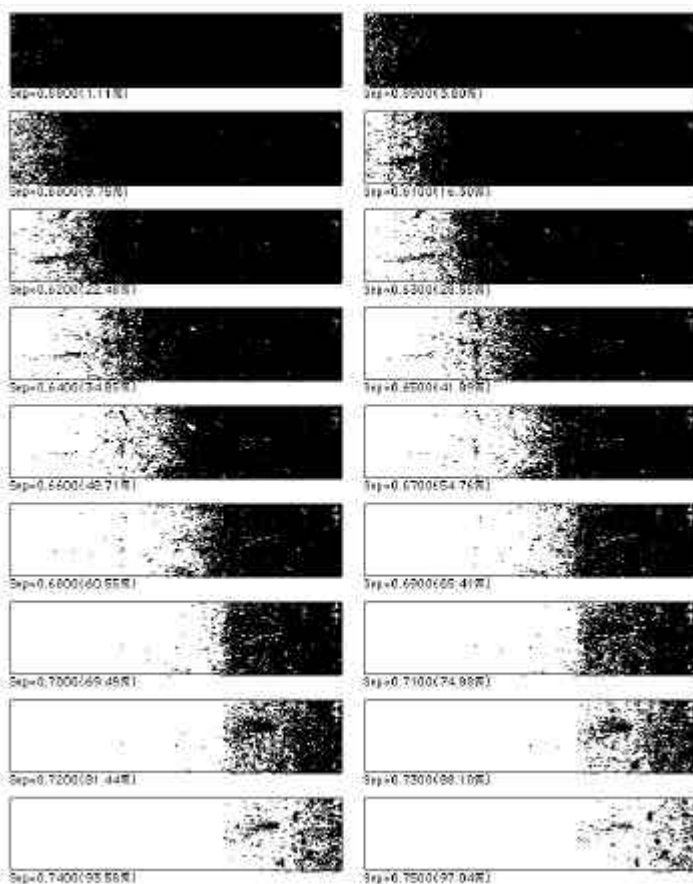


Figure 3. Pictured above are a series of FAPS showing the crack growth processes. The plots show hesitation in crack front movement at some locations.

The curve shows that the slope was approximately constant up to Point A, indicating that the condition of crack growth up to this point was steady and unchanged. However, at Point A, the slope changed and became a little steeper. A steeper slope suggests that the material was less resistant to the crack growth. Thus, some change occurred at Point A that changed the characteristics of crack growth. A possible reason for this could be the change of loading conditions—the change from fatigue pre-cracking at room temperature to a supercritical water environment. The state at Point A will be examined in detail later. The change observed at Point B is due to the forced opening of the crack. It was shown later that the crack front position observed in the FAPP at Point B corresponds to the location where surface color changed, as seen in Figure 1. The slope becomes significantly less steep after Point B, suggesting that the crack growth in this region required more plastic deformation than that in the environment.

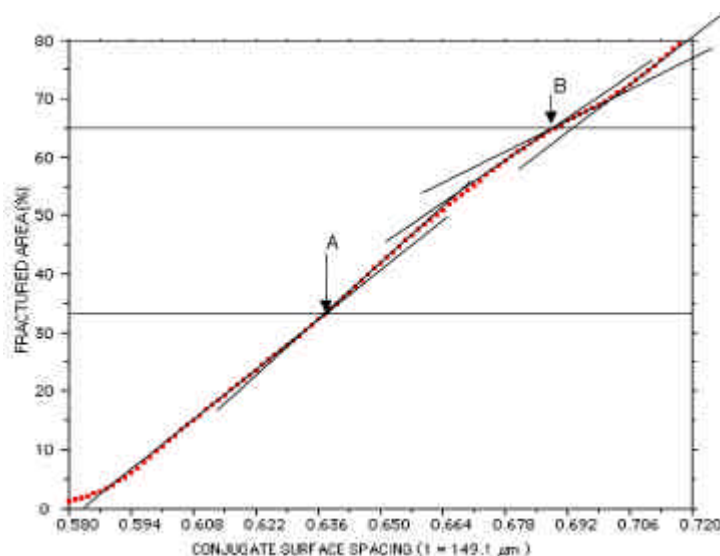


Figure 4. The graph illustrates the fractured area increasing the slope of the curve as a function of conjugate surface spacing.

Planned Activities

Two parallel activities are planned for years two and three of the project: (1) Electrochemical studies of properties of the oxide films and (2) fracture surface analysis for candidate structural materials.

Tasks scheduled for "An Electrochemical Characterization of the Oxide Film Properties on Candidate Materials in Supercritical Conditions in the Bulk and within the Crack" follow:

- Characterize the formation and reduction kinetics and the properties of metal oxide films by using the Contact Electric Resistance (CER) technique.
- Measure the solid contact impedance spectra of oxide films by using Contact Electric Impedance (CEI).
- Characterize the oxidation and reduction kinetics and mechanisms of metals as well as the properties of metal oxide films by using Thin-Layer Electrochemical (TLEC) impedance measurements.
- Perform CDE measurements in simulated crack conditions. The influence of adding ionic species/contaminants on the oxide film formed on the surface of candidate materials will be explored experimentally in a static autoclave under simulated conditions corresponding to those existing inside a stress corrosion crack.

- Rank the influence of ionic species on the oxide films forming on metal surfaces exposed both to simulated supercritical LWR bulk coolant and to simulated crack chemistry conditions, using advanced electrochemical techniques.
 - Quantify and interpret the rate-limiting processes in the corrosion phenomena and the role of electrochemical reactions and properties of oxide films in the crack growth mechanism under supercritical conditions.
 - Derive material-specific parameters that describe the susceptibility of metals to stress corrosion cracking in supercritical coolant conditions for the materials in which crack growth is controlled by the phenomena in oxide films within the crack.
 - Identify candidate remedial actions (changes in water chemistry, material chemical composition, and metallurgical parameters, in particular the degree of cold work) that can decrease the susceptibility to stress corrosion cracking.
- Tasks in the "Experimental Investigation of Crack Initiation and Propagation and Estimation of Life-Time of Candidate Structural Materials" are as follows:
- Expose loaded specimens to a supercritical aqueous environment simultaneously with electrochemical studies of the oxide films on the same materials.
 - Examine fracture surfaces of specimens (they will be broken after the tests) by using the FRASTA technique.
 - Identify crack nucleation sites and times for specimens made of different candidate materials.
 - Use FRASTA to determine crack front formation and movement, including formation of discontinuities ahead of the crack and their possible coalescence later while the crack is advancing.
 - Estimate crack growth rates for different candidate materials under a set of conditions using FRASTA for examination of conjugate fracture surfaces.
 - Correlate electrochemical information on material-environment interactions with crack nucleation and growth data from FRASTA to delineate the fundamentals of uniform and localized degradation of structural materials in Generation-IV supercritical LWRs and estimate life-times of candidate materials for structural components under a variety of normal

NUCLEAR ENERGY RESEARCH INITIATIVE

New Design Equations for Swelling and Irradiation Creep in Generation IV Reactors

Primary Investigator: Wilhelm G. Wolfer, Lawrence Livermore National Laboratory

Project Number: 01-137

Collaborators: Pacific Northwest National Laboratory; Lawrence Berkeley National Laboratory

Project Start Date: October 2001

Project End Date: September 2004

Research Objectives

The objectives of this research project are to significantly extend the theoretical foundation and the modeling of radiation-induced microstructural changes in structural materials used in Generation IV nuclear reactors, and to derive from these microstructure models the constitutive laws for void swelling, irradiation creep, and stress-induced swelling, as well as changes in mechanical properties.

The need for the proposed research is based on three major developments and advances over the past two decades. First, new experimental discoveries have been made on void swelling and irradiation creep that invalidate previous theoretical models and empirical constitutive laws for swelling and irradiation creep. Second, recent advances in computational methods and power make it now possible to model the complex processes of microstructure evolution over long-term neutron exposures. Third, it is now required that radiation-induced changes in structural materials over extended lifetimes be predicted and incorporated in the design of Generation IV reactors.

The approach in this effort to modeling and data analysis is a dual one in accord with the objectives to both simulate the evolution of the microstructure and develop design equations for macroscopic properties. Validation of the models through data analysis is therefore carried out at both the microscopic and the macroscopic levels. For the microstructure models, results were used from transmission electron microscopy of steels irradiated in reactors and from model materials irradiated by neutrons as well as ion bombardments. The macroscopic constitutive laws will be tested and validated by analyzing density data, irradiation creep data, diameter changes of fuel elements, and post-irradiation tensile data. Validation of both microstructure models and macroscopic constitutive laws is a more stringent test of the internal

consistency of the underlying science for radiation effects in structural materials for nuclear reactors.

Research Progress

A microstructure code was developed that evaluates the full, time-dependent distribution of vacancy clusters and the dislocation density, all within a mean-field framework. The vacancy cluster distribution ranges from monomers to voids of arbitrary size. The stochastic, atomic processes of void growth or shrinkage are included by master equation and Fokker-Planck treatments of the void size distribution function. Void growth and fluctuation rates are determined from a self-consistent calculation of the thermal and radiation-induced vacancy and interstitial monomer populations. The dislocation subsystem is modeled entirely as network dislocations, in terms of a single density parameter. Interstitial aggregation is not allowed, as dislocation loops are not explicitly considered. However, it will be included in the future. Dislocation bias factors are calculated according to previously described methods (Sniegowski and Wolfer 1983). There is a cutoff distance used in the derivation that is related to the average density of dislocations.

In the research, two choices are made for that parameter. The first is to calculate dislocation bias factors assuming a density of $6 \times 10^{14} \text{ m}^{-2}$, a typical terminal density under steady irradiation. This is the procedure in Wehner and Wolfer (1985), where it would be expected to give the experimentally observed asymptotic swelling rates for calculations with a fixed dislocation density. The second choice is to calculate the bias factors using a cutoff obtained from the instantaneous value of the evolving dislocation density. That density is evolved according to a model (in Wolfer and Glasgow 1985) that incorporates dislocation-dislocation annihilation processes along with a dislocation multiplication from pinned dislocations

undergoing irradiation-driven, biased climb. The model includes one free parameter—namely, the mesh length or pinning density (set to a value of 400 nm to fit the observed terminal dislocation densities in irradiated steels), which is determined by the density of carbide precipitates in the steel.

It was verified that this team's implementation of the dislocation evolution model reproduces earlier results for annealing in 316 stainless steel. Likewise, the combined void plus dislocation simulations were checked to verify they conserve mass, both with and without irradiation. The method is computationally efficient to temperatures of 650°C, at which point the stable void size becomes too large for efficient simulations. For all lower temperatures, the simulations extend to much longer times than previous treatments of stochastic void nucleation. This method is applied to a model of a high-purity, type-316 austenitic stainless steel.

It is easy to see a temperature-dependent, incubation-like period in the simulated void swelling versus time. Volumetric swelling curves are presented in Figure 1 for a series of temperatures (340°C to 540°C) for an irradiation dose rate of 10^{-6} dpa/s and an initial dislocation density of $6 \times 10^{13} \text{ m}^{-2}$. The data shown in Figure 1 is obtained using a constant dislocation bias factor, as in Wehner and Wolfer (1985). The values for 316 stainless steel are 1.63 for interstitials and 1.04 for

vacancies. The simulations show a brief incubation period, which increases in duration at lower temperatures. Subsequently, the swelling rates at different temperatures are comparable, around 0.85 percent/dpa. This asymptotic rate is largely dictated by the dislocation bias factors. Overall, the predicted swelling behavior is similar to experimental data, both in the appearance of an incubation-like feature and in terms of the numerical value of the asymptotic slope. However, the duration of the incubation period is short compared to commercial steels, being more similar to irradiation results obtained for pure binary and ternary austenitic steels.

The swelling predictions are very sensitive to the choice of dislocation bias factors. Figure 2 displays the swelling curves using dislocation bias factors that are calculated according to the instantaneous dislocation density. The predicted dislocation bias factors are found to be smaller at low dislocation densities, for example 1.39 and (1.03) for interstitials (vacancies) at a dislocation density of $6 \times 10^{13} \text{ m}^{-2}$, and they increase with dislocation density. This gives rise to a prolonged period of void nucleation in solution-annealed metals, producing a striking, incubation-like behavior that lasts from 2 to 15 dpa of total fluence. Besides lengthening the incubation period, the density-dependent bias also causes the asymptotic rates of swelling to depend noticeably on temperature. This change in behavior occurs because the terminal dislocation density is temperature-dependent, the calculated dislocation bias factors are now density-

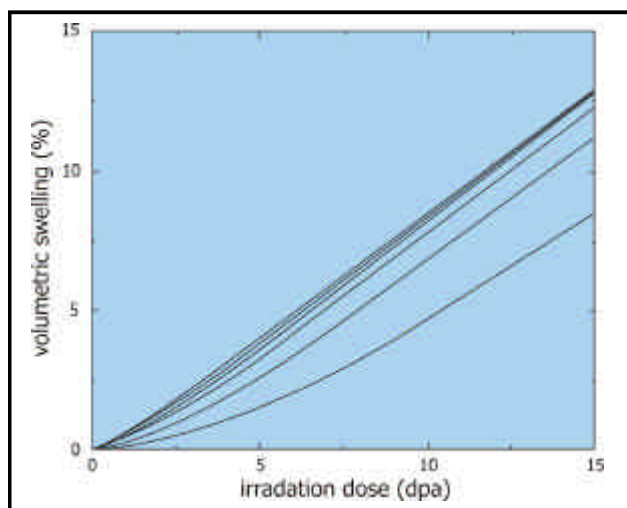


Figure 1. The graph plots volumetric swelling, DV/V in percent, versus total irradiation dose for a pure, type-316 stainless steel. The dose rate is 10^{-6} dpa/s; the starting dislocation density is $6 \times 10^{13} \text{ m}^{-2}$. The various curves correspond to temperatures of 340°C to 540°C in increments of 40°C. The 340°C curve has the longest incubation period. While the dislocation density is allowed to evolve with time, the dislocation bias factors derived from the stress-induced interaction with the vacancy and interstitial defects are taken to be constant.

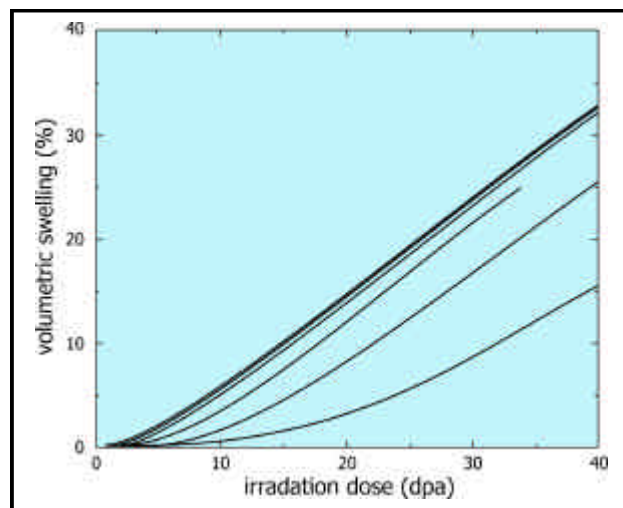


Figure 2. The graph plots volumetric swelling, DV/V in percent, versus total irradiation dose (equivalently, the irradiation time, in Msec) for a pure, type-316 stainless steel. The system parameters are exactly as in Figure 1, except that here, the dislocation bias factors are allowed to vary with the dislocation density. Again, the lowest temperature curves display the longest incubation delays.

dependent, and the final swelling rates are strongly bias-dependent.

There is a striking difference in the predicted number density of voids between the constant and the variable dislocation-bias simulations. The predicted terminal void population is several times smaller with the variable dislocation bias than in the constant dislocation-bias case (Figure 1).

In summary, the present microstructural code for void nucleation and concurrent dislocation network evolution is generating swelling-fluence-temperature correlations which closely resemble that obtained by Garner from recent data sets on EBR-II irradiated 304 stainless steels. At the same time, the new correlations are dramatically different than the empirical swelling design equations still in use for LWR and breeder reactors. In particular, it was found that irradiation temperature does not have a large effect on the steady-state swelling rate, but does have a large influence on the incubation dose.

Planned Activities

During the initial stage of dislocation evolution in solution-annealed stainless steels, a high density of small dislocation loops are present. While these loops merge with the network dislocations at higher doses, they are expected to influence the void nucleation, and hence the incubation dose for void swelling.

During FY02, appropriate models will be developed for loop evolution and will be incorporated into the microstructural evolution code. Additional algorithm development will be undertaken to improve the numerical stability of the code and thereby improve the efficiency.

Collision cascades lead to atomic mixing in materials with small precipitates. An analogous effect should lead to the destruction of small void embryos. This should result in an increase of the incubation dose for void swelling with increasing neutron energy. To quantify this potential effect of the neutron energy spectrum on incubation, collision cascade simulations will be carried out near small clusters of vacancies with and without helium.

NUCLEAR ENERGY RESEARCH INITIATIVE

Development and Validation of Temperature Dependent Thermal Neutron Scattering Laws for Applications and Safety Implications in Generation IV Nuclear Reactor Designs

Primary Investigator: Ayman I. Hawari, North Carolina State University

Project Number: 01-140

Project Start Date: September 2001

Collaborators: Oak Ridge National Laboratory
Instituto Balseiro, Argentina

Project End Date: September 2004

Research Objectives

The overall objectives of this work are: to critically review the currently used thermal neutron scattering laws for various moderators and fuel cells as a function of temperature, to use the review as a guide in examining and updating the various computational approaches in establishing the scattering law, to understand the implications of the results obtained on the ability to accurately define the operating and safety characteristics (e.g. the moderator temperature coefficient) of a given reactor design -- that is, to know not only the reactivity coefficients but also their errors, sensitivity coefficients and covariance matrices, and finally to test and benchmark the developed models within the framework of a neutron slowing down experiment. In particular, the studies will concentrate on investigating the latest ENDF/B thermal neutron cross sections for reactor grade graphite, beryllium, beryllium oxide, zirconium hydride, high purity light water, heavy water and polyethylene at temperatures greater than or equal to room temperature. These materials are neutron moderators that will be used in the development of Generation IV nuclear power reactors and in many applications in the nuclear science and engineering field. Of major importance is graphite, which is the moderator in the modular pebble bed reactor (MPBR) that is being examined internationally as a possible Generation IV power reactor, as the subcritical reactor in accelerator driven concepts, and as the incinerator of radioactive waste and weapons' plutonium. Furthermore, a newly developed highly conductive form of graphite, known as graphite foam, is currently under study as a reactor material.

Research Progress

During the first year, the effort of this project has concentrated on establishing the methodology and the tools that are required for evaluating the thermal neutron scattering laws for the materials of interest. Due to the recent interest in high temperature gas reactor (HTGR) concepts, including the pebble bed reactor, the research focused on evaluating the scattering kernel for graphite. This included updating it by implementing previously unused phonon frequency distributions, exploring the use of "ab initio" methods as a general approach for generating the phonon frequency distributions for crystalline moderators, identifying a set of experimental benchmarks to test the new kernel, and designing the temperature dependent neutron slowing-down-time experiment that will be used to test and validate the standard (i.e., ENDF/B-VI based) and the new thermal neutron scattering kernels for graphite.

As a starting point, the LEAPR methodology of the NJOY99 code system was used to reproduce the graphite scattering kernel using the phonon distribution function established by Young and Koppel in 1965, which is the basis of the ENDF/B-VI data. Once that was achieved successfully, the Young-Koppel data were replaced by a phonon frequency distribution function that was established by Nicklow, Wakabayashi, and Smith at Oak Ridge National Laboratory (ORNL) in 1972. While the general features of the ORNL phonon distribution are similar to the Young-Koppel phonon distribution, the detailed features are quite different. It was found that the resulting "scattering law" $S(a,\beta)$ curves using the ORNL phonon distribution for moderator temperatures 296°K, and 1,200°K were shifted to somewhat higher values compared to the Young-Koppel results. The inelastic cross

sections for the two different phonon distributions were determined using the THERMR module of NJOY99. The figure below shows these results for graphite moderator temperatures of 296°K and 1,200°K.

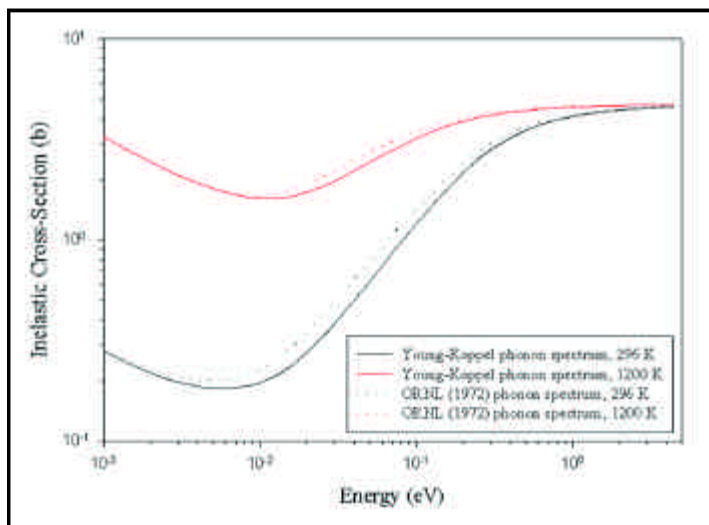


Figure 1. The graph illustrates an inelastic cross-section for graphite at 296°K and 1,200°K

Subsequently, the above data were formatted to be used in the MCNP code using the ACER module of NJOY99 and are currently being tested in computational HTGR benchmarks for sensitivity calculations of the values of k_{eff} and the total capture and reaction rates of actinides as a function of fuel and graphite temperatures.

Furthermore, we have initiated the use of the ab initio code VASP coupled to the PHONON code to establish the phonon spectra of solid moderators based on first principal quantum mechanical calculations. The work during this phase concentrated on optimizing our graphite models and subsequently applying the developed methodology to Be, BeO and ZrH.

In addition, we began a series of Monte Carlo simulations to design an experiment to benchmark the thermal neutron scattering kernel of graphite as a function of temperature. The simulations were performed using the MCNP code and its standard libraries. The simulated temperatures ranged from 300°K to 1,200°K. The model was based on introducing a neutron pulse at the surface of a 75 x 75 x 75 cm graphite pile and monitoring the time dependent reaction rate in a detector placed outside the pile at distances ranging from 0.25 m to 2 m from the surface opposite to the source. The neutron source was assumed to be the Oak Ridge Electron Linear Accelerator (ORELA). To create a realistic model, we assumed that

the graphite pile would be located at the end of one of ORELA's beam tubes. Therefore, to ensure maximum source intensity, we chose the shortest beam tube, which is 10 m long. In addition, we assumed a 20-nanosecond pulse width and a 1000 Hz frequency. Under such conditions, the source strength at the surface of the pile is expected to be approximately 108 n/s. Furthermore, upon analyzing the ORELA energy spectrum we found that despite its spread, it is, in effect, a fast neutron spectrum peaking around 600 keV in $\ln(E)$. This only becomes apparent if the spectrum is expressed as $\ln(E)$ vs. E as opposed to the usual E vs. E . Based on this model, the time dependent reaction rate in a Pu-239 detector was calculated. The figure below shows the time spectra at a distance of 0.25 meters from the pile surface and for temperatures of 300, 800, and 1,200°K. The general features of the time spectra are dictated by the time dependent neutron energy spectrum that is leaking from the pile and the energy dependent fission cross-section of Pu-239. The close coupling of the leakage energy spectrum to the time after the neutron pulse can be predicted based on the principals of time dependent neutron slowing down theory. For both temperatures, the time spectra are nearly identical at early times (i.e., high energies). However, once thermal effects become important (around 10⁻⁴ seconds), the spectra begin to deviate due to the temperature dependence of the thermal neutron scattering kernel.

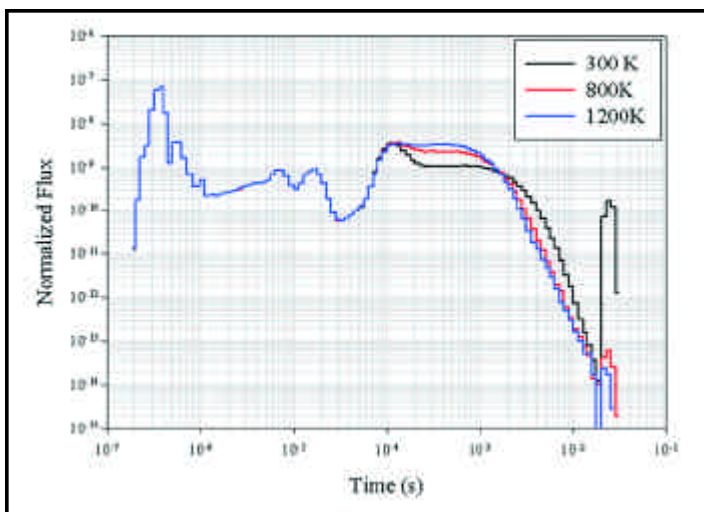


Figure 2. The plot is of the calculated time dependent reaction rates for a Pu-239 detector

Planned Activities

During the upcoming phases of this project, work will continue on exploring new methods for generating the scattering kernels for the proposed materials and comparing them to the standard kernels. This will include ab initio methods and the synthetic kernel approach. In addition, computational benchmarks will be used to examine the validity of the new data and methods relative to current knowledge. During phase 2, this work will

extend to understanding the implications of the results obtained on the ability to accurately define the operating and safety characteristics of a given reactor design. Work will also continue on the design of the graphite benchmark experiment. Preliminary experiments, at ORELA, are expected to begin during phase 2 of this project. The final experiments are planned to take place during phase 3 of the project.

NUCLEAR ENERGY RESEARCH INITIATIVE

Oxidation of Zircaloy Fuel Cladding in Water-Cooled Nuclear Reactors

Primary Investigator: Digby MacDonald,
Pennsylvania State University

Project Number: 02-042

Project Start Date: September 2002

Project End Date: September 2005

With the development of higher burn-up fuels for nuclear power reactors, much greater demands are being placed on the performance of the Zircaloy fuel sheaths. The principal threat to the integrity of the sheath is oxidation/corrosion and hydriding, leading to somewhat uniform thinning, and in some instances to localized corrosion in the form of nodular attack and/or hydriding. Failure leads to the release of fission products into the coolant, which in turn contributes to the man-REM costs of operating the system. Extensive fuel failures may require shutdown, which results in the unit being unavailable for normal operation. Thus, strong operational and economic reasons exist for enhancing fuel reliability. The principal goal of the proposed work is to develop sophisticated physico-electrochemical models for the corrosion of Zircaloy fuel sheaths that can be used by reactor operators to actively manage the accumulation of damage and thereby minimize the risk of fuel cladding failure in operating reactors.

While the kinetics and mechanisms of the oxidation of zirconium and zirconium alloys have been extensively studied, little effort has been made to develop deterministic (as opposed to empirical and semi-empirical) models that can be used to predict fuel sheath performance and reliability at very high burn-ups in operating reactors. Those attempts at developing algorithms have employed semi-empirical, parabolic, or cubic models (e.g., $L^2 = kt + C$, where L is the oxide thickness, t is time, k is the parabolic rate constant, and C is a constant) to extrapolate oxide thickness data to longer times, but the validity of these models is highly uncertain. Furthermore, the models generally ignore the cathodic reaction(s) that occur on the fuel sheath surface and none attempt to model the actual electrochemical conditions that exist within porous deposits at the fuel sheath/coolant (fs/c) interface. Other problems include the simplicity of the diffusion model that predicts parabolic growth, particularly when viewed in light of more modern models

for the growth of anodic oxide films; the inability of the models to predict the transition that occurs in growth kinetics from parabolic (or cubic) to linear at a more-or-less specific oxide film thickness in terms of fundamental, atomic scale processes; the exclusion of effects due to second phase particle (SPPs) on the cathodic processes that occur within the outer layer; the lack of an atomic scale model for the formation of hydrides; and the inability of the present models to describe the influence of solution-phase species, such as Li^+ , on the oxide film growth kinetics. On reflection, it is apparent that the most glaring deficiency in the current theories and models is the lack of a sound electrochemical basis for the corrosion process under free corrosion conditions. By focusing only upon the oxidation of zirconium, these models in effect attempt to treat only half of the problem, in that the cathodic processes are ignored. Because the cathodic processes must be included in order to satisfy the conservation of charge, the existing models are "non-physical" and hence cannot constitute a deterministic basis for describing the oxidation phenomenon. Furthermore, some evidence exists to suggest that the cathodic reactions, which must occur at the same rate as the zirconium oxidation reaction, may actually control the overall rate, with the apparent dependence of the rate on oxide thickness reflecting the rate of electron transfer across the film.

The issue with respect to the underlying mechanisms of oxidation and hydriding is important and timely, because of the considerable advances that have been made on these subjects over the past several years. For example, work by the authors over the past twenty years, under DOE/BES sponsorship, has developed the Point Defect Model (PDM) for the growth and breakdown of anodic passive films that form on metal surfaces. Recent work has shown that the PDM provides a much better description of oxide film growth than does the classical "high field" model [HFM], and indeed one attempt has

already been made to apply the PDM to the oxidation of Zircaloy-4. Furthermore, the formation of hydride is readily described by the PDM and a strong possibility exists that a unified, predictive model may be developed for oxidation and hydriding.

As noted above, electrochemical effects are almost totally ignored in the current models, but as with all corrosion processes they are actually dominant. Thus, the radiolysis of the coolant produces a number of electroactive species, including H_2 , O_2 , and H_2O_2 , which react at the cladding/environment interface to consume the charge that is produced by the oxidation of the Zircaloy. The conservation of charge requires that the sum of the anodic partial currents due to Zr and H_2 oxidation be equal to that for the reduction of oxygen and hydrogen peroxide and any other reducible species in the system. The potential at which this condition is satisfied defines the corrosion potential (ECP), which is known to have a major impact on the corrosion of materials in reactor coolant circuits. Over the past decade, the author and his colleagues have developed sophisticated models for the radiolysis of water and the electrochemistry of the coolant circuits in boiling water reactors (BWRs) and more recently in pressurized water reactors (PWRs). Similar models will be developed in the proposed work to accurately describe the electrochemical conditions that exist at the cladding/coolant interface. The objectives of this program are to develop fundamentally new mechanisms for Zr oxidation and hydriding in reactor primary coolant environments that address issues arising from the specific chemistry employed (BWR vs. PWR) as well as from reactor-specific issues related to the mode of operation. The mechanisms will include the important phenomenon of boiling within porous CRUD deposits that exist on the fuel surface. This work is expected to yield new technologies for predicting the rate of growth of ZrO_2 on Zircaloy under high burn-up conditions that can be used to the great benefit of the U.S. nuclear power industry. The technologies will be based on recent advances that this team has made in discerning the mechanism(s) of oxidation and hydriding of metals and alloys, as well as on advanced models that will be developed to describe the electrochemistry of reactor coolants at the fuel cladding/coolant interface, in terms of the bulk coolant chemistry, interfacial boiling, and the operating conditions in the reactor. Thus, the goal is to produce a predictive model that relates fuel sheath performance to coolant chemistry and reactor operating history, so that an operator can devise the most cost-

effective operating strategies that minimize the risk of fuel failure. The technology will be produced in the form of an algorithm that is readily incorporated into power plant computers and hence can be used as both a risk assessment tool and as an operating planning guide.

The proposed research will represent a major departure from work being carried out elsewhere, by undertaking the following activities:

- Incorporating the PDM in place of the diffusion models to describe oxide and hydride growth
- Incorporating the cathodic reactions that occur at the fuel cladding/coolant interface including the role of intermetallic precipitates in the film as catalytic sites for these reactions
- Incorporating an advanced coolant radiolysis model for estimating the concentrations of electroactive species (O_2 , H_2O_2 , H_2 , etc) at the cladding surface, as a function of the chemistry of the coolant (pH, [Li], [B], [H_2]) and the operating conditions of the reactor
- Including mechanisms (cation vacancy condensation) for passivity breakdown as a means of describing the onset of nodular attack
- Developing a model based upon the generation and annihilation of point defects (oxygen vacancies, cation vacancies, and zirconium interstitials) at the Zircaloy/zirconia and zirconia/solution interfaces to describe the generation of stress in the interphasial region
- Incorporating a model for the concentration of solutes into porous deposits (CRUD) on the fuel under boiling (BWRs) or nucleate boiling (PWRs) conditions, in order to more accurately describe the environment that is in contact with the Zircaloy surface
- Integrating the damage over the operating history of the reactor, including start-ups, shut downs, and variable power operation
- Exploring the electronic structure and measure kinetic parameters for ZrO_2 film growth on Zircaloy under accurately simulated reactor operating conditions; following film growth in situ by electrochemical impedance spectroscopy (EIS)/capacitance measurements, while determining the electronic structure by using Mott-Schottky analysis

- Measuring kinetic parameters (exchange current densities and transfer coefficients) for the reduction of oxygen and the oxidation of hydrogen on Zircaloy under prototypical reactor operating conditions to accurately model the cathodic processes that occur on the cladding surface

The output of this project will be a more comprehensive understanding of the oxidation and hydriding of Zircaloy fuel cladding in reactor coolant environments, with particular emphasis on linkage between the plant operating parameters and the damage incurred due to oxidation and hydriding. Additionally, the

project will yield a set of models and codes that will be made available to the nuclear power industry for managing the accumulation of corrosion damage to reactor fuel cladding as a function of the coolant chemistry and reactor operating conditions and history.

Finally, the development of the models and codes outlined in this proposal could greatly aid in the development of Generation IV reactors, by exploring water chemistry, materials/environment compatibility, and fuel design options that would minimize corrosion (oxidation and hydriding) damage to fuel cladding under specified operating regimes.

NUCLEAR ENERGY RESEARCH INITIATIVE

Incorporation of Integral Fuel Burnable Absorbers Boron and Gadolinium into Zirconium-Alloy Fuel Clad Material

Primary Investigator: K. Sridharan, University of Wisconsin

Project Number: 02-044

Project Start Date: September 2002

Collaborators: Sandia National Laboratory;
Westinghouse Savannah River Company

Project End Date: September 2004

Long-lived fuels require the use of higher enrichments of ^{235}U or other fissile materials. Such high levels of fissile material lead to excessive fuel activity at the beginning of life. To counteract this excessive activity, integral fuel burnable absorbers (IFBA) are added to some rods in the fuel assembly. The three commonly used IFBA materials are gadolinium oxide and erbium oxide, which are added to the UO_2 powder, and zirconium-diboride that is applied as a coating on the UO_2 pellets using plasma spraying or chemical vapor deposition techniques. These operations are performed as part of the fuel manufacturing process in the fuel plants. Due to the potential for cross-contamination with fuel that does not contain IFBA, these operations are performed in a facility that is physically separated from the main plant. These operations tend to be very costly because of their small volume, and can add from 20 to 30 percent to the manufacturing cost of the fuel. Other manufacturing issues that impact cost are maintenance of the correct levels of dosing and reduction in the fuel melting point due to additions of gadolinium and erbium oxide.

The goal of the proposed research is to develop an alternative approach that involves incorporation of boron or gadolinium into the fuel cladding material rather than as a coating or additive to the fuel pellets. This paradigm shift will allow for the introduction of the IFBA in a non-nuclear regulated environment and will obviate the necessity of additional handling and processing of the fuel pellets. This could represent significant cost savings and

potentially lead to greater reproducibility and control of the burnable fuel in the early stages of the reactor operation.

To achieve this objective, state-of-the-art, ion-based, surface engineering techniques will be applied. This will be performed using the IBEST (Ion Beam Surface Treatment) process being developed at Sandia National Laboratories, which involves the delivery of high energy ion beam pulses onto the surface of a target material. These pulses melt the top few microns of the target material's surface. The melt zone then solidifies rapidly at rates in excess of 10^9K/sec due to rapid heat extraction by the underlying substrate heat sink. This rapid solidification allows for surface alloying well in excess of the thermodynamically dictated solubility limits. This effect can be beneficially applied to the objectives of the proposed research for incorporating boron or gadolinium into the near-surface regions of Zircaloy-4 and Zirlo material used for fuel cladding. Several variants of this approach will be investigated with the goal of optimizing the process parameters to achieve the desired structure, composition, and compositional gradient in the near-surface regions of the Zircaloy-4 and Zirlo. Detailed materials characterization of the modified surface regions will be performed at the University of Wisconsin. The durability of the modified zirconium alloys against corrosion and oxidation will be tested in steam autoclaves at Westinghouse Science & Technology Department.

NUCLEAR ENERGY RESEARCH INITIATIVE

Neutron and Beta/Gamma Radiolysis of Supercritical Water

Primary Investigator: David M. Bartels, Argonne National Laboratory

Collaborators: University of Wisconsin

Project Number: 02-060

Project Start Date: September 2002

Project End Date: September 2005

Commercial nuclear reactors provide a source of heat, used to drive a "heat engine" (turbine) to create electricity. A fundamental principle of thermodynamics is that the higher the temperature at which any heat engine is operated, the greater its efficiency. Consequently, an obvious way to increase the operating efficiency and profitability of future nuclear power plants is to heat the water of the primary cooling loop to higher temperatures. Current pressurized water reactors (PWRs) run at roughly 300°C and 100 atmospheres pressure. Designs under consideration would operate at 450°C and 250 atmospheres, i.e., well beyond the critical point of water. This would improve the thermodynamic efficiency by about 30 percent. A major unanswered question is, what changes occur in the radiation-induced chemistry in water as the temperature and pressure are raised beyond the critical point, and what does this imply for the limiting corrosion processes in the materials of the primary cooling loop?

The cooling water of any water-cooled reactor undergoes radiolytic decomposition, induced by gamma, fast-electron, and neutron radiation in the reactor cores. Unless mitigating steps are taken, oxidizing species produced by the coolant radiolysis can promote intergranular stress-corrosion cracking and irradiation-assisted, stress-corrosion cracking of iron- and nickel-based alloys. These will alter corrosion rates of iron- and nickel-based alloys, and of zirconium alloys, in reactors. One commonly used remedial measure to limit corrosion by oxidizing species is to add hydrogen in a sufficient quantity to chemically reduce transient radiolytic primary oxidizing species (OH, H₂O₂, HO₂/O₂⁻), thereby stopping the formation of oxidizing products (H₂O₂ and O₂). It is still unclear whether this will be effective at the higher temperatures proposed for future reactors. While an earlier NERI project has investigated some of the most

important radiation chemistry in supercritical water, there is no information at all on the effect of neutron radiolysis, which is the main source of the troublesome oxidizing species.

The collaboration proposed here is ideally suited to discover most of the fundamental information necessary for a predictive model of radiation-induced chemistry in a supercritical water reactor core. Electron pulse radiolysis coupled with transient absorption spectroscopy is the method of choice for measuring the kinetics of radiation-induced species, as well as product yields for fast electron and gamma radiation. The Argonne Chemistry Division's linac is capable of producing 20 MeV electron pulses of 30 picoseconds duration, and the principal investigators at Argonne have extensive experience in measuring transients on a nanosecond and sub-nanosecond timescale. The University of Wisconsin's Nuclear Reactor Facility is a very convenient source of neutron radiation that can be exploited for radiolysis experiments from room temperature to 500°C. The combined capabilities of these facilities will make it possible to create a quantitative model for water radiolysis in both current PWR systems and supercritical water-cooled plants in the future.

The subject of this proposal touches on several areas of research mentioned in the NERI call for proposals. At its heart, the work is fundamental chemical science, which can be applied to both current and future reactor problems, and other areas of endeavor such as supercritical water oxidation technology. The direct application to nuclear engineering research is the design of reactors with higher performance and efficiency. The work proposed here is a follow-up and extension of research in a previous NERI project (276) on the same subject.

NUCLEAR ENERGY RESEARCH INITIATIVE

Innovative Approach to Establish Root Causes for Cracking in Aggressive Reactor Environments

Primary Investigator: S. M. Bruemmer, Pacific Northwest National Laboratory

Collaborators: GE Global Research Center; Electric Power Research Institute; Framatome ANP, Inc.

Project Number: 02-075

Project Start Date: September 2002

Project End Date: September 2005

The successful development of Generation IV nuclear power systems must address and mitigate several materials-degradation issues now strongly impacting existing light water reactors (LWRs) after very long periods of operation. In addition, the more aggressive radiation and environmental exposures envisioned for various advanced reactor concepts will require materials with improved high-temperature properties and resistance to cracking. Although previous fast reactor and fusion device programs have focused on the development of improved structural materials for their relevant conditions, no comparable effort has been directed toward the conditions unique to water-cooled fission reactors since the inception of nuclear-powered propulsion units for submarines. The paramount issues impacting both LWR economics and safety have been corrosion and stress-corrosion cracking in high-temperature water. These degradation processes have continued to limit performance as the industry has changed operating parameters and materials. Mechanistic understanding and non-traditional approaches are necessary to create durable corrosion-resistant alloys and establish the foundation for advanced reactor designs. Less down time and longer component lifetimes are the drivers motivating this research for both Generation III and IV nuclear power systems.

Proposed research will focus on the characterization of critical Fe- and Ni-base stainless alloys tested under well-controlled conditions where in-service complexities can be minimized. Quantitative assessment of crack-

growth rates will be used to isolate effects of key variables, while high-resolution analytical transmission electron microscopy will provide mechanistic insights by interrogating crack-tip corrosion/oxidation reactions and crack-tip structures at near atomic dimensions. Reactions at buried interfaces, not accessible by conventional approaches, will be systematically interrogated for the first time. Novel mechanistic "fingerprinting" of crack-tip structures tied to thermodynamic and kinetic modeling of crack-tip processes will be used to isolate causes of environmental cracking. Comparisons will be made with results on failed components removed from LWR service (funded separately by industry collaborators).

The proposed research strategy capitalizes on unique national laboratory, industry, and university capabilities to generate basic materials and corrosion science results with immediate impact to next generation nuclear power systems. This proposed work will be integrated with existing NERI projects, with fundamental research funded by the DOE Office of Basic Energy Sciences, and with focused U.S. and international projects dealing with current LWR degradation issues. This leveraged approach will facilitate the revolutionary advances envisioned by NERI by creating a multi-faceted effort combining the basic and applied science necessary to drive mechanistic understanding and promote development of next generation materials that meet the performance goals of advanced reactors.

NUCLEAR ENERGY RESEARCH INITIATIVE

Design of Radiation-Tolerant Structural Alloys for Generation IV Nuclear Energy Systems

Primary Investigator: Todd R. Allen, Argonne National Laboratory

Project Number: 02-110

Collaborators: Pacific Northwest National Laboratory; University of Michigan; Japan Nuclear Cycle Development Institute

Project Start Date: September 2002

Project End Date: September 2005

Under the Generation IV Reactor initiative, revolutionary improvements in nuclear energy system design are being pursued in the areas of sustainability, economics, and safety and reliability. To meet these goals, advanced nuclear energy systems demand materials that minimize resource use, minimize waste impact, improve proliferation resistance, extend component lifetime, and reduce uncertainty in component performance. Simultaneously, they will potentially operate in higher temperature environments, with greater radiation dose, and in unique corrosion environments compared to previous generations of nuclear energy systems. Additionally, the material choices must provide for construction and operating costs that allow the nuclear energy system to compete in the marketplace.

The irradiation performance of structural materials will likely be the limiting factor in successful nuclear energy system development. The limits of the structural and fuel-related materials determine the performance of new nuclear energy systems. Satisfactory performance in a nuclear energy system is unusually demanding. In addition to the best characteristics and performance of materials that have been achieved in other advanced high-temperature energy systems, nuclear energy systems require exceptional performance under high fluence irradiation. Based on experience, materials not tailored for irradiation performance generally experience profound changes in virtually all important engineering and physical properties because of fundamental changes in structure caused by radiation damage.

This project will develop and characterize the radiation performance of materials with improved radiation resistance. Material classes will be chosen that are expected to be critical in multiple Generation IV technologies. The material design strategies to be tested fall into three main categories: (1) alloying, by adding oversized elements to the matrix; (2) engineering grain boundaries; and (3) designing the microstructure/nanostructure, such as by adding matrix precipitates.

The materials to be examined include both austenitic and ferritic-martensitic steels, both classes of which are expected to be key structural materials in many Generation IV concepts. The irradiation program will consist of scoping studies using proton and heavy-ion irradiations of key alloys and tailored alloy condition, and examination of materials irradiated in BOR-60 to confirm charged particle results. Examinations will include microstructural characterization, and mechanical properties evaluation using hardness and shear punch and stress-corrosion cracking.

The teaming of Argonne National Laboratory, Pacific Northwest National Laboratory, and the University of Michigan joins together institutions with critical skills and demonstrated capability in evaluating irradiation performance, along with experience in water reactor and liquid metal fast reactor systems. This project builds on the successes of NERI projects being performed jointly at these three institutions over the last three years.

NUCLEAR ENERGY RESEARCH INITIATIVE

Enhanced Control of PWR Primary Coolant Water Chemistry Using Selective Separation Systems for Recovery and Recycle of Enriched Boric Acid

Primary Investigator: Ken Czerwinski,
Massachusetts Institute of Technology

Project Number: 02-146

Collaborators: Los Alamos National Laboratory;
Florida Power and Light; Pacific Southern Electric and
Gas Co.; (n,p) Energy, Inc.; University of California,
Berkeley

Project Start Date: September 2002

Project End Date: September 2005

The economics of operating existing and advanced pressurized water reactors (PWRs) clearly identify that increasing nuclear fuel enrichment will produce more energy. To operate within the nuclear reactor safety requirements, the concentration of natural boric acid used as a flux chemical shim would have to be increased. Enriched boric acid (B-10) has a greater cross section than natural boric acid and is favored over natural boric acid. This occurs because of primary side-water, corrosion-cracking issues associated with the increased requirement for higher lithium hydroxide (Li-7) concentrations to maintain operational pH with an increased natural boric acid concentration. However, the cost of producing and using enriched isotopes such as B-10 and Li-7 requires a means to cost-effectively recover and reuse them.

Under the NERI category of fundamental chemistry, under fundamental science, work is proposed to develop and field test polymeric sequestering systems designed to efficiently and selectively recover enriched boric acid/lithium hydroxide from the primary coolant water of reactors. These advanced separation materials will reduce the cost of operating existing and advanced light water reactor systems by improving the chemical control of the primary reactor coolant. Contaminants present in the coolant system will be characterized regarding their potential for interfering with the selective recovery of B-10 and Li-7, and counter measures will be developed to mitigate their interference. Cost benefits will result from greater energy production per reactor unit, reduced operational radiation exposure, and protection from accelerated corrosion of critical core components.

